APTD-0704

PB 201 422

INFRARED SPECTROSCOPIC STUDY OF GAS-SOLID INTERACTIONS
REPORT NO. III

FINAL REPORT

MAY 1971

Division of Controlled Systems
Office of Air Programs
Environmental Protection Agency
3914 Virginia Avenue
Cincinnati, Ohio 45227

Contract No. CPA 70-63

Submitted By

General Technologies Corporation
A Subsidiary of Cities Service Company
1821 Michael Faraday Drive
Reston, Virginia 22070

by

Edwin F. Rissmann

Reproduced by
NATIONAL TECHNICAL
INFORMATION SERVICE
Springfield, Va. 22151

85

PB 201 422

BIBLIOGRAPHIC DATA SHEET	1. Report No. APTD-0704	2.	3. Recipient's Accession No.

4. Title and Subtitle
Infrared Spectroscopic Study of Gas-Solid Interactions - Report No. III

5. Report Date
May 1971

6.

7. Author(s)
Edwin F. Rissmann

8. Performing Organization Rept. No.

9. Performing Organization Name and Address
General Technologies Corporation
A Subsidiary of Cities Service Company
1821 Michael Faraday Drive
Reston, Virginia 22070

10. Project/Task/Work Unit No.

11. Contract/Grant No.
CPA 70-63

12. Sponsoring Organization Name and Address
Division of Controlled Systems
Office of Air Programs
Environmental Protection Agency
3914 Virginia Avenue
Cincinnati, Ohio 45227

13. Type of Report & Period Covered
Final

14.

15. Supplementary Notes

16. Abstracts

Investigations have been conducted in an effort to develop rapid reliable methods for analysis of reacted limestone and limestone slurries. In this area new thin film infrared cells have been developed and demonstrated. The cells developed were then used to obtain calibration curves for species of interest in several solvent systems which would be of use in analyzing either reacted solid limestones or limestone slurries. In another phase of this program, a study was made of the influences of impurities on the dead-burning of limestone. Specifically, a study using infrared spectroscopy, electroprobe investigations and auger spectroscopy revealed both the occurrence of chemical reactions between lime and limestone and impurities at higher calcination temperatures and diffusion of impurities to surfaces and into pores.

17. Key Words and Document Analysis. 17a. Descriptors

Air pollution
Scrubbers
Chemical analysis
Limestone
Reactivity
Activation
Temperature
Chemical reactions
Calcines
Infrared spectroscopy
Electron microprobe

17b. Identifiers/Open-Ended Terms
Air pollution control
Auger spectroscopy

17c. COSATI Field/Group 13B, 7B

18. Availability Statement Unlimited	19. Security Class (This Report) UNCLASSIFIED	21. No. of Pages 86
	20. Security Class (This Page UNCLASSIFIED	22. Price

FORM NTIS-35 (10-70) USCOMM-DC 40329-P71

C

DISCLAIMER

This report was furnished to the Office of Air Programs by

General Technologies Corporation
A Subsidiary of Cities Service Company
1821 Michael Faraday Drive
Reston, Virginia 22070

in fulfillment of Contract No. CPA 70-63

INFRARED SPECTROSCOPIC
STUDY OF GAS-SOLID INTERACTIONS
REPORT NO. III

FINAL REPORT

MAY 1971

Division of Controlled Systems
Office of Air Programs
Environmental Protection Agency
3914 Virginia Avenue
Cincinnati, Ohio 45227

Contract No. CPA 70-63

Submitted By

General Technologies Corporation
A Subsidiary of Cities Service Company
1821 Michael Faraday Drive
Reston, Virginia 22070

by

Edwin F. Rissmann

ABSTRACT

This report constitutes work conducted during the third year of effort to study gas-solid interactions by infrared techniques. Reports of the first two year's work have been published by the National Technical Information Service for contract numbers PH 86-68-78 and CPA 22-69-59.

The major effort in this investigation has been directed toward development of rapid reliable methods for analysis of reacted limestone and limestone slurries. In this area, new thin film infrared cells have been developed and demonstrated. These cells are free of several of the problems possessed by the thin film silver chloride cells developed during earlier studies in that they are both more wear resistant and easier to fill and handle. The materials used, Irtran 2 and silver (for the thin film) were chosen on the basis of water and wear resistance tests run on several possible materials and the final design of cell was selected on the basis of experimental results obtained with several possible varieties.

The cells developed were then used to obtain calibration curves for species of interest (i.e. nitrate, nitrite, sulfate and sulfite) in several solvent systems which would be of use in analyzing either reacted solid limestones or limestone slurries. Specifically, the solvent systems studied were tetrasodium EDTA (ethylenediaminetetraacetic acid) saturated water, saturated aqueous KF and pure water. Calibration curves for the ions of interest in these solvents were obtained in all cases in the 0.1-2.0 g/100 cc concentration range. These curves, and the cells were then used to analyze a number of reacted slurries and results, for a few cases, were compared with those obtained by other methods with satisfactory results.

In another phase of this program, a study was made of the influences of impurities on the deadburning of limestone. Specifically, a study using infrared spectroscopy, electro-microprobe investigations and Auger spectroscopy revealed both the occurrence of chemical reactions between lime and limestone and impurities at higher calcination temperatures and diffusion of impurities to surfaces and into pores. Specifically, diffusion of aluminum into pores and to bulk surfaces was noted at higher calcination temperatures and evidence was obtained which showed that large amounts of the impurities present occurred in discrete phases, many of which tended to be located at or near the surfaces of pores, which could well explain the lower reactivities of impure limestones.

TABLE OF CONTENTS

Page

I INTORDUCTION AND SUMMARY 1

II EXPERIMENTAL RESULTS AND DISCUSSION 3

A. ANALYTICAL STUDIES 3

1. Introduction 3
2. Experimental Results and General Statement 4
3. Selection and Evaluation of Cell Materials 4
4. Design and Testing of Improved Cells 10

B. CALIBRATION STUDIES 18

1. General Procedures 18
2. Results and Discussion 19
3. Discussion of Calibration Studies 39
4. Quantitative Analyses 45

C. DEADBURNING STUDIES 47

1. Introduction 47
2. Experimental 47
3. Results and Discussion 52

III CONCLUSIONS AND RECOMMENDATIONS 72

IV REFERENCES 74

V ACKNOWLEDGMENTS 75

LIST OF FIGURES

Figure		Page
1	Germanium - Effect of Exposure to EDTA Solutions	6
2	KRS 5-Top Portion Exposed to EDTA Solutions Bottom Portion Unexposed	7
3	Silicon, Bottom Portion Exposed to EDTA (note eroded regions)	8
4	ZnSe (note difference between bottom (exposed) and top (unexposed) regions)	9
5	ZnS - Effect of Exposure to EDTA Solutions	11
6	Infrared Cell for Use with Limestone Solvent	13
7	Diagram of One Proposed Model of Evacuable Thin Film Cell	15
8	Modified Cell Holder	16
9	Evacuable Infrared Cell	17
10	Spectra of NO_3^- and CO_3^- and Interferences Between Them	20
11	Calibration Curve for Sulfite	22
12	Calibration Curve for Nitrite	23
13	Calibration Curve for Sulfate on EDTA at 1110 cm^{-1}	24
14	Calibration Curves $Ca(NO_3)_2^-$ in EDTA 1340 cm^{-1} in H_2O 1340 cm^{-1}	25
15	Calibration Curve $CaCO_3$ in EDTA - 1440 cm^{-1}	26
16	EDTA - pH 12.0	27
17	Nitrite - KF 1235 cm^{-1}	28
18	Carbonate - KF - 1410 cm^{-1}	29
19	Nitrate 1390 cm^{-1} Sat KF	30

LIST OF FIGURES (contd.)

Figure		Page
20	Sulfate - KF - 1110 cm^{-1}	31
21	NO_3^- in KF	32
22	$CaSO_3$ - KF - 940 cm^{-1}	33
23	$NaHSO_3$ - KF	35
24	Ca Nitrite - H_2O - 1240 cm^{-1}	36
25	Calibration Curves for Sulfates in H_2O	37
26	Calibration Curves for $SO_4^=$ in H_2O	38
27	Calibration Curves for SO_3 in H_2O	40
28	$Ca(OH)_2$ - D_2O - Analysis for OH	41
29	Silicon Rich Limestone 1700°F, 800X	50
30	Iron Rich Limestone 2000°F, 800X	51
31A	Dolomite High in Silica at 1700°F	54
31B	Dolomite High in Silica at 2600°F	55
32A	Iron Containing Dolomite at 1700°F	56
32B	Iron Containing Dolomite at 2600°F	57
33	Microprobe Trace for Silicon on 1700°F Calcined Limestone	63
34	Microprobe Trace for Iron on 1700°F Calcined Limestone	64
35	Microprobe Trace for Aluminum on 2600°F Limestone	67
36	Auger Spectrum of 2600°F Limestone Calcine	73

LIST OF TABLES

Table		Page
IA	Infrared Window Material for Thin Film Cells	5
IB	Further Evaluation of Satisfactory Window Materials by Exposure Testing	5
II	Reproducibility with Single New Cell of Sulfate Absorbance at 1110 cm^{-1}	12
III	Positions of Band Maxima Used in Calibration Curves for Species of Interest	19
IV	Solvent Systems for Limestone Analyses	43
V	Analysis of Scrubber Solutions	46
VI	Chemical Analyses in Weight Percentage (Analyses by Analytical Chemistry Section of the Illinois State Geological Survey)	49
VII	Band Positions and Intensities for Calcination Studies	53
VIII	Band Positions Near 1000 cm^{-1} for Known Silicates	58
IX	Spectra of HCl Insoluble Residues from Limestone Calcines	59
X	Spectra of HCl Soluble Residues from Limestone Calcines	60
XI	Spectra of EDTA Insoluble Residues	61
XII	Surface to Bulk Concentration Ratios for Impurities as a Function of Calcination Temperature	68
XIII	Correlation Between Scanning Electron Microscope Positions of Pores and Phases and Microprobe Concentration Maxima - High Silica 2000°F Calcine Partilces	69
XIV	Effect of Calcination Temperature on Concentrations of Impurities in Pores	69
XV	Effect of Calcination Time on Surface/Bulk Impurity Ratios	71
XVI	Fraction of Pores Possessing Specific High Concentrations of Impurities (More than 10 Times Bulk Impurity Level)	71

SECTION I

INTRODUCTION AND SUMMARY

The removal of sulfur dioxide and nitrogen oxides from power plant flue gases is increasingly becoming a subject of considerable concern. Several processes have been proposed to satisfactorily remove these pollutants by converting them into either saleable or non-toxic, easily discardable, products. Two potentially economical methods, which result primarily in formation of discardable calcium salts, are the wet and dry limestone scrubbing processes.

For these techniques to be adequately studied, several problems must first be solved. New analyses which are sufficiently rapid so as to be able to handle large numbers of process control samples must be developed. The classical wet chemical techniques already in use are simply too time consuming if a number of reacted limestone constituents must be determined on a routine basis. Also, information on the causes of phenomena such as deadburning of limestone must be obtained sothat problems involving losses of reactivity of limestone can be solved and knowledge gained of which types or compositions of limestone are suitable for use in the gas cleaning processes.

The aim of this program has been to utilize infrared spectroscopic methods to identify and solve some of the above problems. Specifically, three areas have been studied in considerable detail:

1. Improved thin film infrared cells have been developed for use in analyzing aqueous solutions.

2. The development of rapid, accurate infrared methods for the routine analysis of the constituents of reacted limestone and aqueous limestone slurries using the thin cells has been studied.

3. A study was made of the possible influences of specific impurities in the deadburning (i.e. loss of reactivity) of limestone as a function of calcination conditions.

For the first two tasks, studies centered around development of improved infrared cells. In earlier studies, cells made of silver chloride were used. These cells were found to have erosion and filling problems which would make their routine use somewhat difficult. In these current studies, an investigation was first performed to determine which window and film materials possessed the greatest water and wear resistance. These best materials, Irtran 2 and silver, were then used for construction of several different possible types of cells, of which one type, a demountable variety, was found to possess few if any handling or filling problems.

Using matched pairs of the demountable variety thin film cells, calibration curves were obtained in saturated tetrasodium EDTA aqueous solutions, in saturated aqueous KF and in pure water for solutions of the sulfates, nitrate, nitrite and sulfite of calcium. Other salts of the same types (i.e. $MgSO_4$, $Mg(NO_3)_2$, etc. were also studied and calibration curves were then constructed for absorbance versus concentration of the ions of interest. Salt concentrations for these calibrations were in the 0.1-2.0 g/100 cc range.

After the necessary calibration curves had been developed, a number of slurries were analyzed by this infrared method and the results, for a few cases, compared with those obtained by other techniques. Reasonable agreement was found.

For the third task, a study using infrared spectroscopy, electron microprobe investigations and Auger spectroscopy was performed of the influence of impurities on the thermal deactivation (deadburning) of limestones. In this study, spectra were obtained by the KBr pellet method of different limestones calcined at various temperatures for specific times. Analysis of the results showed that chemical reactions were occurring at higher calcination temperatures to yield materials with spectra quite different from those obtained on the lower temperature calcines. Infrared studies performed on the HCl insoluble residues from these calcines further confirmed that the amount of free silica present in the samples decreased, for silica and iron rich samples, with increasing calcination temperature. These results have been interpreted in terms of reactions between SiO_2 or sample silicates with lime or limestone to yield more complex materials.

Electron microprobe studies were also conducted on the different calcines. Results of the line trace microprobe studies showed that many of the impurities were present in discrete phases in the samples and that, with increasing calcination temperature, larger amounts of higher impurity phases tended to be present at pore sites. The microprobe studies also indicated that aluminum (probably in the form of alumina or some aluminate) diffused to surfaces of the samples at higher calcination temperatures. This finding was confirmed by Auger spectroscopy studies for one set of samples.

SECTION II

EXPERIMENTAL RESULTS AND DISCUSSION

The work performed under this contract was aimed at the solution of two discrete sets of problems:

1. Analytical investigations and development of improved thin film infrared cells and,
2. Studies of the effects of impurities on the thermal deactivation (deadburning) of limestone.

In this report, each of these areas will be treated, in whole, in a separate section. This, it is felt, will yield a more easily understandable presentation.

A. ANALYTICAL STUDIES

1. Introduction

Over the past few decades, the field of infrared spectroscopy has made significant advances. However, the problem of being able to perform quantitative infrared studies of aqueous solutions has to a large degree escaped solution. To date, water has been employed as a solvent in several infrared investigations, most of which, because of difficulties with the very thin cells of less than 10 microns thickness required, have been of essentially a qualitative nature(1-4). However, recent advances in cell technologies have made it possible to design single cells of a few microns in thickness which can be used for quantitative studies(5-6). The methods of cell preparation, which consisted of deposition of a thin film of polymer on the outer edges of a flat salt plate by solution evaporation, have been useful only for preparation of single cells and are, essentially, of little use for construction of matched pairs of cells, as would be required, for some quantitative studies.

More recently, work has been presented on a method of sulfate analysis in aqueous solution using cells of 3 micron thickness which had been prepared by vacuum evaporation of uniform thin silver films onto the outer edges of polished silver chloride plates(7). However, the approach taken in that study, while overcoming the difficulties involved in preparation of matched pairs of thin cells, possessed problems involving removal of trapped air bubbles formed on filling the cells. Removal of such air bubbles particularly in corners, in the past, has proven both troublesome and time consuming(8). Problems of erosion of the silver chloride windows with time were also encountered to some degree.

To overcome some of the above problems and develop cells, which are both easy to use, several studies were initiated under this program which are described in the following sections.

2. Experimental Results and General Statement

The experimental work under this portion of the program consisted of three phases:

a. Selection and evaluation of improved material for cell construction.

b. Design and testing of improved cells.

c. Use of new cells to prepare calibration curves for some species of interest and performance of some analytical studies to determine the accuracy of the infrared methods developed.

Below are given detailed descriptions of the experimental procedures involved in each of these phases.

3. Selection and Evaluation of Cell Materials

A detailed evaluation was conducted of all potentially useable infrared window materials for use in improved thin film cells. In these studies, the criteria adopted were:

a. The materials must be more wear resistant and less deformable than the silver chloride windows used earlier.

b. The materials must be transparent out to at least 800 cm^{-1}.

c. The materials must be resistant and inert to water, saturated aqueous tetrasodium EDTA solutions, and saturated KF solutions, the three solvent systems of interest.

A detailed literature search was then made to locate all materials which satisfied the first criteria and were water resistant. These are listed in Table I along with reasons which were discovered for exclusion of some of these from further consideration. Thus, materials such as quartz and sapphire could be rejected because they do not transmit over a wide enough region. Other materials, such as MgO or CaF_2, could be rejected because of their known solubility in EDTA containing solutions; and a few others, such as AgBr could be rejected because of their softness or sensitivity to ultraviolet light.

As can be seen from Table I, five materials were seen to meet all of the requirements as could be determined by detailed investigation of the literature. These materials were further examined for their resistance to water and aqueous tetrasodium EDTA saturated solutions in the following manner. The samples (all one inch diameter disks) were mounted in a half immersed position in beakers of the solution at room temperature. The stirred solutions of EDTA or water were kept in contact with the samples for a 36 hour period, after which the samples were removed, washed and examined under a microscope. For four of the materials differences, as can be seen from Figures 1-4, could be seen

Table IA Infrared Window Material for Thin Film Cells

Material	Reason for Exclusion from Further Consideration
MgO	Listed as soluble in EDTA solutions
CaF_2	" " " " " "
MgF_2	" " " " " "
BaF_2	" " " " " "
LiF	Transparency limit of approximately 1400 cm^{-1}
Silicon	Appears satisfactory from literature search
Germanium	" " " " "
AgBr	Very light sensitive, soft like AgCl
KRS-5	Appears satisfactory from literature search
ZnS (Irtran 2)	" " " " "
ZnSe (Irtran 4)	" " " " "
CdS	Soft, like AgCl, low hardness (121 Knoop) reported
CdTe	Not readily available in useable form
Quartz	Transparency limit approximately 2500 cm^{-1}
Diamond	Optically, chemically and mechanically ideal, however prohibitive in cost
Sapphire	Transparency limit approximately 1400 cm^{-1}
As_2S_3 Glass	Attacked by alkaline solutions

Table IB Further Evaluation of Satisfactory Window Materials by Exposure Testing

Material	Result
ZnS	No evidence for corrosion or erosion on EDTA solution exposure
Silicon	Slight erosion and formation of a glossy film (SiO_2) over portions of the exposed region
Germanium	Much evidence for erosion - pits etc. - on exposed areas
KRS-5	Much evidence for erosion - exposed regions changed from organge to yellow and there was evidence of dissolution of material from these regions
ZnSe	Small amount of erosion was seen in EDTA exposed areas

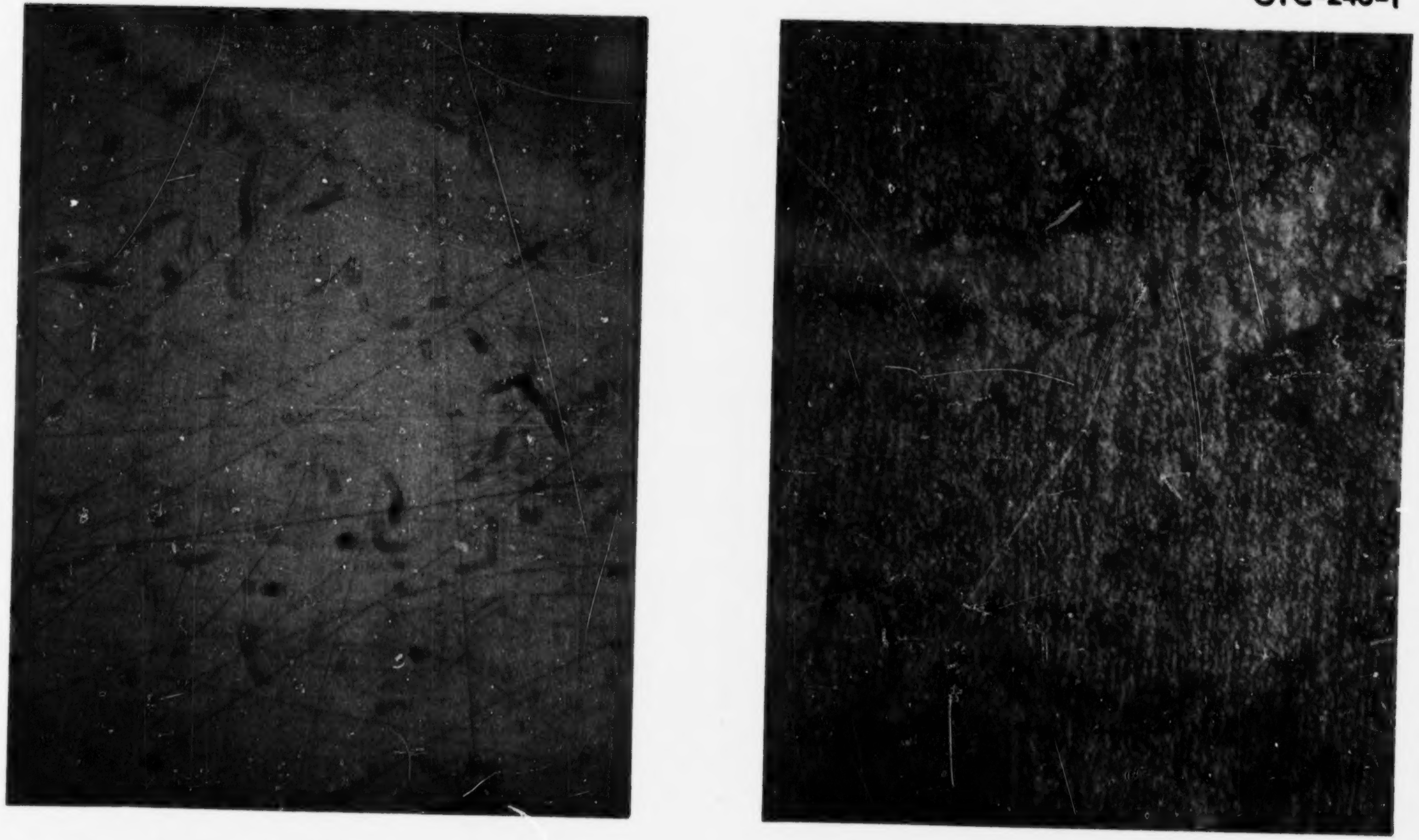

a. Ge Unexposed (400X)

b. Ge After Exposure to EDTA (400X)

Figure 1. Germanium – Effect of Exposure to EDTA Solutions

GTC-246-2

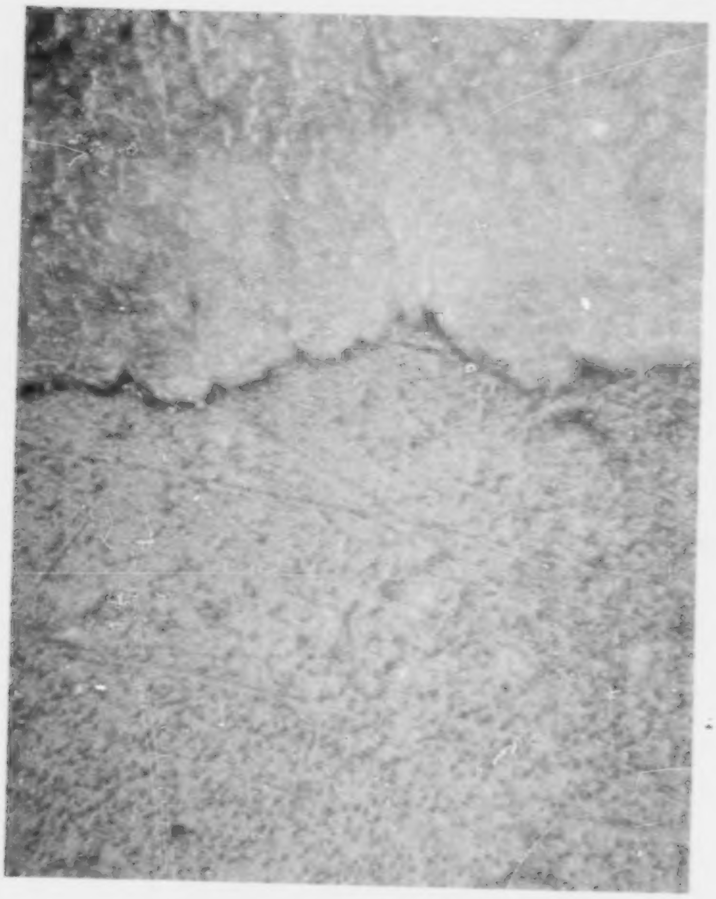

Figure 2. KRS 5
Top Portion Exposed to EDTA Solutions
Bottom Portion Unexposed

GTC-246-3

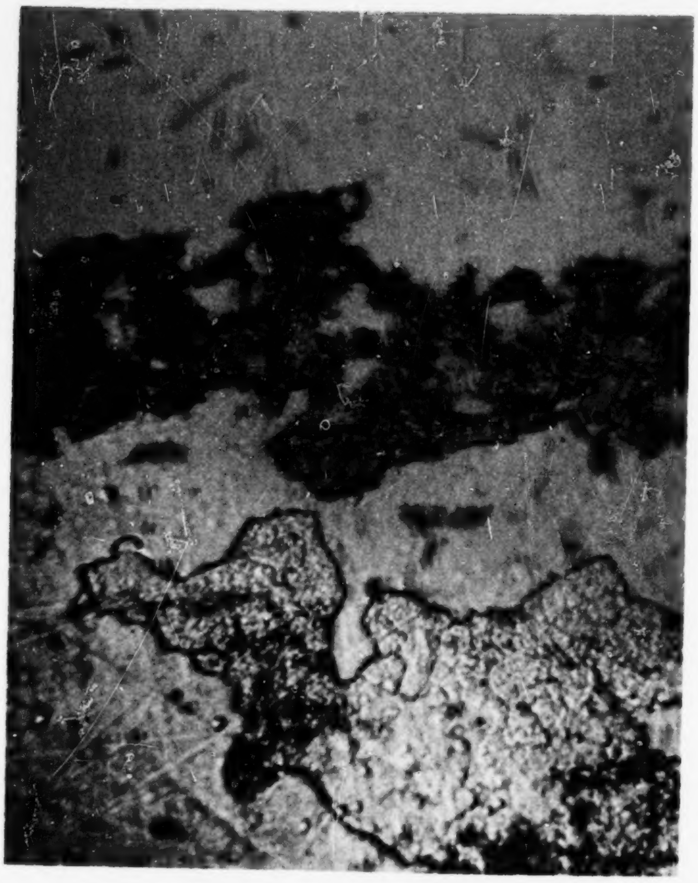

Figure 3. Silicon, Bottom Portion Exposed to EDTA (note eroded regions)

GTC-246-4

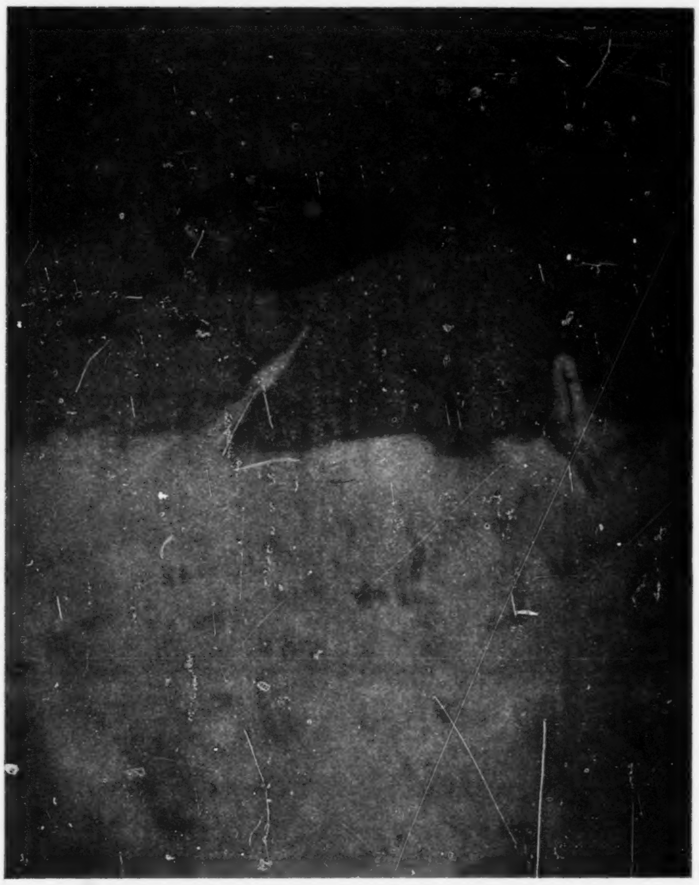

Figure 4. ZnSe (note difference between bottom (exposed) and top (unexposed) regions)

between the exposed and unexposed portions of the polished disks for the EDTA exposure experiments. Thus, for KRS-5, the exposed portion both changed color (orange to yellow) and showed visible signs of corrosion. The germanium and silicon samples also were seen to be corroded somewhat on the EDTA solution exposed portions. The Irtran 4 material (ZnSe) was, likewise, seen to be eroded somewhat by EDTA. The Irtran 2 material, on the other hand, as can be seen from Figure 5, was seen to be completely unchanged by EDTA exposure. Thus, this material was seen to be best suited for use. For the above exposure studies, separate EDTA solutions were used for each of the materials investigated.

Studies of potential spacer materials were performed using the same techniques mentioned above. Tantalum, silver, platinum and Teflon were all found to be suitably resistant to EDTA solutions. Gold, due to its extreme softness and poor wear characteristics was not studied.

A check was then made with the McMinn Optical Company who prepared the earlier AgCl thin film cells by vacuum evaporation of silver, to determine if methods existed for suitable deposition of Teflon on Irtran 2. A literature search, and some brief experimental work revealed that vacuum deposition of Teflon is not feasible. Further work also showed that preparing the film from deposited zinc sulfide itself was not feasible under this program due to the large amount of developmental work required to obtain satisfactory films with this material. Of the remaining spacer materials (i.e. tantalum, platinum and silver), considerations of cost led to selection of silver as the spacer material. Studies showed all three materials to be satisfactory for our purposes and adherent in the form of evaporated films to zinc sulfide.

4. Design and Testing of Improved Cells

a. General Statement

Two possible types of improved cells were examined. The first consisted of a relatively simple demountable variety of a type similar to that employed by Thompson(5). The second was a sealed evacuable variety, which could be cleaned or filled by drawing liquid through it under reduced pressure. For calibration and analytical studies, the first variety proved more suitable for use. Below are given both detailed descriptions of the devices studied and reasons for the choice of the demountable variety.

b. Demountable Cell

The possibility of designing a thin film cell, in which the spacer consists of a thin film of material deposited onto the outer edges of a salt plate was first proposed by Thompson(5), who used thin polymer films deposited by solution evaporation techniques. In these cells there were no holes for admission of samples. Instead, a drop of the liquid to be examined was simply placed on the bottom plate and the excess liquid then squeezed out by mounting the top plate.

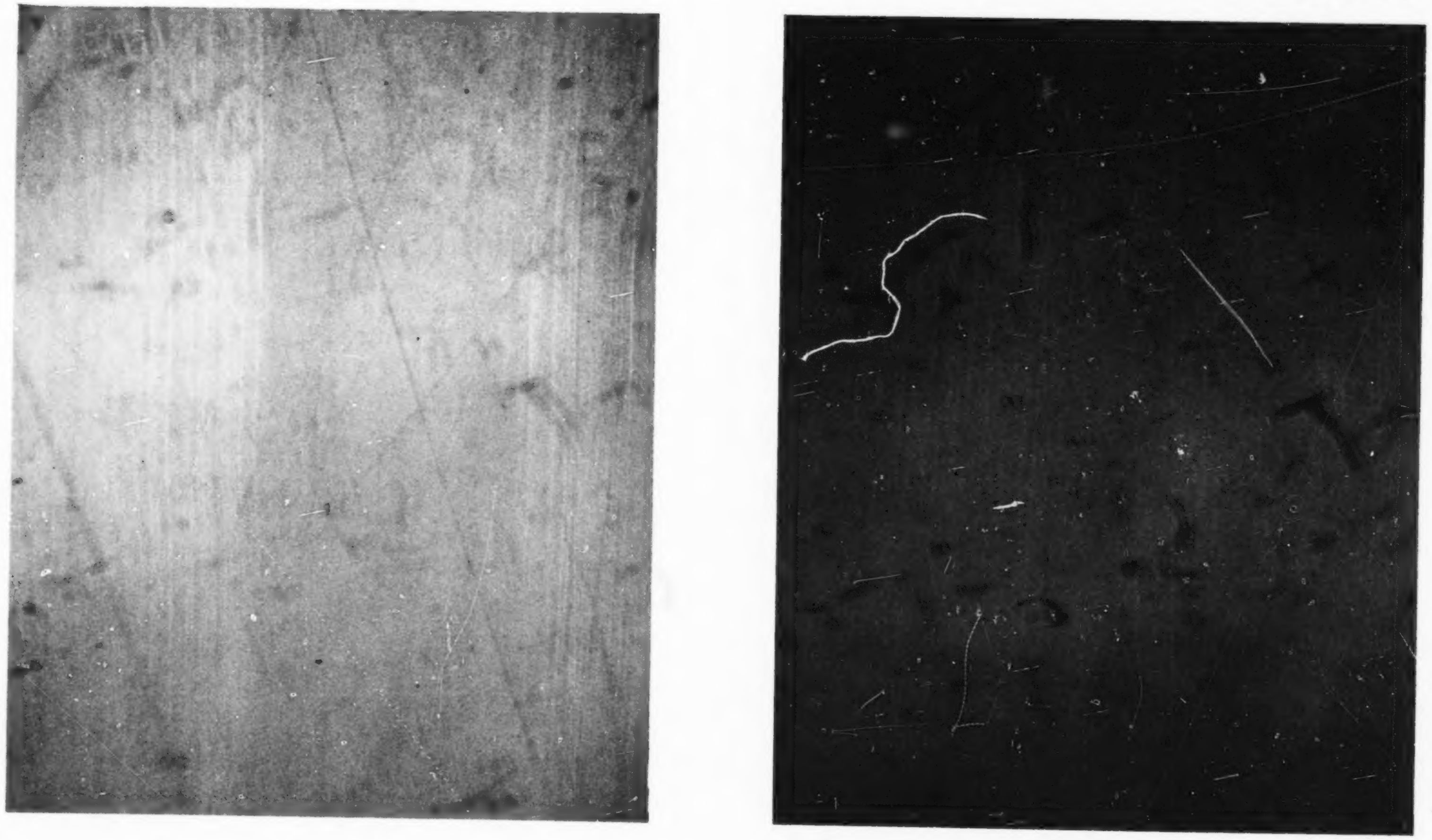

a. ZnS Unexposed to EDTA

b. ZnS Exposed to EDTA

Figure 5. ZnS - Effect of Exposure to EDTA Solutions

The results presented by Thompson and later by others(6), made it appear that this approach might prove to be satisfactory for our purposes. While Thompson's polymer film techniques are useless for preparing matched pairs of cells, it was felt that the approach of using vacuum evaporated films(7, 8) and the same cell arrangements would yield cells free of the filling problems encountered earlier. Accordingly, the following experiment was performed:

(1) An old standard cell holder was modified so that its upper plate was screwed to the lower plate at six positions symmetrically located around the cell.

(2) For the cell, a AgCl bottom plate (with Ag film) and an undrilled top plate were used.

(3) A drop of Na_2SO_4 solution was placed between the plates, the excess squeezed out, the arrangement assembled and a spectrum run. The sulfate absorbance at 1110 cm^{-1} was measured and recorded.

The above procedure was repeated ten times with the cell being washed between determinations. Table II lists relevant data. As can be seen, the sulfate band intensity is reproducible from determination to determination to within the accuracy of the spectrometer (~ ± 2%). Thus, a simple cell, such as that shown in Figure 6, used in conjunction with a modified cell holder, such as described above was seen to readily solve all of the filling problems encountered earlier. Indeed, to fill and assemble such a device required less than 5 minutes, as opposed to the long time required for the earlier AgCl cells due to bubble formation, filling, and leakage problems encountered with the old design.

Table II Reproducibility with Single New Cell of Sulfate Absorbance at 1110 cm^{-1}

Determination Number	Absorbance	Deviation from Average
1	0.66	.00
2	0.63	-.03
3	0.63	-.03
4	0.64	-.02
5	0.69	.03
6	0.67	.01
7	0.64	-.02
8	0.68	.02
9	0.68	.02
10	0.65	-.01
Average absorbance	0.66	
Standard deviation	0.02	
Mean deviation	0.02	

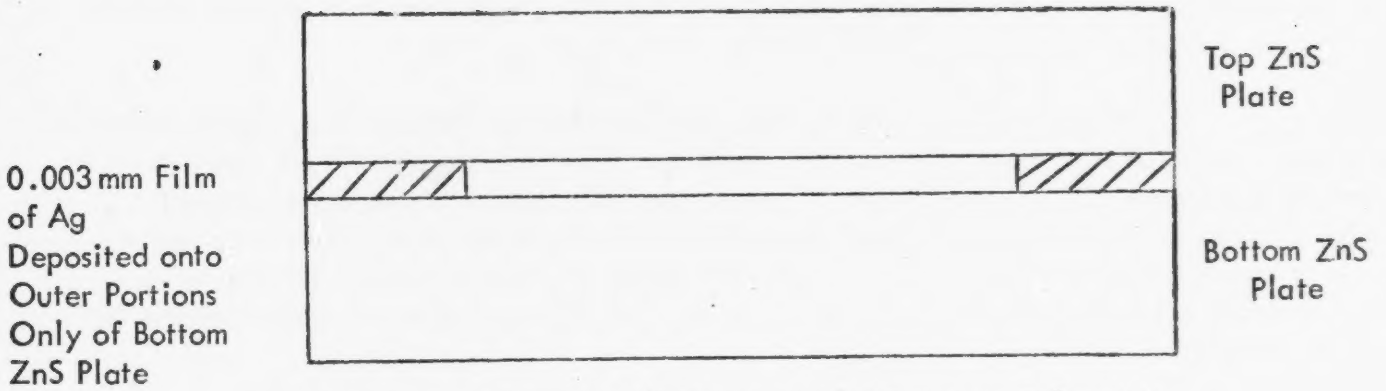
Top ZnS Plate
0.003 mm Film of Ag Deposited onto Outer Portions Only of Bottom ZnS Plate
Bottom ZnS Plate

Figure 6. Infrared Cell for Use with Limestone Solvent

c. Evacuable Cell

A second approach taken to the design of a thin film infrared cell free from filling problems was to construct an evacuable cell which could be filled by drawing liquid into and through it at reduced pressure. For this approach, two different types of such a device were constructed and evaluated.

The first version, as is shown in Figure 7, had holes for admission of samples and connection to vacuum line at the top of the cell. For the test cell constructed, the holes were precisely drilled into a set of Ag plated, one of which contained a 3 micron silver film. As can be seen from the diagrams (Figure 7) both admission of samples and evacuation occur from the top of the cell, thus preventing drainage problems. In this arrangement 2 mm stainless steel tubing was used. The tubing was sealed into its desired position with polymethyl methacrylate resin and the cell then mounted into a modified cell holder. To one of the stainless steel tubes was attached some Teflon tubing, through which the solutions to be used could be passed from a storage vessel. The other stainless steel tube was attached to a Kovar seal and glass joint, for connection, via vacuum tubing to a vacuum system.

This arrangement was briefly tested, using the same sodium sulfate solutions employed in evaluations of the demountable devices. However, problems were encountered due to strains imposed on the steel tubes by attachment of tubing. Indeed, this caused breakage of the polymeric sealant layer between the tubes and the AgCl plates and led to air leaks at these positions. As strain due to attachment to tubing was expected to be a constant problem in actual useage of such a system, this approach did not appear promising and was abandoned.

A second design of evacuable cell with drilled holes in the top ZnS plate was then assembled and tested. The cell, it was found, could be readily filled by evacuation which resulted in drawing liquid readily into and through the cell. Some minor problems were encountered with solvent evaporation using this approach, however, these could be overcome by drawing of sufficient liquid through the cell and into a reservoir area. A sketch and picture of this arrangement are given in Figures 8 and 9. Here, the base plate P had dimensions suitable for the holder in the Beckman unit and a foot F to enable it to stand upright when not in the holder. The window nearest the plate W, contained the thin film spacer. It rested on the plate but was cushioned by two pieces of heavy paper C. The second window W_2 was then placed on top of the first. This window contained two 1/32" diameter holes for admission of sample.

This sandwich arrangement was held together tightly by two clamp bars B, in the center of which are 3/32" holes D. The latter had threaded tubing for attachment to external vacuum and filling arrangements. Solvent tight seals were obtained by amalgamated lead washers between the top window and the bars and at the allen head screws. Even pressure on the windows was obtained by adjustment of the four binding post nuts N, the cardboard pieces C serving to relieve minor inequalities and strains.

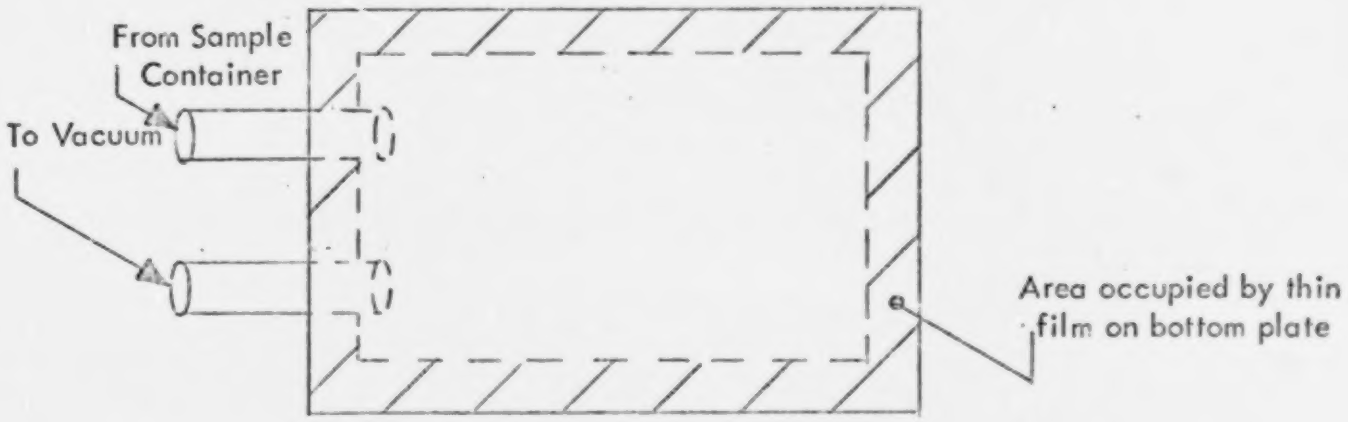
From Sample
Container
To Vacuum
Area occupied by thin
film on bottom plate

a. Top View

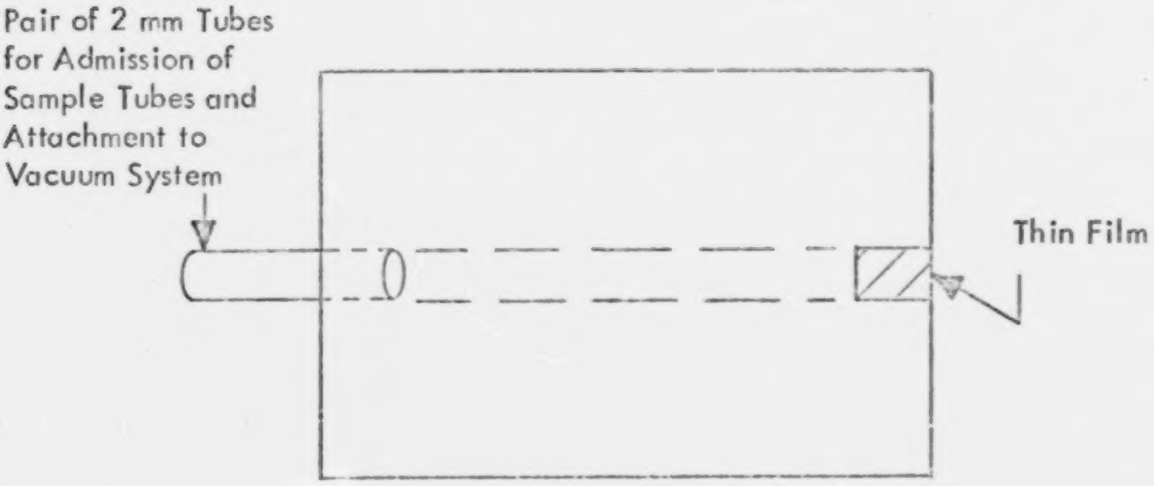
Pair of 2 mm Tubes
for Admission of
Sample Tubes and
Attachment to
Vacuum System
Thin Film

b. Side View

Figure 7. Diagram of One Proposed Model of Evacuable Thin Film Cell

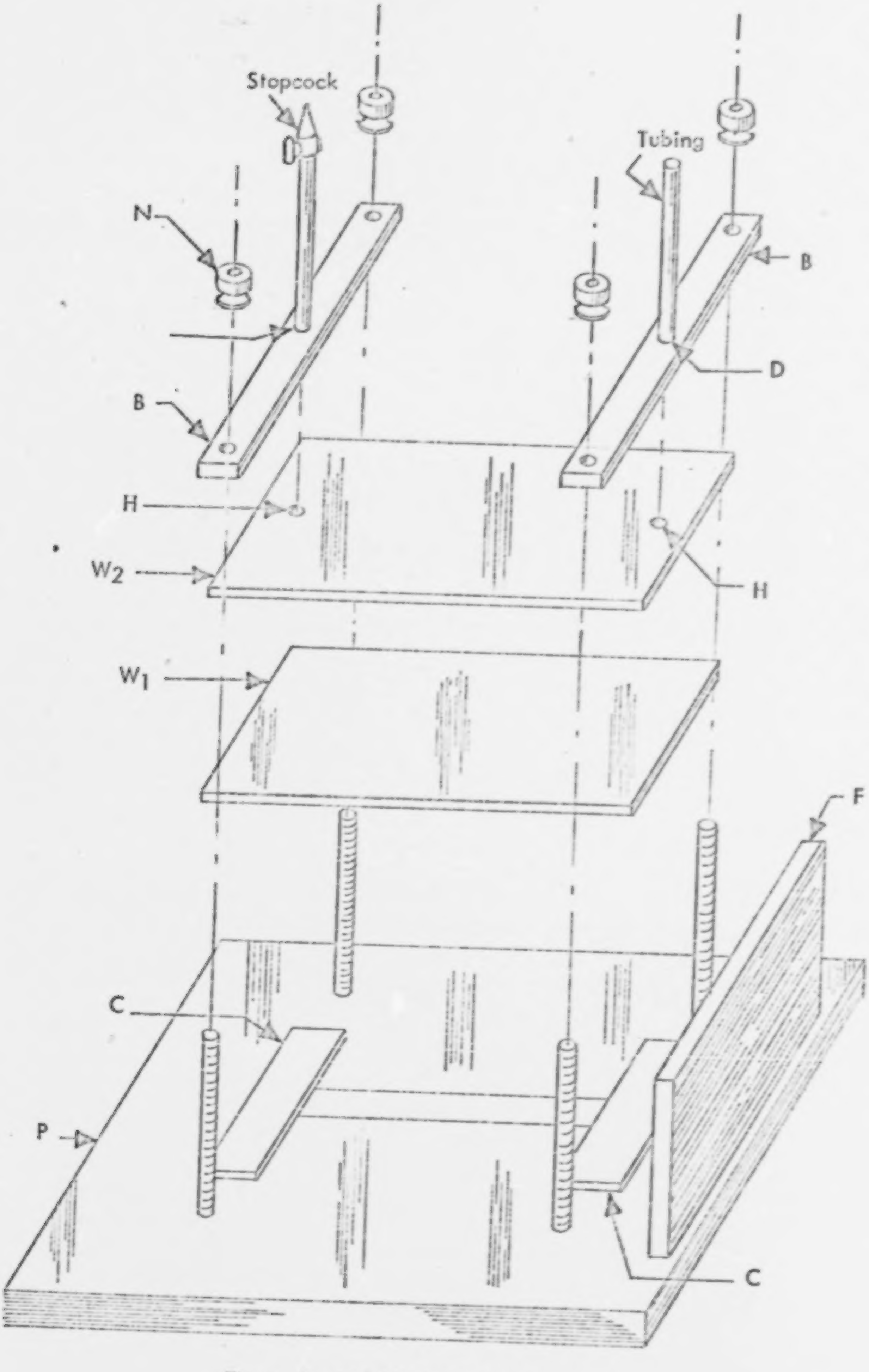
Stopcock
Tubing
N
B
B
D
H
W2
H
W1
F
C
P
C

Figure 8. Modified Cell Holder

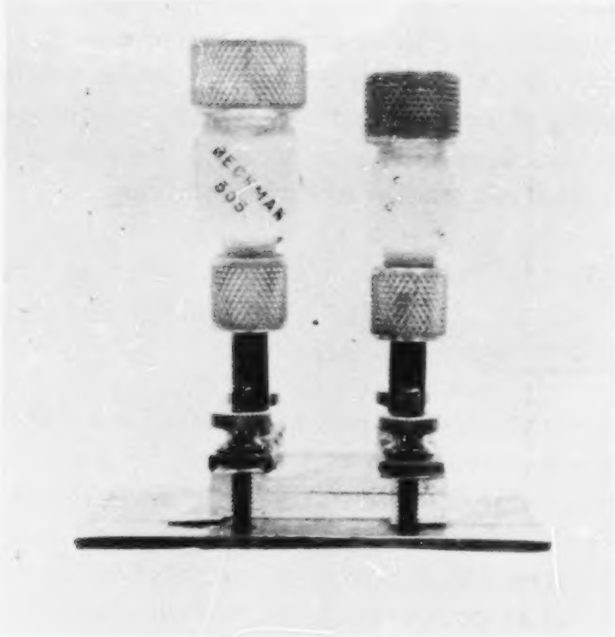
BECKMAN
505

a. Side View

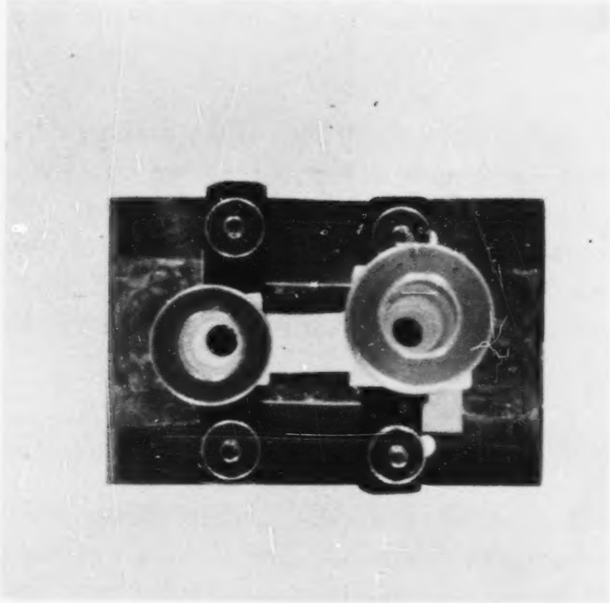

b. Top View

Figure 9. Evacuable Infrared Cell

A pair of such devices were built and evaluated. While reproducible spectra could be obtained using such devices the problems of maint_ining the sealed arrangement necessitated cleaning of the cells by drawing pure solvent into and through them. In practice, this constituted a very time consuming procedure, due to the need for special care to avoid breaking or straining the glass attachment parts. After a number of studies using this device, it was found that the times required for cleaning were of the same order as those required to fill the silver chloride cells used in earlier studies(8). Hence, it was felt that this evacuable model cell did not present any advantages over the old model and further work with it was abandoned in favor of using the demountable cell for all calibration and quantitative analysis studies to be undertaken.

B. CALIBRATION STUDIES

1. General Procedures

Calibration studies were performed using the demountable cells shown previously in Figure 6. For these studies, a matched pair of the cells were used. The cells consisted of two optically flat Irtran 2 (zinc sulfide) plates. On the outer portions of the bottom plate was deposited a 0.003 mm silver film which served as a spacer. Samples in all cases were added to the cells by placing a drop of the solution on the lower plate and then positioning the upper plate. In so doing, excess liquid was forced out of the cavity and no air pockets remained. For these analytical studies, a pair of such cells, equal in thickness to ± 2 percent were used; one containing the solvent alone was always placed in the spectrometer reference beam and the other containing the solution with sample to be studied was placed in the sample beam. All spectra were run on a Beckman IR 10 infrared spectrometer.

The saturated tetrasodium EDTA and KF solutions used were prepared by dissolving these materials in distilled water to saturation and storing the resulting solutions over an excess of the salt used.

Solutions of the salts of interest were prepared by dissolving known amounts of these materials in specified volumes of solvents. In the cases where water or saturated EDTA solutions were used, all of the materials dissolved with stirring. With KF solutions, on the other hand, special sample preparation consisting of grinding of the salt of interest into a highly divided powder before weighing had to be employed. Using the calcium salts of interest in all cases, the mechanism by which the ions of interest dissolve in aqueous KF can be expressed as:

$$\mathrm{Ca\,X(or\,X_2)_{(solid)}} + \mathrm{2KF_{(aq)}} \longrightarrow \mathrm{CaF_{2(solid)}} + \mathrm{2KX\,(or\,X_2)_{(aq)}}$$

where the added calcium salt dissolves and CaF_2 precipitates. This procedure appeared to be satisfactory, even in the cases of $CaCO_3$ and $CaSO_4$, probably due to the greater insolubility of CaF_2. In all cases, in preparing these solutions, about 2 days with stirring were allowed for this exchange reaction to be completed and the solutions were then filtered to remove the solid CaF_2. Analysis of this material after washing for the $CaCO_3$ solutions, showed the solid to be CaF_2 (i.e. carbonate free). After filtering, the solutions were then analyzed using procedures explained above.

In the data analyses, the absorbances at the band maximum for all cases were measured assuming the background over the band regions were linear. For all species except sulfite, this was found to be rigorously true. For sulfite, a linear but sloping background was generally seen. The position of the band maxima in the 3 solvents used for all of the species examined are given in Table III. Detailed procedures for each of the analyses to be treated in this report have been presented in a manual(9).

Table III Positions of Band Maxima Used in Calibration Curves for Species of Interest

	Solvent			
Species of Interest	H_2O	EDTA	KF	KF/D_2O
NO_3^-	1340 cm^{-1}	1340 cm^{-1}	1390 cm^{-1}	---
NO_2^-	1240 cm^{-1}	1250 cm^{-1}	1235 cm^{-1}	---
$CO_3^=$	$CaCO_3$ insoluble Na_2CO_3 1410 cm^{-1}	1440 cm^{-1}	1410 cm^{-1}	---
HCO_3^-	---	---	---	---
$SO_4^=$	1110 cm^{-1}	1110 cm^{-1}	1110 cm^{-1}	---
$SO_3^=$	920 cm^{-1}	925 cm^{-1}	940 cm^{-1}	---
HSO_3^-	---	---	950 cm^{-1}, 1050 cm^{-1} and 1195 cm^{-1}	---
OH^-	---	---	---	3400 cm^{-1} and 1610 cm^{-1}

It should be noted here that HCO_3^- and $CO_3^=$ were found to be not analyzable in the presence of each other due to problems of CO_2 pickup from the atmosphere and a high degree of band overlap. Nitrate and carbonate analyses were also found to interfere with each other due to severe overlap problems, such as are demonstrated in Figure 10 for the case of aqueous solutions. As can be seen, the two bands overlap over most of their expanses making separation into individual components almost impossible. As a result of these difficulties, a method for bicarbonate analysis could not be developed and the analyses for nitrate are valid only in the case of pure aqueous solutions, in which $CaCO_3$ is extremely insoluble.

For the other species of interest, i.e. $SO_3^=$, $SO_4^=$ and NO_2^-, no overlap problems were found to exist.

2. Results and Discussion

As was mentioned above, three solvents were used in these studies, saturated aqueous tetrasodium EDTA, saturated aqueous KF and pure water. Below are given the results for each.

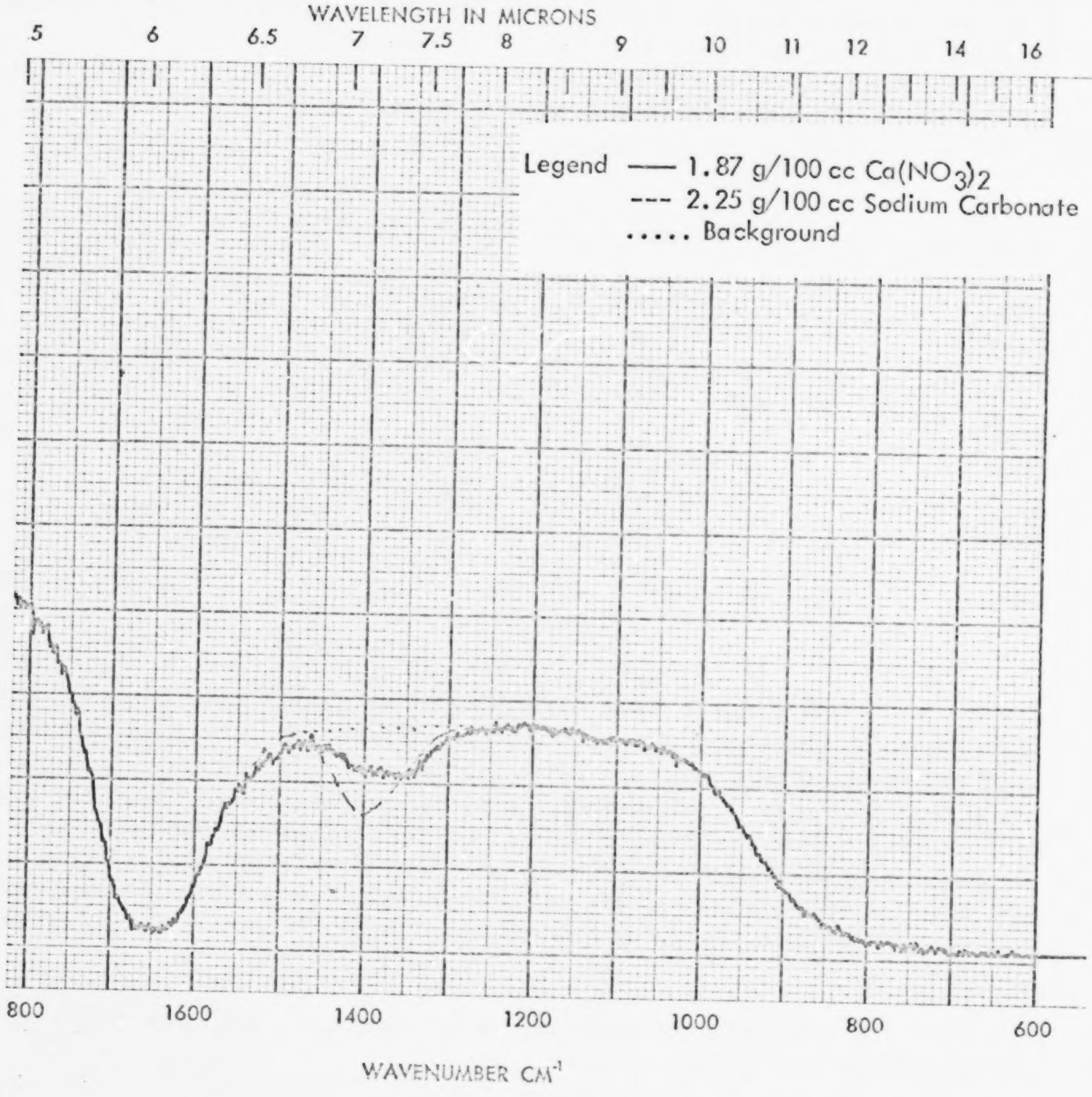

Figure 10. Spectra of NO_3^- and CO_3^- and Interferences Between Them

a. EDTA Solutions

Calibration curves, in concentration ranges of interest (0.1-3.0 g/100cc) were obtained for Ca $(NO_2)_2$, $CaSO_3$, $CaCO_3$, $CaSO_4$ and $Ca(NO_3)_2$ in saturated aqueous tetrasodium EDTA solutions using the dual cell technique with pure saturated tetrasodium EDTA solutions in the reference beam and using the matched cells and techniques described earlier. These curves are shown in Figures 11-15. As can be seen from Figures 2 and 3, very little scatter appears in these calibration data for sulfite and nitrite. Brief investigations of the pH dependencies of EDTA spectra, in addition, showed no pronounced pH dependencies at either 1250 cm^{-1} (nitrite) or 925 cm^{-1} (sulfite) such as were seen earlier for the sulfate case(7, 8).

Figure 13 shows the calibration curve obtained for sulfate at 1110 cm^{-1} as well as the calibration curve obtained earlier with the old AgCl cells and for that earlier work. As can be seen there is good agreement. The small differences seen are attributed to thickness differences of a few percent between the present Irtran 2 cells and the old set of AgCl cells.

Figures 14 and 15 show the calibration data for NO_3^- and $CO_3^=$ respectively. There is considerable scatter, particularly for the carbonate case, as was encountered in earlier work(9). Figure 16 shows a spectrum of EDTA at ca. pH 12. As can be seen, the most intense bands (aside from the 1660 cm^{-1} OH vibration are at 1405 and ~1330 cm^{-1}. The calibration curves for nitrate and carbonate, at their band maxima, were obtained respectively at 1340 and 1440 cm^{-1}. As a result of these conditions, any small mismatch in cells, small spacing error on assembling, etc. could give rise to appreciable scatter as the absorbances of EDTA at 1405 and 1330 cm^{-1} are quite large. As can be seen from Figure 16, this solvent absorption problem is worse for the 1405 cm^{-1} band, this accounts for all of the problems encountered in trying to develop an analysis method for $CO_3^=$ in EDTA.

b. KF Studies

After having solved the problems of obtaining reproducible solutions, calibrations curves were obtained in KF solutions for $CaCO_3$, $Ca(NO_3)_2$, $Ca(NO_2)_2$ and $CaSO_4$. The results are shown in Figures 17-21. As can be seen, in all of these cases good reproducible curves have been obtained. For carbonate and nitrite, no unusual effects were noted. For nitrate, however, interesting effects could be seen. As can be seen from comparison of Figure 19 with Figure 14, both the absorbance and position of the nitrate band appear to be different in KF. Thus, in this solvent the absorbance appears to be significantly higher, a fact which may prove beneficial in developing some specific analytical techniques. Also, the band maximum in KF solutions reproducibly occurred at 1390 cm^{-1} instead of at 1340 cm^{-1} where it was encountered in water and EDTA. The shape of the band, as shown in Figure 21, differs significantly from that in water in that it appears to be somewhat sharper. The spectrum of Figure 22 from 2000 to 1100 cm^{-1} was obtained using a single cell. The difference obtained for KF solution suggests some sort of specific interaction for NO_3^- in this medium. The

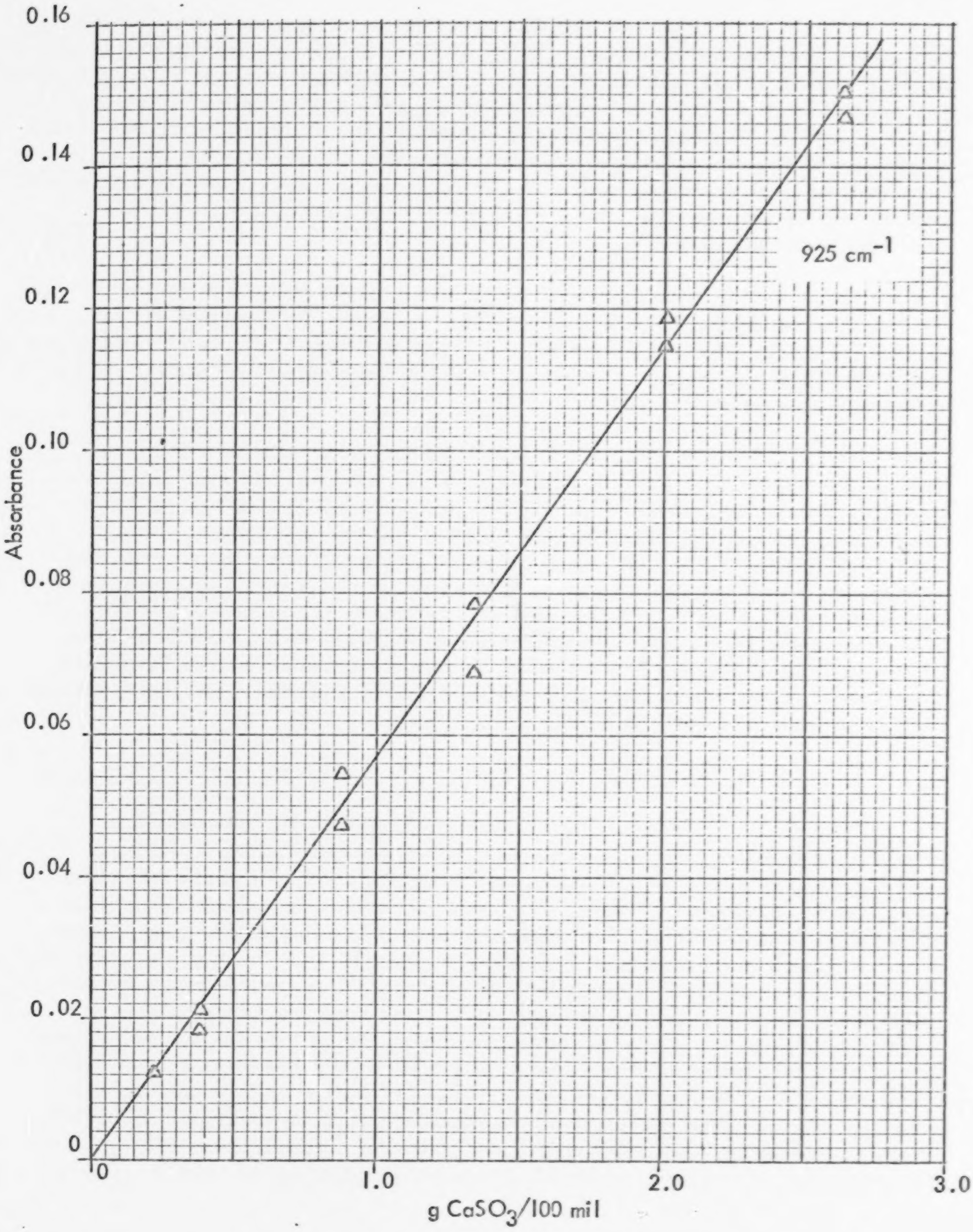

Figure II. Calibration Curve for Sulfite in EDTA

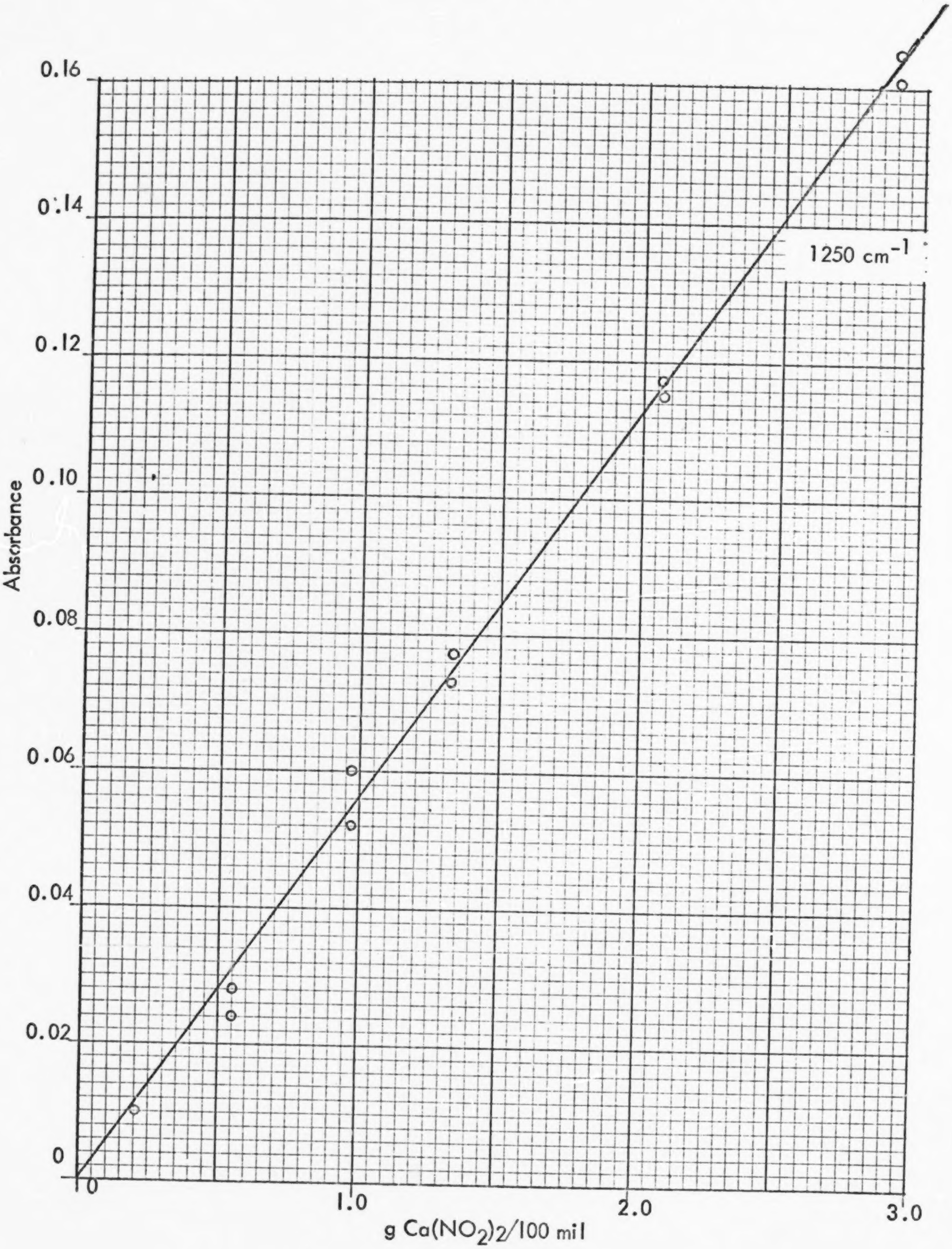

Figure 12. Calibration Curve for Nitrite in EDTA

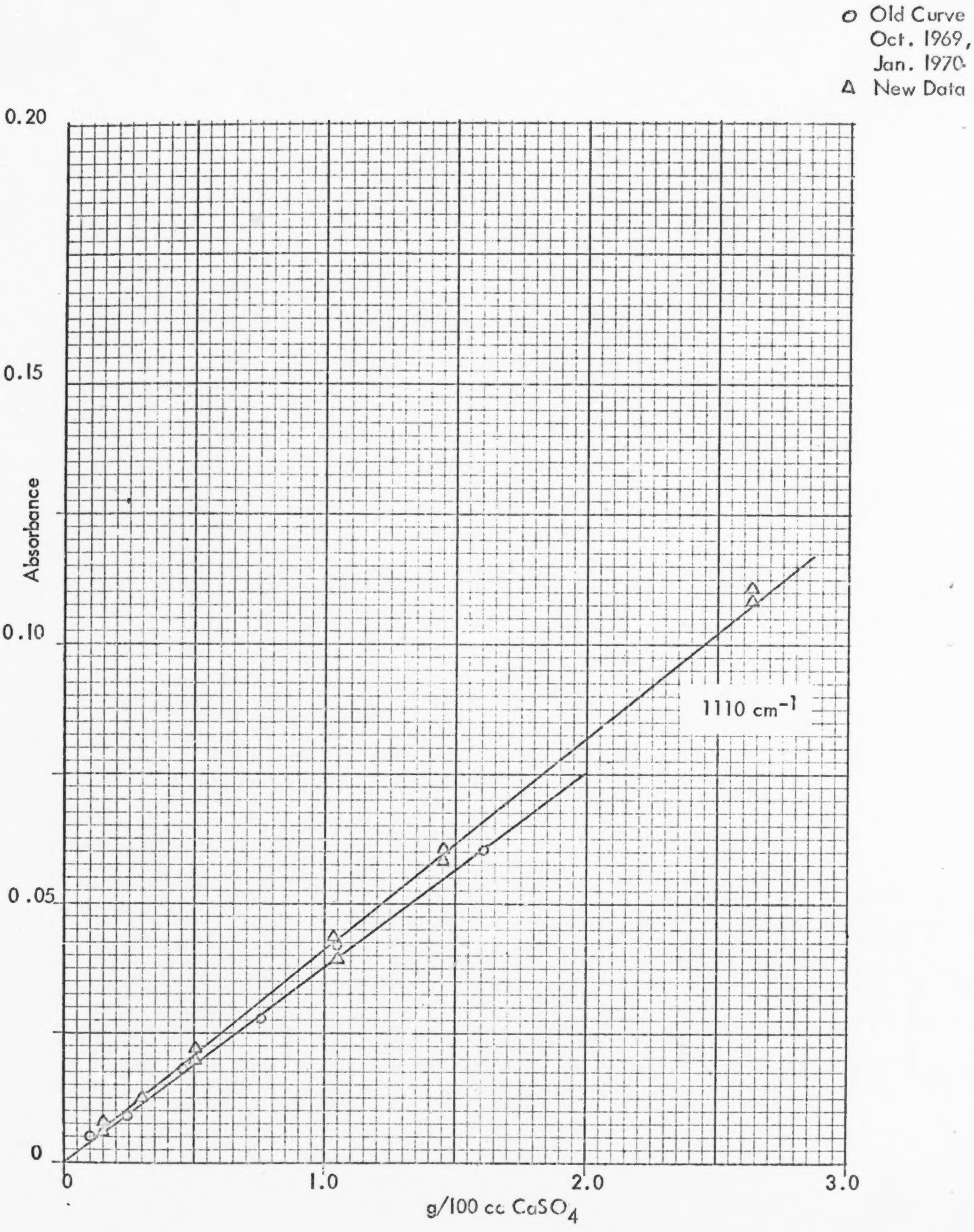

Figure 13. Calibration Curve for Sulfate in EDTA at 1110 cm^{-1}

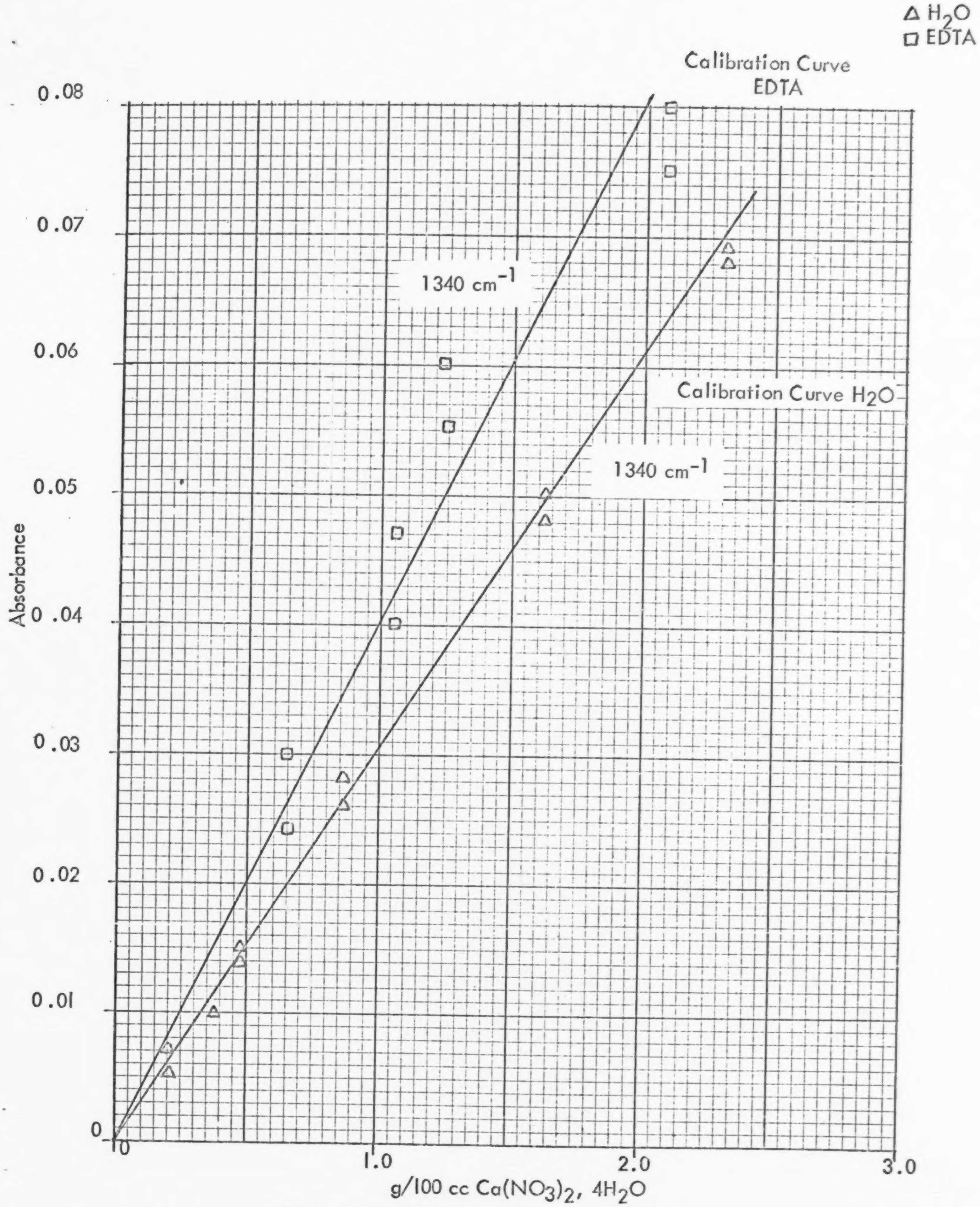

Figure 14. Calibration Curves $Ca(NO_3)_2$ -
in EDTA 1340 cm^{-1}
in H_2O 1340 cm^{-1}

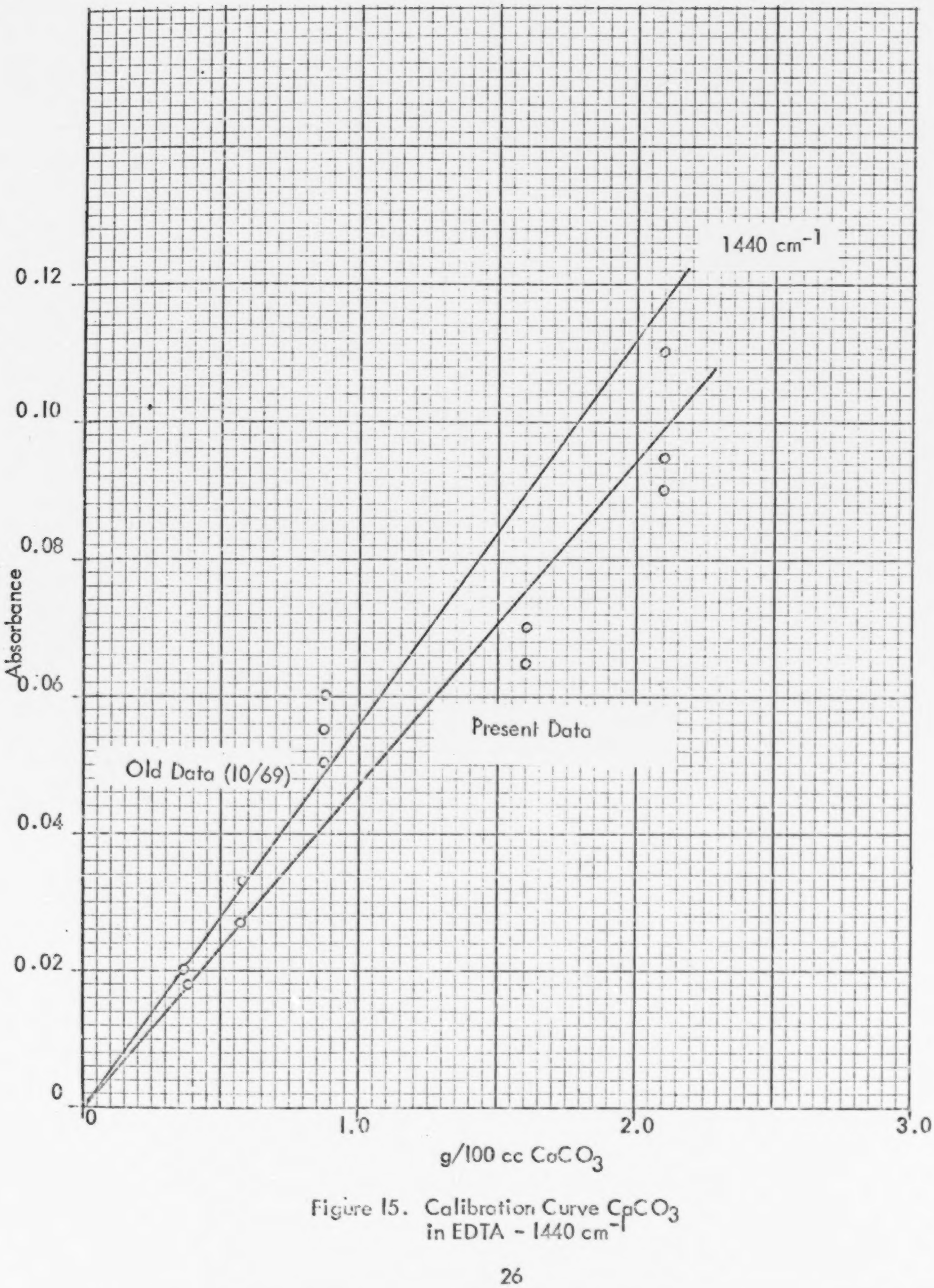

Figure 15. Calibration Curve CaCO$_3$ in EDTA - 1440 cm^{-1}

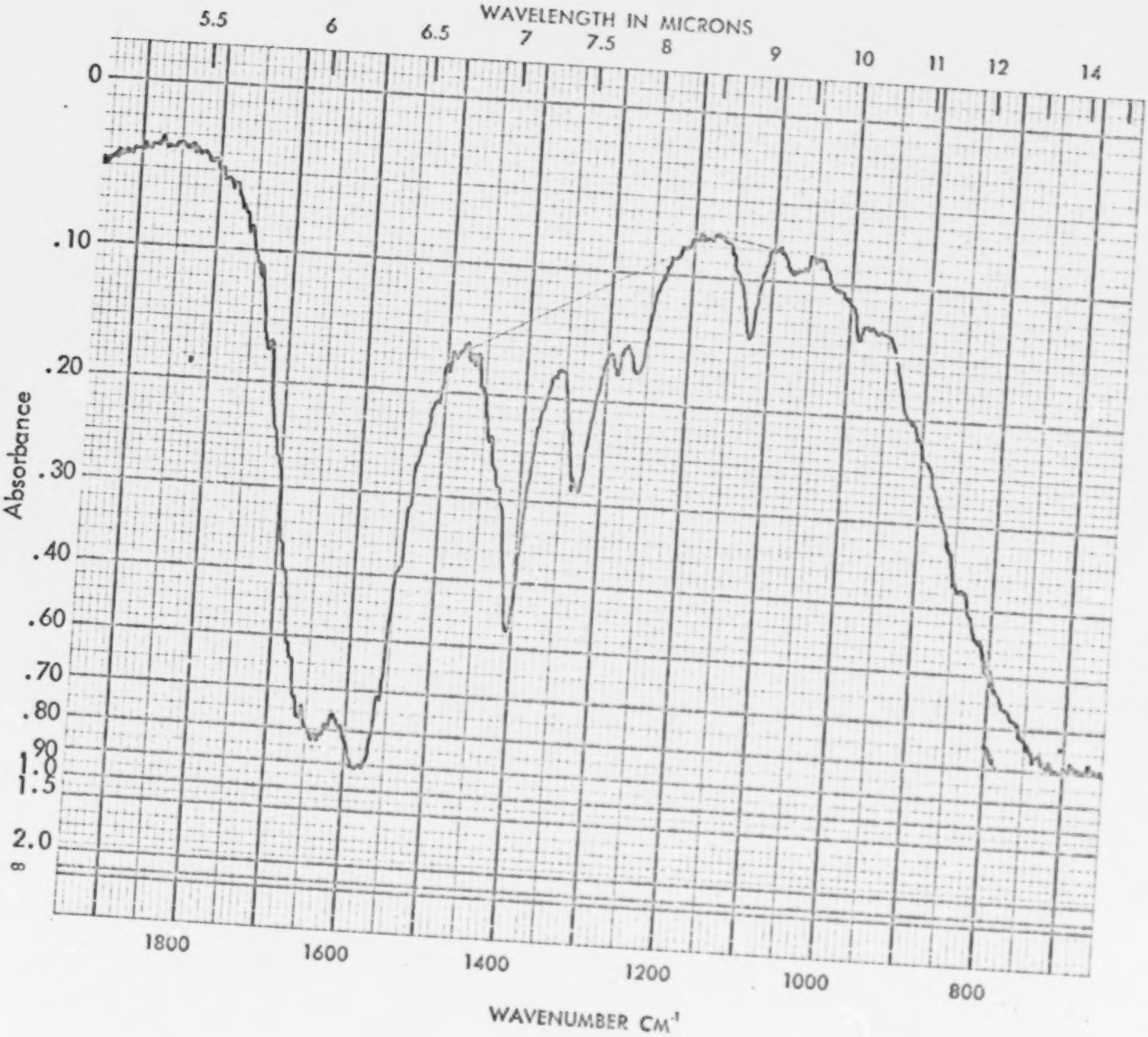

Figure 16. EDTA-pH 12.0

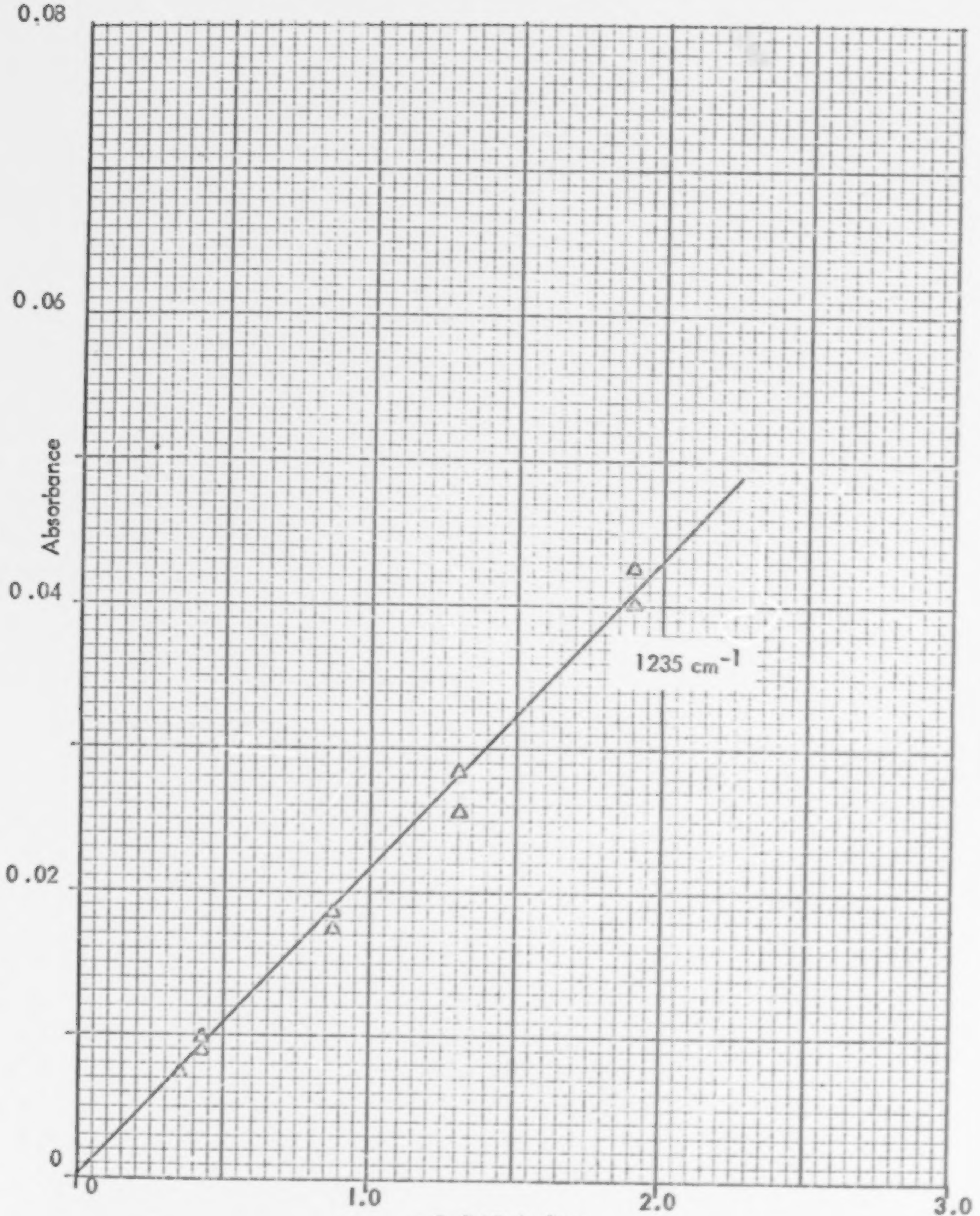

Figure 17. Nitrite--KF 1235 cm^{-1}

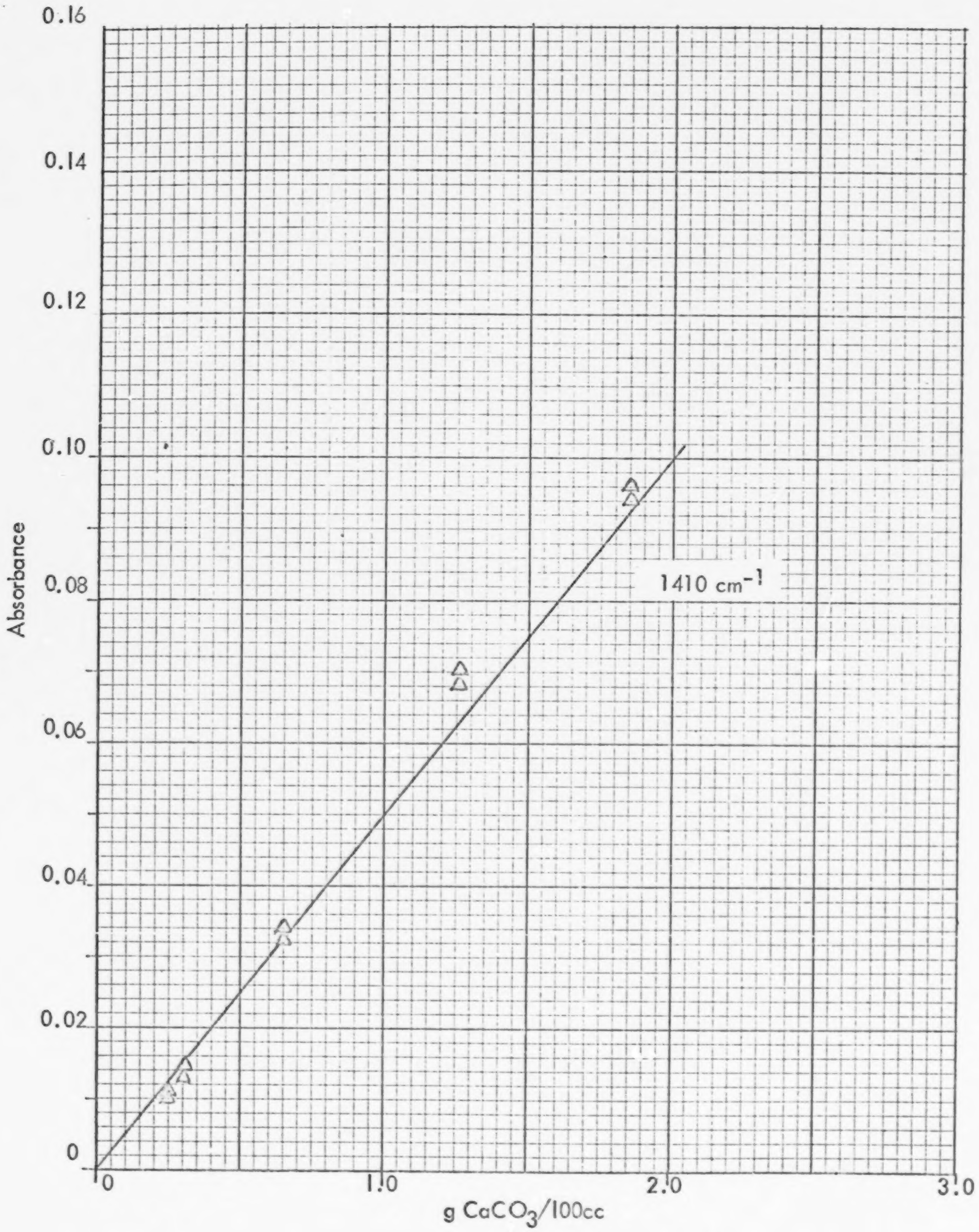

Figure 18. Carbonate - KF - 1410 cm^{-1}

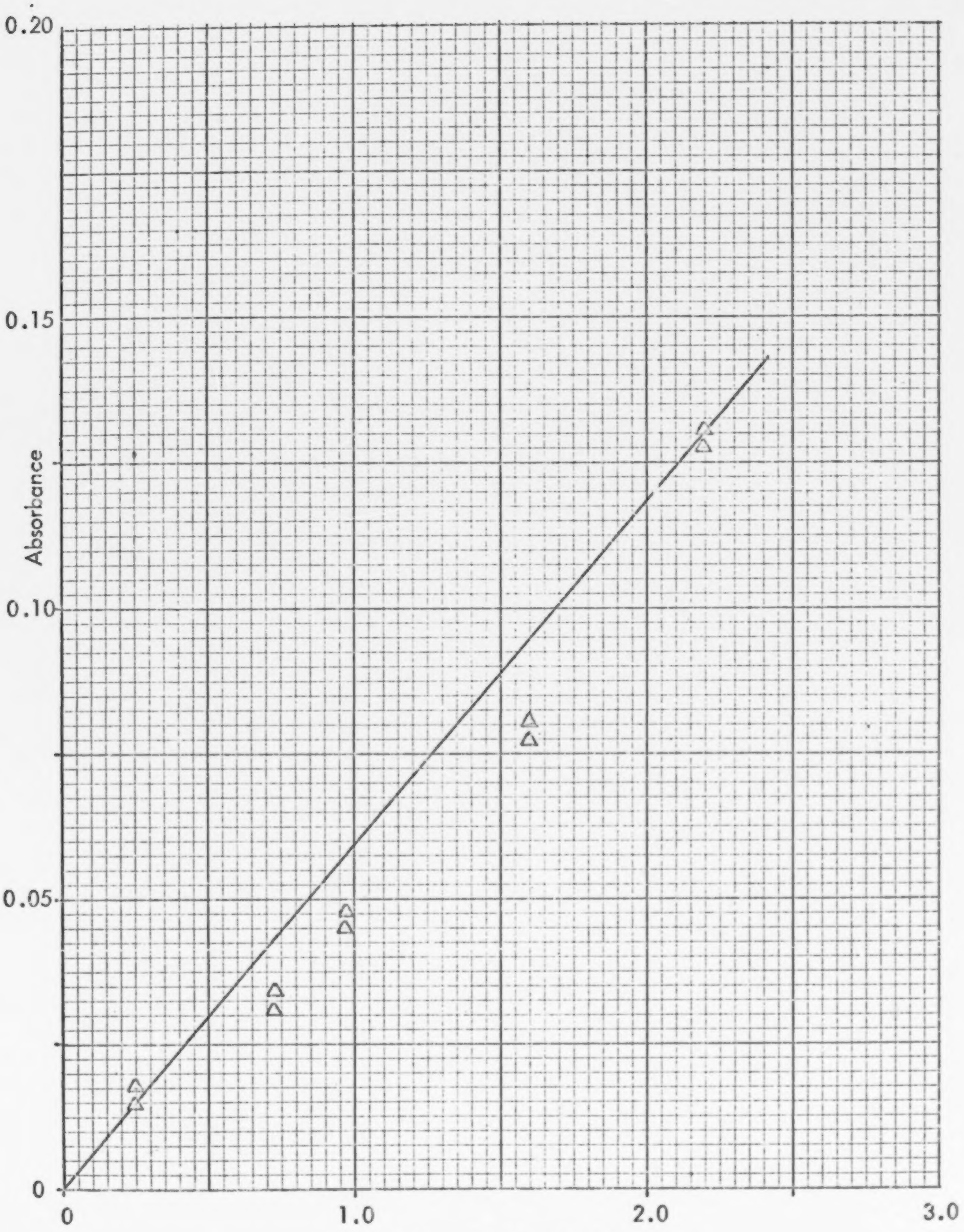

Figure 19. Nitrate 1390 cm^{-1} – Sat KF

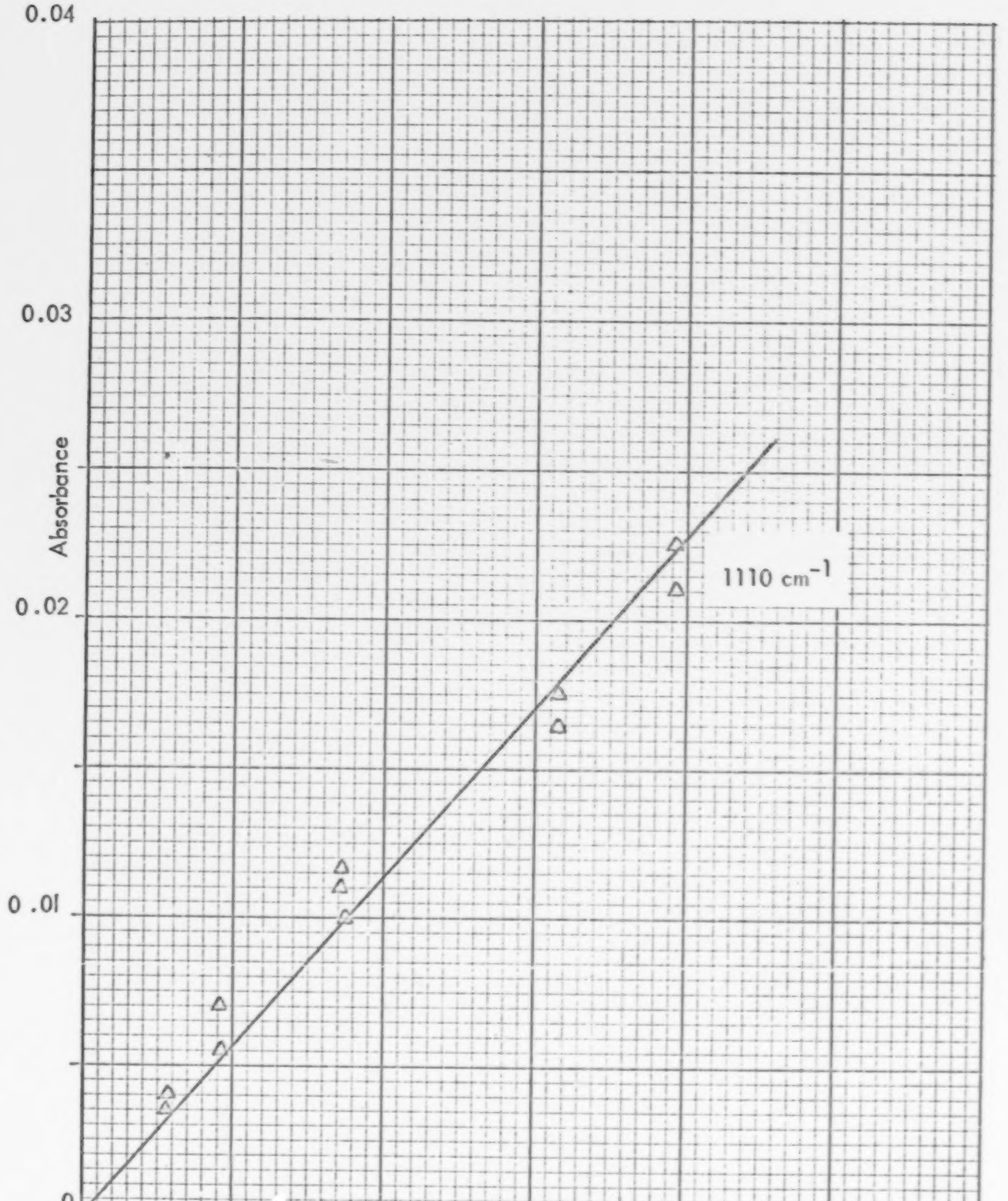

Figure 20. Sulfate - KF - 1110 cm^{-1}

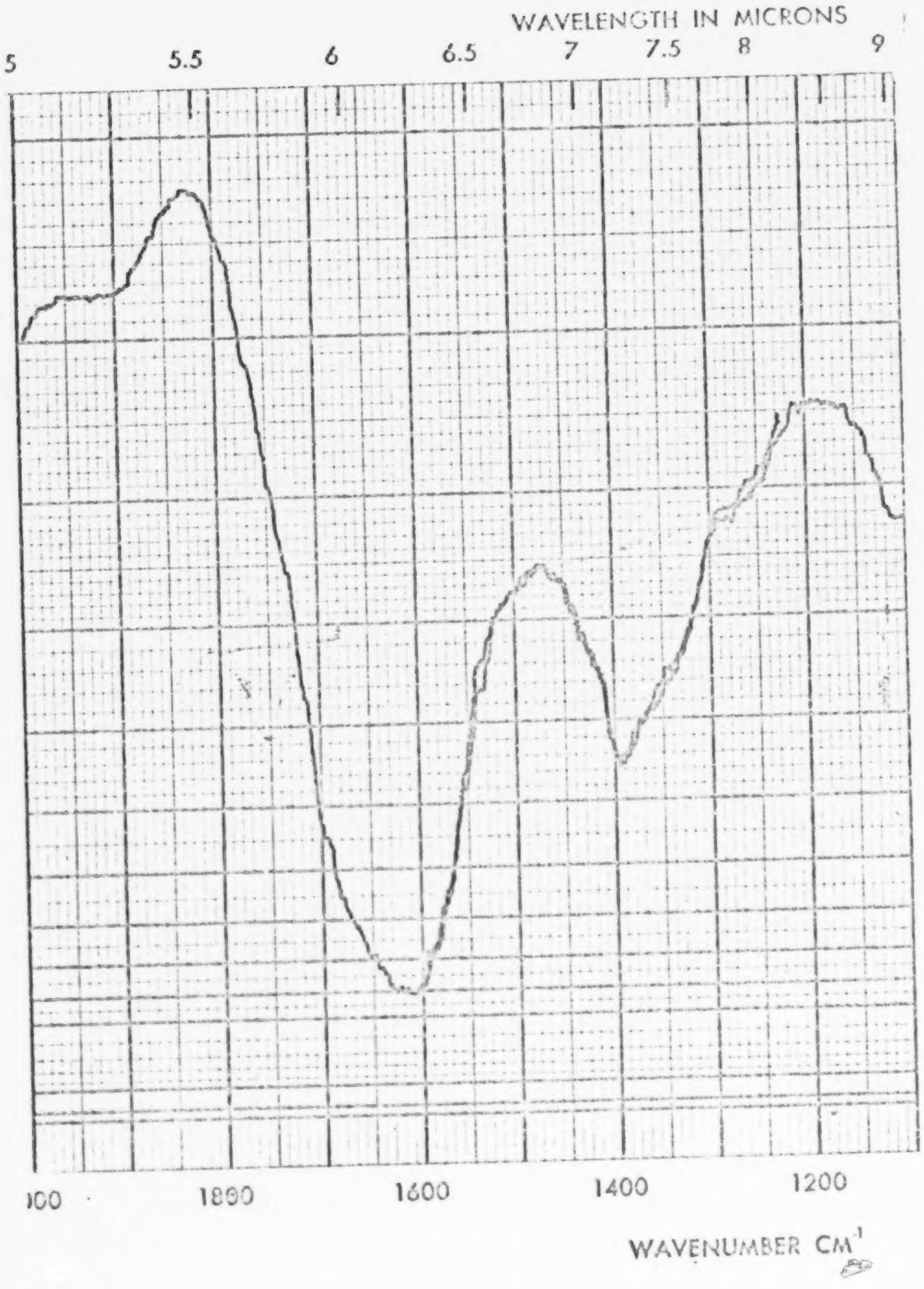

Figure 21. NO_3^- in KF

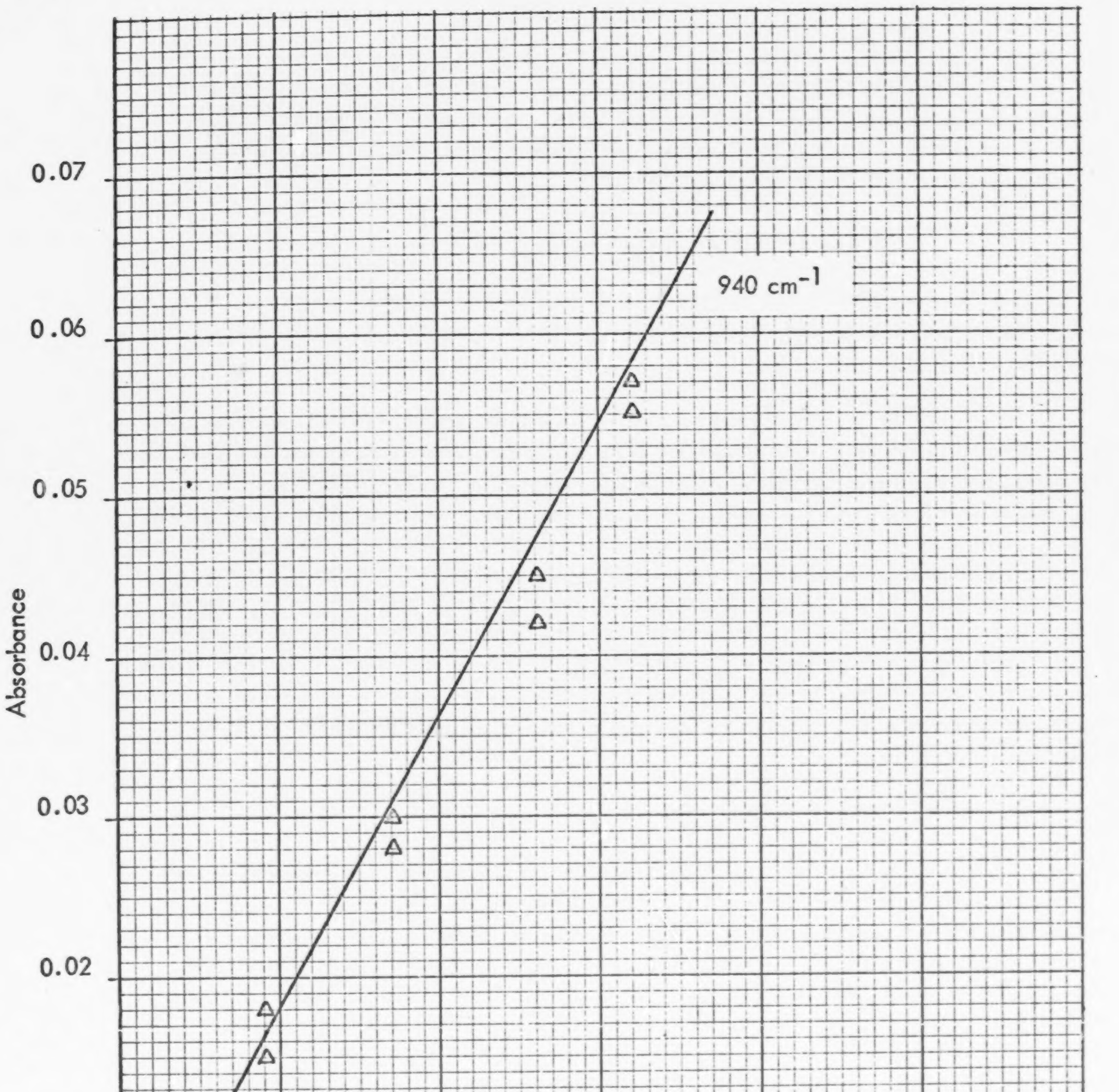

Figure 22. $CaSO_3$ - KF - 940 cm^{-1}

exact nature of this interaction is at present unknown; however the effect may prove to be beneficial in development of an infrared method for determination of low NO_3^- ion concentrations.

The results for $SO_4^=$, as can be seen from Figure 20, show a reproducibly lower absorbance in KF solutions than was encountered in EDTA. This lower absorbance is not due to insufficient time for equilibration as the same curve was generated for solutions standing for two days and for one week after mixing. The lower absorbance values suggest that the specific equilibrium:

$$2F^-_{(aq)} + CaSO_{4(s)} \rightleftharpoons CaF_{2(s)} + SO_4^={}_{(aq)}$$

does not lie as far to the right for the sulfate case as it does for the other species. This result can be taken to indicate that the KF solvent system is probably less useful for $SO_4^=$ than was EDTA.

Using saturated aqueous KF solutions, calibration curves were also obtained for $SO_3^=$ and HSO_3^-. The curve for $SO_3^=$ (940 cm^{-1}) in KF is shown in Figure 22. As can be seen, there is little scatter and reasonable absorbances. For HSO_3^-, as can be seen from Figure 23, there are three bands, for which calibration curves has been obtained. The 950 cm^{-1} band, by far the most intense, however lies in the same region as sulfite. As bisulfite is expected to be present in the slurries to be studied in concentrations far lower than sulfite, the 950 cm^{-1} band appears, in spite of its high intensity, to be useless for bisulfite analysis. The other two bands, at 1050 and 1195 cm^{-1} are of lower intensity but are in regions where no interferences by other species present are expected. Of these two bands, the 1050 cm^{-1} appears the more intense and should be used for analytical purposes. As can be seen from Figure 24, good reproducible calibration data has been obtained for all three HSO_3^- bands.

c. Pure Aqueous Solutions

Spectra were also obtained of the calcium salts of interest in pure water. The calibration curve for nitrate was shown in Figure 14. Figure 24 shows the curve for NO_2^- along with the curves from EDTA for comparison. There is little scatter and good reproducibility in the data obtained. One interesting feature which can be noted is that the absorbance ratio between EDTA and H_2O solutions of the nitrites and nitrates is ca. 0.74 (H_2O/EDTA) in both cases. The reproducibility of the data clearly shows that this is not an artifact and is probably due to differences in interactions of nitrate and nitrite ions with these two solvent systems. It would be of interest to see if such effects also exist for other ions in EDTA and water, however, the solubilities of the other calcium salts of interest ($CaCO_3$, $CaSO_4$ and $CaSO_3$) are too low in water to obtain similar data.

Calibration curves for $CaSO_4$, $MgSO_4$ and Na_2SO_4 in aqueous solution in the 0.01 - 1.0 g/100 cc concentration range were also obtained. For $CaSO_4$ due to solubility limits, only the lower portion of the concentration range could be studied. Figure 25 shows plots of absorbance vs. concentration for the magnesium and sodium salts. Figure 26 shows plots of the same data expressed as absorbance vs. concentration of $SO_4^=$.

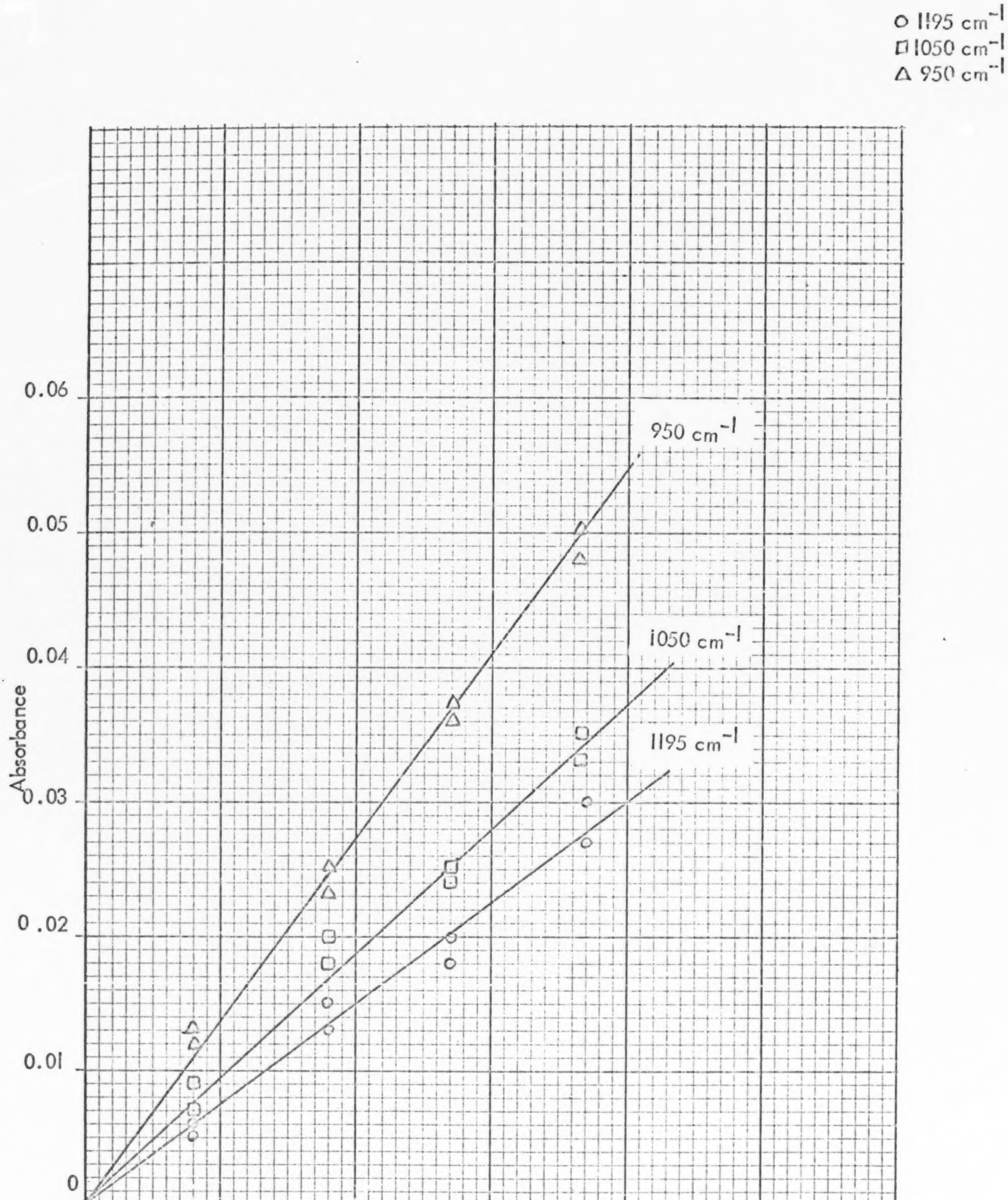

Figure 23. $NaHSO_3$ - KF

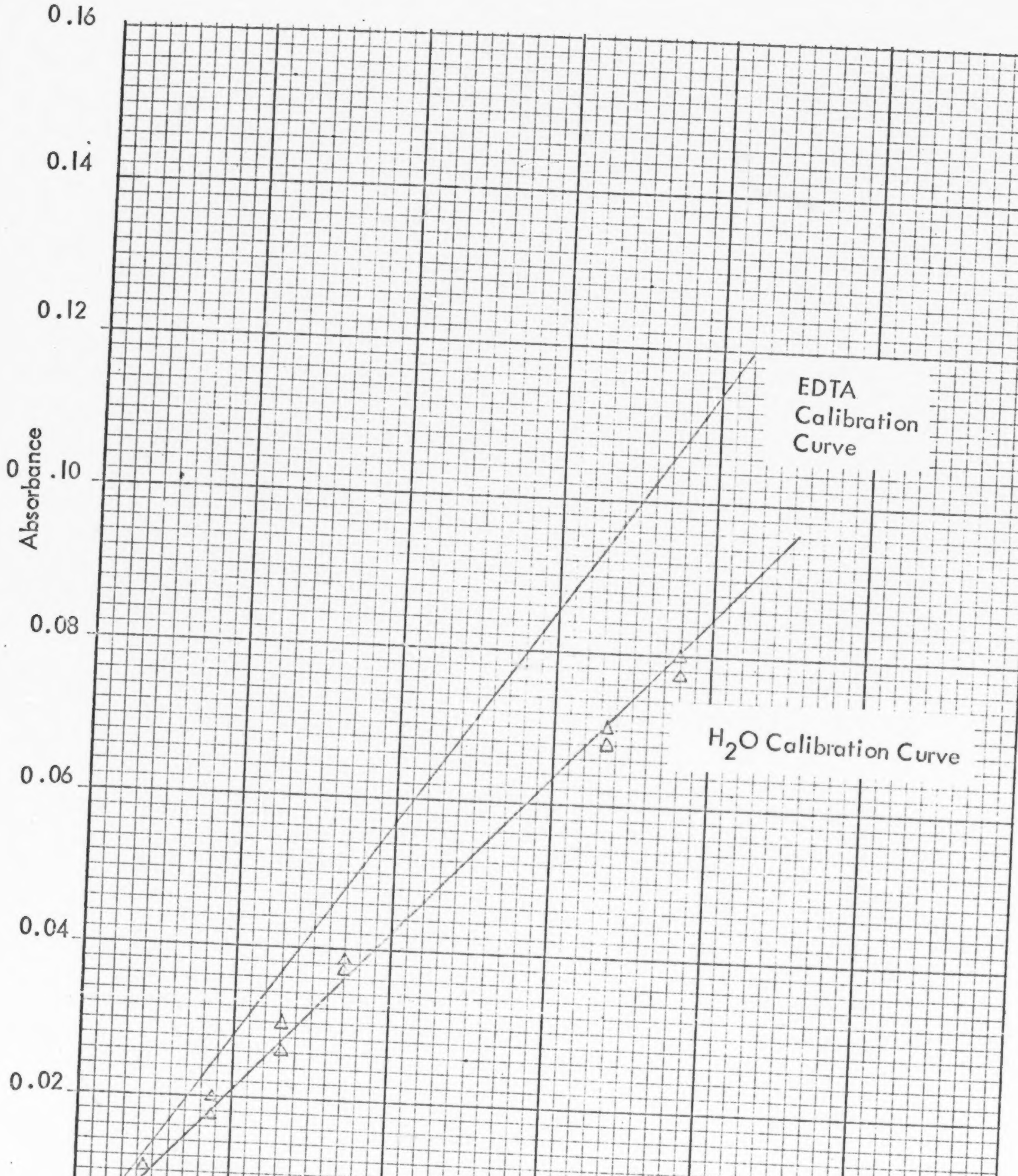

Figure 24. Calcium Nitrite - H_2O - 1240 cm^{-1}

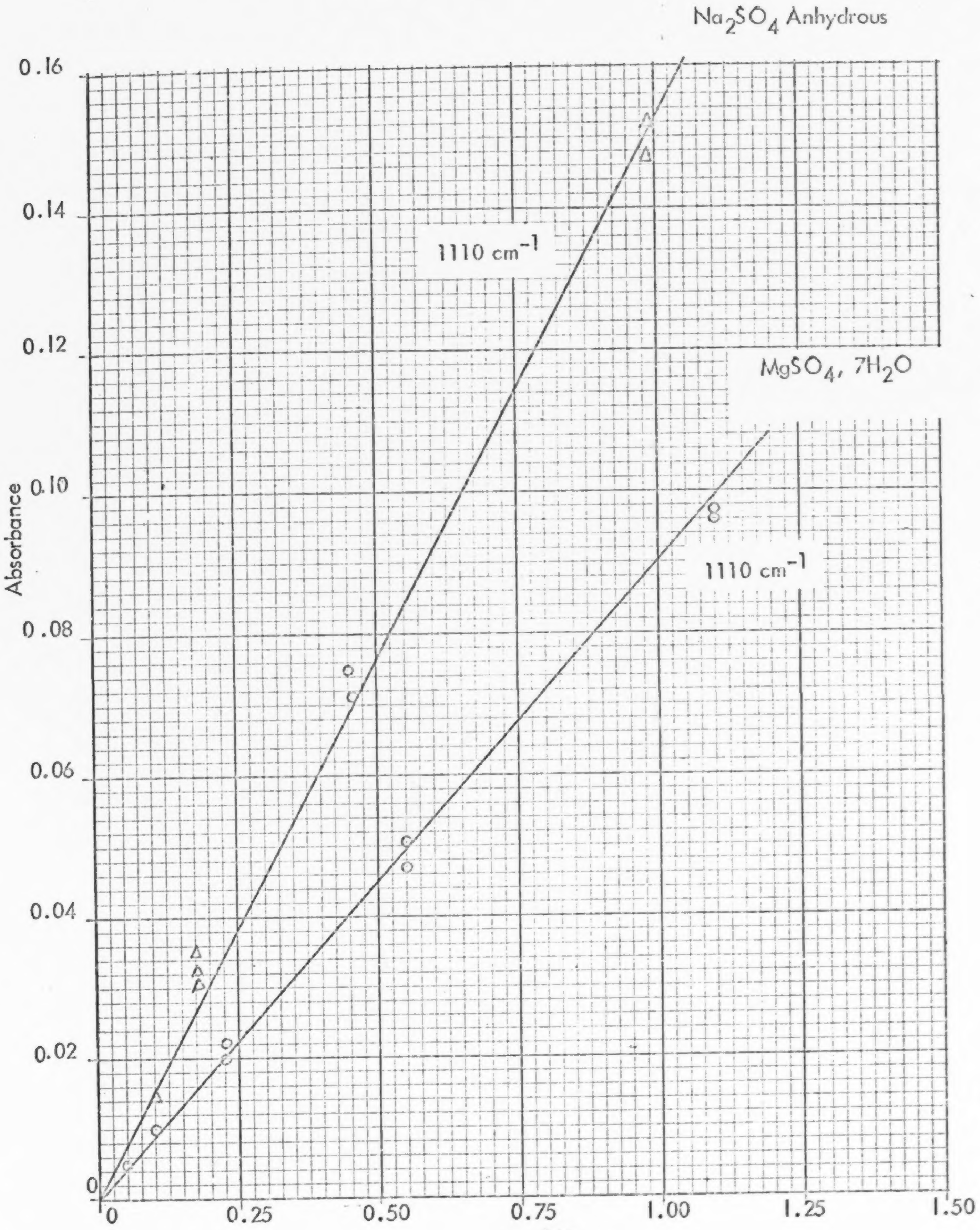

Figure 25. Calibration Curves for Sulfates in H_2O

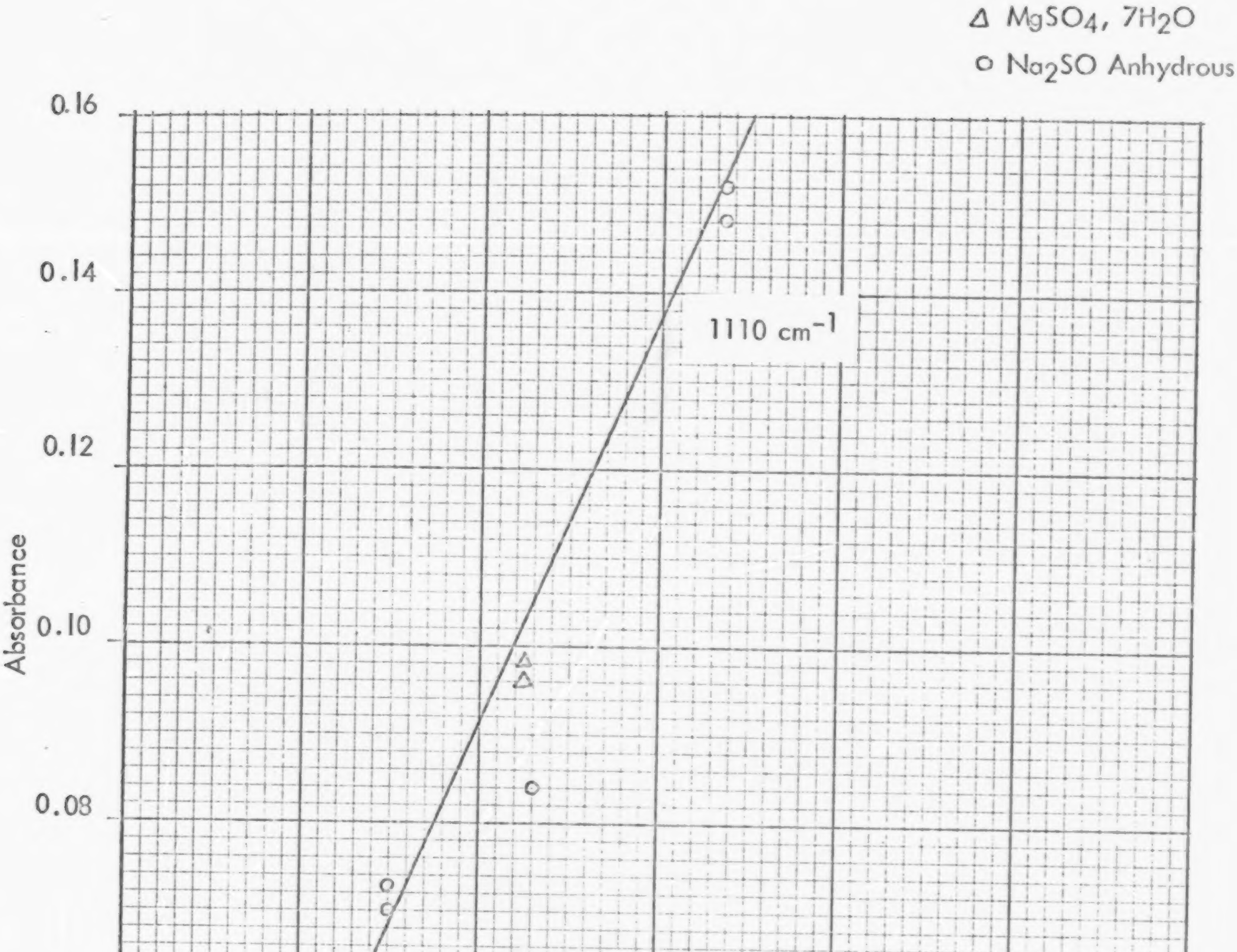

Figure 26. Calibration Curves for $SO_4^=$ in H_2O

The calcium data points (not shown) also fit this curve. The sulfate absorbance seems, in the concentration ranges studied and of interest, to be independent of the positive ions present.

Figure 27 shows a plot, for the same concentration range of absorbance (at 920 cm^{-1}) vs. concentration for $SO_3^{=}$. These values were obtained for calcium and sodium sulfites, and, as can be seen, at least for these two cases, the sulfite absorbance appears to also be independent of thepositive in species present.

d. Calibration for OH^- in KF Saturated D_2O

Calibration curves of OH^- in KF saturated D_2O were also obtained during this program. For this work, special precautions had to be employed to exclude pickup of H_2O, which would interfere in these studies. The following precautions were taken;

(1) The KF used for solution preparation was vacuum dried for 24 hours before use and was added to the D_2O under dry conditions in a glove bag with dry N_2 flowing.

(2) The $Ca(OH)_2$ used was also vacuum dried and was added to the KF saturated D_2O under inert conditions.

(3) The exchange reaction between $Ca(OH)_2$ and KF to yield CaF_2 and KOH occurred in the stoppered flasks with care being taken to minimize contact of the solutions with moist air.

(4) The cells were filled rapidly with the $Ca(OH)_2$ solutions in D_2O-KF and were washed with D_2O-acetone. All contact with water was avoided and the cells were assembled as rapidly as possible.

With the above precautions, good calibration data, as shown in Figure 28 were obtained for the 3400 and 1610 cm^{-1} OH bands. In cases where one or more of the above precautions were not employed, considerable scatter and nonreproducibility due to H_2O pickup resulted.

Unfortunately, this method of OH^- determination is expected to be of use only for dry solid samples. For slurries, where water is present in large amounts, such a technique is expected to be of little value.

3. Discussion of Calibration Studies

Analysis of the calibration results in the previous section was calculated

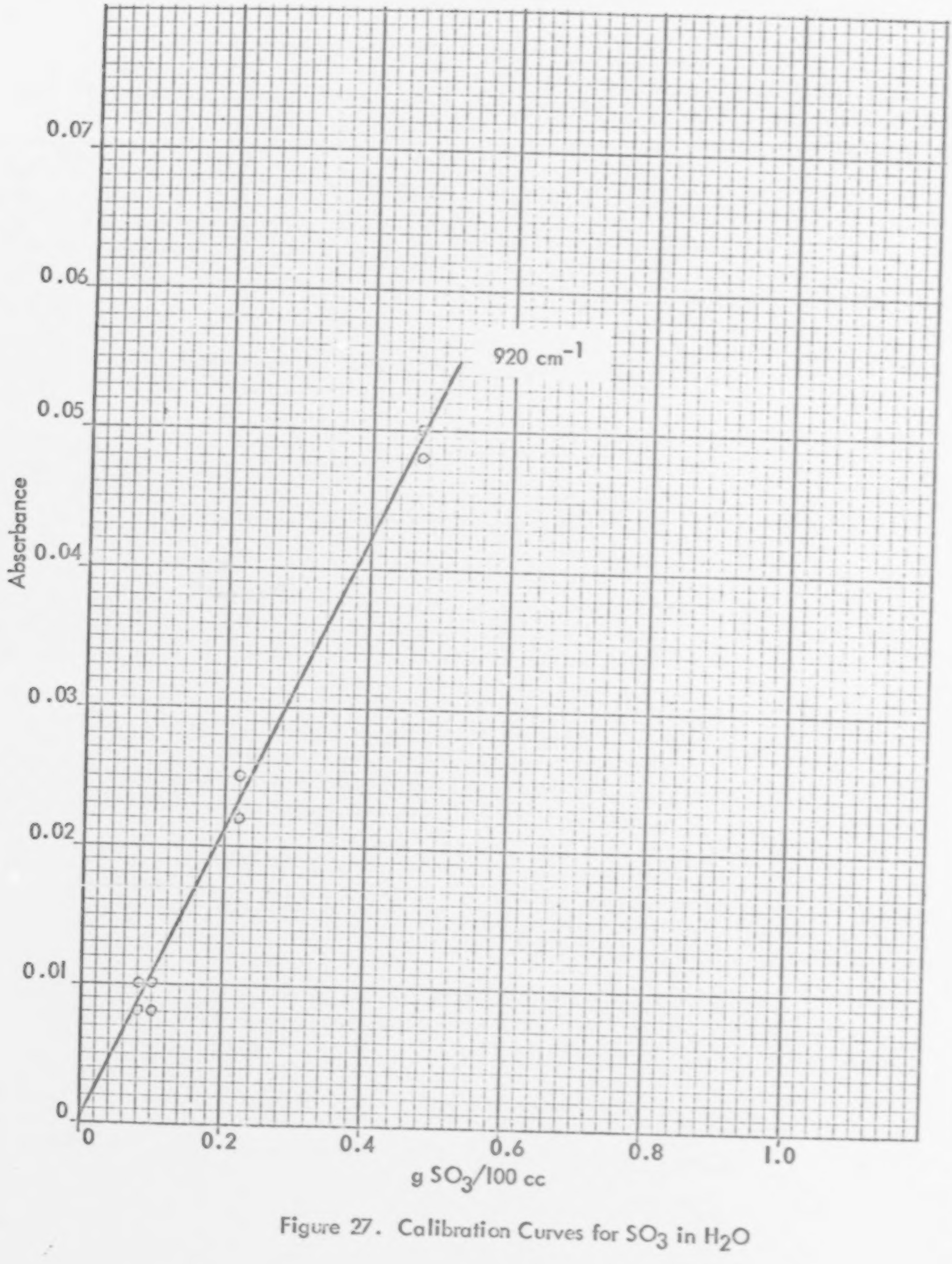

Figure 27. Calibration Curves for SO_3 in H_2O

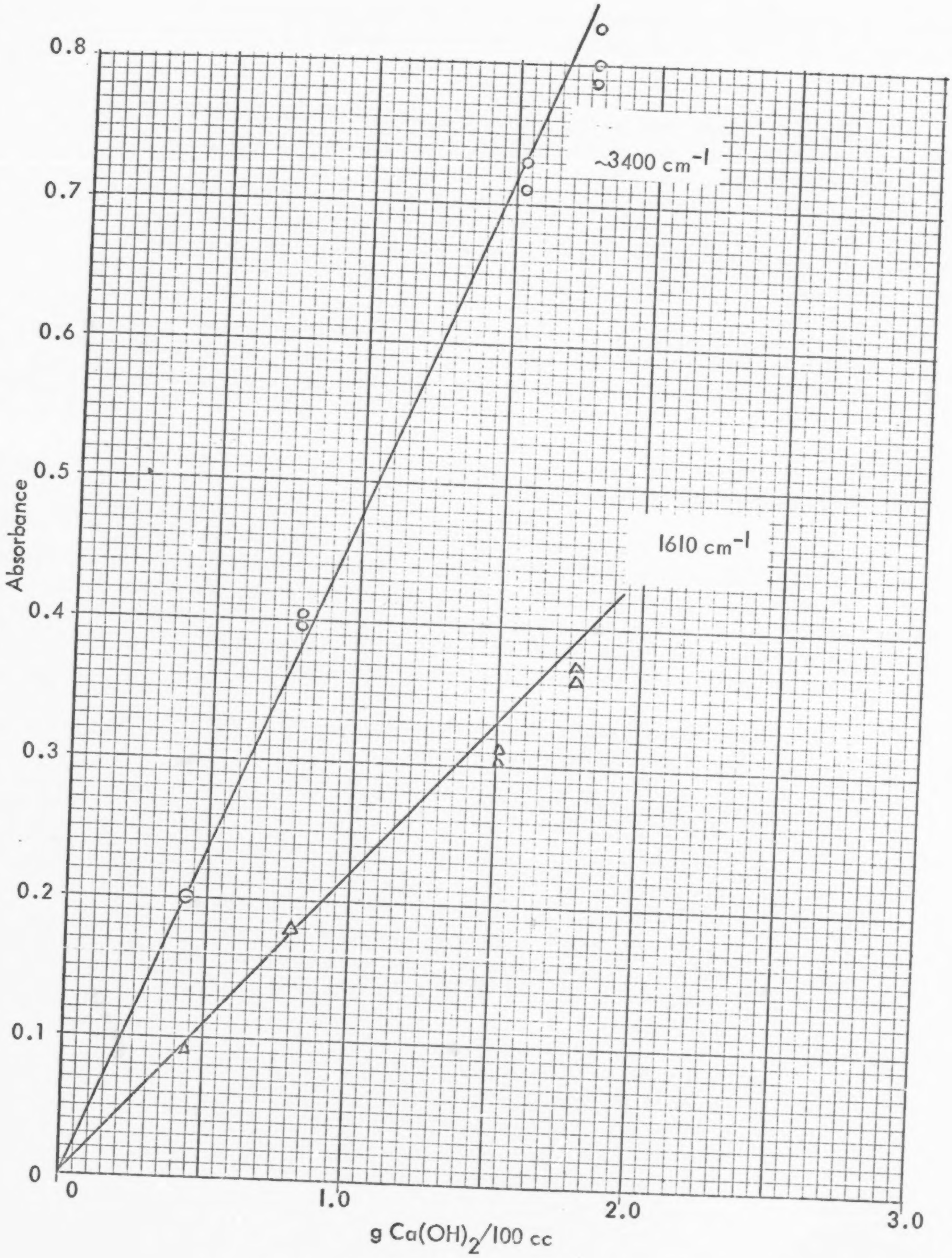

Figure 28. $Ca(OH)_2 - D_2O$ - Analysis for OH

with two aims: 1) to determine the minimum quantities of materials analyzable by the infrared thin film cell method and 2) to determine which solvent systems are most suited for specific analyses.

Using the approaches developed in earlier studies(7, 8), an effort was made to determine the minimum concentrations which could be analyzed in aqueous solution using the various techniques presented earlier in this report. With a background absorbance variation of ca. ± .003, the limit for sulfate with the instrumentation available to this program appeared to be $\sim 2 \times 10^{-4}$ g/ml. For sulfite a value of about 4×10^{-4} g/ml $SO_3^=$ was found. For nitrate and nitrite, minimum values of 0.001 g/ml and 0.0015 g/ml respectively were found.

It should be noted here, that these values are related to equipment used for these studies only. For other spectrometric equipment in which better control of background noise is possible lower levels should be achievable. Also, the above values are for a cell of 3 microns in thickness. As it is possible to study aqueous solutions in cells of thicknesses up to ~10 microns, use of somewhat thicker cells (~6-7 microns) could act to further lower minimum observable concentrations. Using a more intense spectrometer infrared source, also may aid in detecting and measuring lower concentrations.

In passing, it may also be pointed out that the choice of solvent may aid to a small degree in some cases in increasing the extinction coefficients (absorbances). In earlier work, it was reported, for example, that in saturated EDTA solutions, the absorbances of NO_3^- and NO_2^- were ~20% higher than in water. Comparison of the sulfate data reported above with that found earlier, however does show such a large effect for sulfate indicating that such effects may vary from ion to ion to some degree.

All of the calibration studies conducted are summarized in Table IV. By simple inspection, the following conclusions can be drawn:

a. For EDTA Solvent Systems

(1) Analysis for nitrite and sulfite should be straightforward with no need for pH corrections as there are no pH dependent EDTA bands at either 1240 or 920 cm^{-1}. Method limitations (which may depend on instrument noise level, scale expansion accessories available, etc.) should be $\sim 5 \times 10^{-4}$ g/ml for a 3 μ cell using present equipment.

(2) Analysis for carbonate and nitrate is not advisable using EDTA because of intense solvent peaks at frequencies close to those of absorption bands of interest. This overlap leads to considerable scatter in the calibration data and, hence, considerable errors are expected.

Table IV Solvent Systems for Limestone Analyses

Ion	Solvent System			
	EDTA	KF	H_2O	D2O/KF
$SO_3^=$	satisfactory no pH corrections needed	satisfactory no corrections needed	insoluble calcium salt, otherwise satisfactory	---
HSO_3^-	no good - solvent alkaline	satisfactory no corrections needed	insoluble calcium salt, otherwise satisfactory	---
$SO_4^=$	satisfactory with pH corrections	satisfactory but absorbances lower than for EDTA case	insoluble calcium salt, otherwise satisfactory	---
NO_3^-	large scatter due to EDTA absorption band	satisfactory in absence carbonate	satisfactory	---
NO_2^-	satisfactory no pH corrections needed	satisfactory	satisfactory	---
$CO_3^=$	large scatter due to EDTA absorption band	satisfactory in absence of nitrate	insoluble calcium salt	---
HCO_3^-	no good solvent alkaline	no good - problems with uptake of ambient CO_2 by alkaline solutions	insoluble calcium salt	---
OH^-	impossible - solvent water based	impossible - solvent water based	impossible - solvent water based	satisfactory in absence of H_2O

(3) Analysis for HCO_3^- and HSO_3^- are not possible with the EDTA solvent due to its intrinsic alkalinity.

(4) Analysis for $SO_4^=$, as was shown in an earlier study can be conducted with an EDTA solvent provided corrections are made for pH change effects. The magnitudes of these corrections as a function of pH have been reported earlier.

b. For Analysis In Pure Aqueous Solutions

All of the calcium salts except the nitrate and nitrite are reasonably insoluble in pure H_2O. For the extremely insoluble materials, analysis in H_2O solution is obviously not possible. For nitrate and nitrite, which possess high solubility, analysis can be readily conducted. This vast difference in solubilities can be used for selective analysis for the nitrate and nitrite contents of reacted slurries. As carbonate is extremely insoluble, the liquid phases should contain all of the $CO_3^=$ present. Hence, filtering of the solutions followed by IR analysis of the liquid phase should give the total nitrate and nitrite contents. As sulfite and sulfate are only slightly soluble, only lower concentrations of these species in water can be determined. As the solubilities of these materials are .003 g/ml, water is expected to be useful as a solvent only in the .0003-.003 g/ml.

c. For Analysis In KF Solutions

(1) For analysis of nitrite, nitrate, bisulfite and sulfite, saturated KF solution is quite satisfactory. For sulfate, while the absorbances per unit concentration are smaller than in EDTA, no corrections have to be made for pH effects. However, as determination of small amounts of sulfate appears to be of great interest, EDTA, with the needed pH correction appears to be more useful than KF.

(2) For bicarbonate, due to pH effects on dissolution of other constituents or absorption of CO_2 from the air on handling of the solutions, accurate analysis does not appear feasible.

(3) For total carbonate (bicarbonate and carbonate), analysis in KF appears promising provided nitrate is absent. Due to the vast solubility difference between $Ca(NO_3)_2$ and $CaCO_3$ in water, analysis of the water insoluble solids in KF solution appears to be a feasible method, as discussed above, for $CO_3^=$ analysis.

d. For Analysis In D_2O/KF

Solid phase dry hydroxides can be determined by this method. For solutions or slurries, however, this approach is not suitable.

In summary:

EDTA is the preferred solvent for sulfate analysis of solids.

Pure water is preferred for nitrate and nitrite and for sulfate and sulfite already in aqueous solution.

KF solution is preferred for the other species.

4. Quantitative Analyses

The thin film cells developed under this program were demonstrated to APCO personnel at the Fairfax facility. There a matched pair of cells were used to obtain spectra of a number of solutions obtained under varying conditions from the wet scrubber in operation. The scrubber in use employed a simulated flue gas, which, for some of our studies contained only SO_2 and no nitrogen oxides. In a few runs, NO_x was briefly added. For these, however, no nitrate or nitrite in measurable (i.e. greater than trace) quantities could be seen, probably because insufficient time had been allowed for a buildup of these species in the scrubber solutions.

Spectra were run on several filtered or centrifuged scrubber solutions, free of suspended matter and the results have been analyzed at GTC. These are given in Table V. All of the samples, except the 10:00 a. m. sample seem to depict a general trend of sulfate increase with time (the table gives the samples in the order in which they were obtained). The reason for the different behavior of the 10:00 a.m. sample is not understood.

It should be pointed out here that the evaluation of the data was based on calibration curves obtained with a different set of cells and different spectrometer (at GTC). However, errors arising from cell thickness differences and differences between spectrometers should be fairly small (as was demonstrated for NO_3^- calibration curves obtained at APCO and amount to ~10 percent or less.

It should be noted that none of the above solutions studied were found to be saturated in $CaSO_4$ (solubility of ~0.3 g/100 cc). The highest sulfate values reported

Table V Analysis of Scrubber Solutions

APCO Designation (sample)	Species	Concentration (g/100 cc)	Comments
9:50 a.m.	NO_3^-	0	No NO_x used in scrubber
	NO_2^-	0	
	$SO_4^=$	<0.02 g/100 cc	
	$SO_3^=$	0.2 g/100 cc	
9:55 a.m.	NO_3^-	0	
	NO_2^-	0	No NO_x used in scrubber
	$SO_4^=$	0.10 g/100 cc	
	$SO_3^=$	0.08 g/100 cc	
10 a.m.	NO_2^-	0	
	NO_3^-	0	
	$SO_4^=$	<0.02 g/100 cc	
	$SO_3^=$	~ 0.2 g/100 cc	
4	NO_2^-	0	NO_x in flue gas
	NO_3^-	0	
	$SO_4^=$	0.16 g/100 cc	
	$SO_3^=$	0.08 g/100 cc	
5	NO_2^-	0	NO_x in flue gas
	NO_3^-	0	
	$SO_4^=$	0.14 g/100 cc	
	$SO_3^=$	~ 0.04 g/100 cc	

above (as $SO_4^=$) correspond to ~ 0.23 g/100 cc $CaSO_4$. Unfortunately, none of the results in Table V were checked by other methods of analysis.

To further check the methods of analysis developed on this program, an analysis for nitrate and nitrite were performed on a second set of samples from a wet scrubber provided by APCO. From the infrared method values of .018 g/ml and 5×10^{-4} g/ml were obtained respectively for the NO_3^- and NO_2^- contents. Analyses of the same samples by ultraviolet spectroscopy gave values of .020 g/ml for nitrate and 4×10^{-4} for nitrite in good agreement with the infrared values. No further checks were run due to a lack of samples containing nitrate and nitrite in the concentration range to which the infrared method is applicable.

To summarize the analytical studies performed under this program, it can be pointed out that a simple cell has been developed for measurement of concentrations in aqueous solutions of species such as NO_3^-, NO_2^-, $SO_4^=$ and $SO_3^=$ in the .0002-.02 g/ml concentration range. Using simple band intensity (absorbance) measurements, meaningful calibration curves for species of interest can be obtained and using more sophisticated band area integration methods greater accuracy may be achievable using the methods developed.

C. DEADBURNING STUDIES

1. Introduction

The dry and wet limestone processes for sulfur dioxide removal from flue gases offer a number of advantages based on their low cost and simplicity of operation. However in certain cases a number of problems have been found which are related to incomplete reaction of the limestone. One of the possible causes of this incomplete reaction is the phenomenon called deadburning, wherein the calcined limestone becomes relatively inactive toward either hydration or chemical reaction due to either collection of impurities at its surface or to a large loss of surface area and porosity.

A number of studies have been made of the deadburning phenomenon; however, much disagreement still exists as to the importance of several of the variables involved. Thus, while some authors have related reactivity to pore volumes and surface areas available for reaction(10-12), others have stressed the possible influences of various solid state reactions which can occur with impurities during calcination. Impurities such as SiO_2, Al_2O_3, FeO_3, phosphates, sulfates and potassium and sodium salts are known to differ widely with sources(13) and it is known that above 1750°C reactions between CaO and SiO_2 do occur which result in the formation of surface silicates. Indeed, it has been found that limes high in silica may react with water like hard burned (i.e. low surface area) materials even though extensive sintering did not occur(14).

An extensive study of the pyrochemical reactions occurring in impure limestone has been conducted by Lee(15). With increasing calcination temperature several reactions occur including formation of silicates, ferrites and aluminoferrites, all of which lead to inert materials which, at high temperatures, melt and diffuse readily to the surface cuasing particle shrinkage and reduction in porosity. On cooling, it has been found that these materials particularly the ferrites, crystallize on the surface providing a barrier against reaction(15). Thus, it is conceivable that part of the deadburning problem can be traced to formation layers of inert materials over portions of surfaces. An earlier infrared study has, indeed shown that higher calcination temperatures result in formation of complex silicates, but did now show where with respect to the surface such silicates were located(8). This report presents a more detailed study using a combination of infrared spectroscopic, electron microprobe and Auger spectroscopic methods which attempts to assess some of the reactions with impurities which occur during the calcination process and to determine the degree of diffusion of impurities to the surface at different calcination temperatures.

2. Experimental

The six series of limestones used in this study were supplied by the Office of Air Programs, Cincinnati, Ohio. These samples were calcined at the specified temperatures or specified times, (generally two hours unless noted otherwise), in a rotary kiln under inert atmosphere. The samples consisted of an Iceland Spar, an Aragonite, a pure dolomite, a pure limestone, an iron rich dolomite and a silica rich dolomite. A detailed petrographic and minerological description of these samples is given by Harvey(16), who also studied their activities for SO_2 adsorption. The compositions of these materials are given in Table VI, where the type numbers are the same as those used by Harvey(16).

Spectra were run on the various samples using the KBr pellet technique. Specifically, all sample pellets were prepared under inert atmosphere using a glove bag arrangement with flowing dry nitrogen. During running of the spectra, the sample compartment of the spectrometer was purged with dry nitrogen to prevent uptake of CO_2, H_2O or other contaminants by the samples. Pellets contained from 1-5 weight percent calcined limestone and were prepared by mechanically mixing the limestone with KBr powder in a Wig L Bug for 30 seconds. The resulting mixtures were then pressed into pellets and spectra run. All spectra were recorded with a Beckman IR 10 spectrophotometer using the double beam mode and slow scan speed.

For microprobe studies, the experimental procedures consisted of making disk type samples in degassed epoxy resin, allowing the resin to cure and polishing the disk with diamond until flat cross sections of a number of limestone particles were observed. Care was taken in these steps to avoid contamination of the surfaces with either silica, alumina or iron compounds. The disks were then taken, coated with carbon and inserted into the microprobe apparatus and line scans across individual particle cross sections for iron, silica and aluminum were run on a number of individual particles for each sample. For some runs, scanning electronmicroscope photographs of the microprobe traces were taken and correlations were then made from these between physical phenomena such as pores, discrete phases, etc. and impurity maxima or minima.

Line analyses for silicon, iron and aluminum were run on cross sections of several particles of each of the 1700 and 2600°F calcined samples of limestones. All materials except the Iceland Spar were studied. This material was deleted because its impurity content was so low that no conclusive results of interest on impurity aggregation and diffusion could be expected. Initially, scan rates of 160 μ/min were used. For samples showing the most interesting results (i.e. the iron and silica rich materials) line scans of 12 μ/min were used to gain more detail. For these samples, studies were also later made of the other calcination temperatures and of the effects of different calcination times. Figures 29 and 30 show types of surfaces examined with the probe.

To verify some of the microprobe results by an independent technique and to gain further insight into the diffusion processes occurring, one specific experiment was performed utilizing Auger spectroscopy. The advantage to be gained from this technique was that Auger measured compositions only for about the first 25-50 Angstroms of surface. The microprobe, on the other hand, averaged values over a one micron depth. Thus, thin inert layers (of a few hundred Angstroms) completely covering pores could be averaged away by the microprobe, but would be demonstrated by Auger.

The experiment performed specifically consisted of measuring the Auger

Table VI Chemical Analyses in Weight Percentage
(Analyses by Analytical Chemistry Section
of the Illinois State Geological Survey)

	Sample Type Number					
	1	4	5	6	8	9
Oxides	Iceland Spar	Pure Limestone	Pure Dolomite	Silica Rich	Aragonite	Iron Rich
SiO_2	ND[a]	1.53	0.03	11.8	0.19	5.88
TiO_2	ND	ND	ND	0.02	ND	0.15
Al_2O_3	ND	0.01	0.02	1.77	0.27	0.69
Fe_2O_3	ND	0.31[c]	0.34[c]	0.13	ND	2.82
Fe	0.13	--	--	0.41	0.01	1.75
MnO	ND	0.09	0.02	0.02	ND	0.21
MgO	ND	0.00	21.40	17.4	ND	15.33
CaO	55.3	54.8	30.30	26.5	55.2	30.82
Na_2O	0.003	0.047	0.008	0.040	0.53	0.16
K_2O	0.02	0.04	0.03	0.90	0.03	0.22
P_2O_5	trace[b]	--	--	0.02	0.01	0.10
CO_2	43.95	43.35	47.30	40.27	42.10	40.68
SO_3	0.01	0.15	0.13	0.03	0.37	0.42
SrO	0.014	0.019	0.019	0.04	0.10	0.04
Cl	ND	ND	0.09	trace	0.24	ND
Ign. loss	43.49	43.15	47.24	40.46[d]	43.33	41.85

---

[a] ND – not detected: Limits of detection for SiO_2, 0.03; TiO_2 and MnO, 0.01; Al_2O_3, 0.05; Fe_2O_3, 0.01; MgO, 0.10; Cl, 0.02.

[b] Trace of P_2O_5, approximately 0.005%.

[c] Percentage of total iron expressed as Fe_2O_3.

[d] Includes 0.30% H_2O+.

[e] Includes 0.61% H_2O+.

GTC 246-7

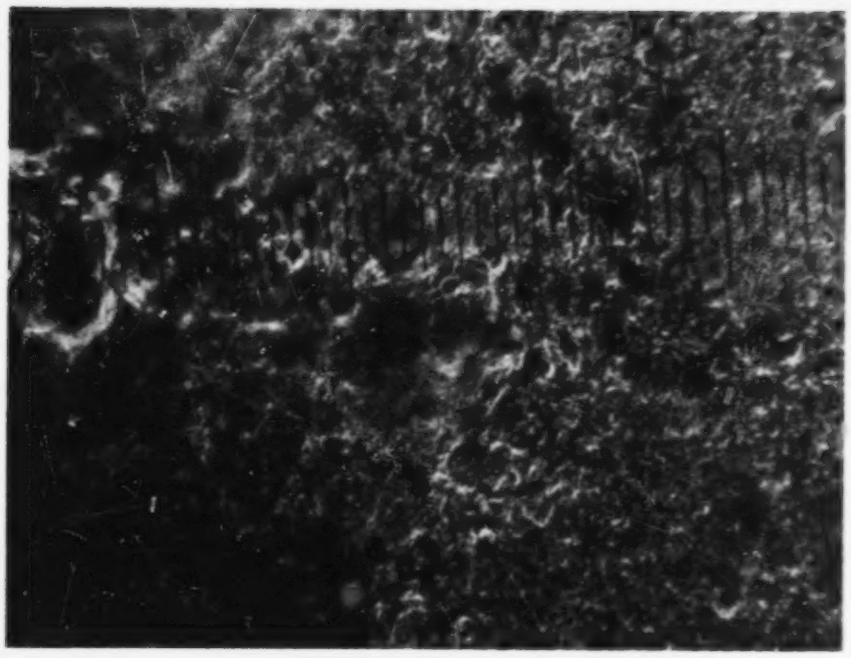

Figure 29. Silicon Rich Limestone 1700°F, 800X

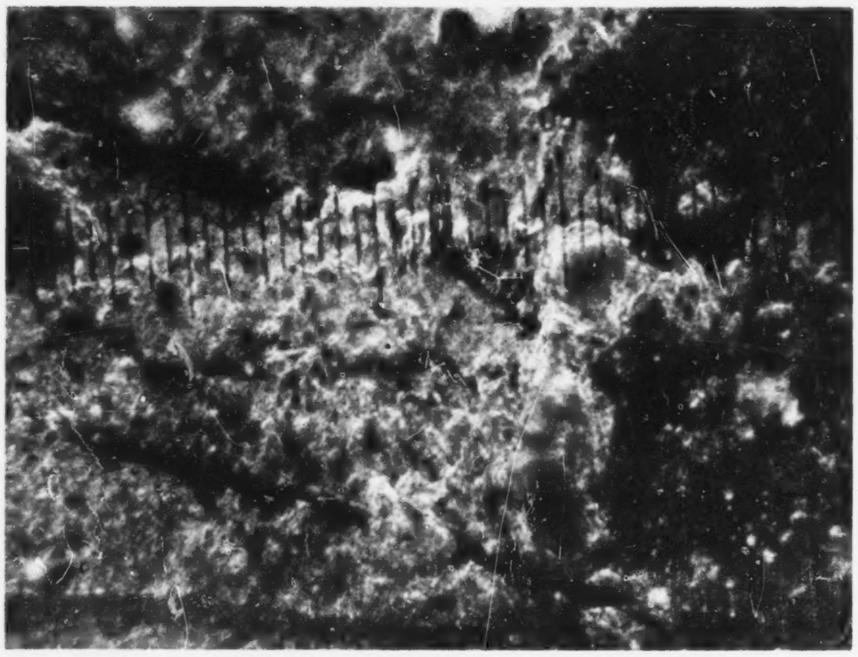

Figure 30. Iron Rich Limestone 2000°F, 800X

spectrum of a few locations on both a 1700°F iron rich type 9 calcined particle, and on particles of the 2600°F calcine of the same material.

3. Results and Discussion

a.. Infrared Studies

The six series of limestones were used for studies of the effect of calcination temperature on the positions and intensities of the SiO stretching bands. The findings of this study are listed in Table VII. It may be noted that, for the Iceland Spar, the bands obtained were very weak (absorbances ~0.05-0.1). For the calcines of the pure limestone and the iron- and silica-rich material, intense bands were found.

From the spectra obtained for the aragonite and Iceland Spar, no band shifts could be observed between the 1700°F and 2600°F calcines. This was probably due to very low concentrations of impurities available for reaction. For the pure dolomite, a shift of ca. 10 cm^{-1} was seen for a band at 1010 cm^{-1} in the silicate region.

The spectra obtained for the pure limestone and the iron- and silica-rich materials were far more revealing. For these three series, as can be seen for example from Figures 31 and 32, there are pronounced changes which mostly occur between 2300° and 2600°F. Thus, the lower temperature silica (Figure 31) or iron (Figure 32) containing calcines exhibit a strong band at ~1000 cm^{-1}. For the 2600°F calcines, on the other hand, the 1000 cm^{-1} band has greatly weakened and the principal absorption is now, in both cases, at 800-900 cm^{-1}. This is clearcut evidence of some type of reaction having occurred. Listed in Table VIII are principal positions of bands in some simple silicates. Some of the silicates listed (such as $CaSiO_3$) show spectra similar to those seen with the low temperature calcines. The highest temperature calcines, on the other hand, show spectra clearly different indicating formation of more complex materials.

In an effort to separate out the complex spectra of the type shown in Figures 31 and 32, an approach was employed wherein the calcines were dissolved in 2N HCl and the insoluble residues then recovered and spectra then run by the KBr pellet method of these. Using this approach, the CaO, unreacted $CaCO_3$ and soluble calcium metasilicates were dissolved away leaving SiO_2 and some of the more complex silicates behind as residues. In these studies, it was difficult to get a sufficient amount of residue for study from the Iceland Spar, as expected.

Spectra of the residues for the 1700°F and 2600°F calcines are listed in Table IX. Comparison of the results with Table VIII strongly suggests most of this material is one or more forms of silica. The small shifts noted with the residues, for some cases, could be explained in terms of degree of crystallinity of the silica and changes in it with temperature. It is of interest to note that, generally, the amounts of insolubles were greater for the low temperature calcines which may indicate that at more elevated temperatures SiO_2 reacts with the CaO and other impurities to form complex silicates. The discovery of free SiO_2 plus a variety of silicates present in these samples is of

Table VII Band Positions and Intensities for Calcination Studies

Material	Band Positions				Assignment
	1700°F	2000°F	2300°F	2600°F	
Iceland Spar	3650 w	--	--	3650 v.w.	OH^-
	1420 w	--	--	1420 v.w.	$CO_3^=$
	1020 v.w.	--	--	1020 v.w.	SiO
	875 w	--	--	870 v.w.	$CO_3^=$
	710 v.w.	--	--	--	$CO_3^=$
Aragonite	1430 b,w			1430 v.w.	$CO_3^=$
	1130 b,m			1130 b,m	SiO
	1020 v.w.			1010 v.w.	SiO
	995 v.w.			995 v.w.	SiO
	875 m			875 w	$CO_3^=$
Pure Dolomite	1420 m			1420 w	$CO_3^=$
	1155 w			1155 v.w.	SiO
	1130 m			1130 v.w.	SiO
	1010 w			1020 v.w.	SiO
	875 m			875 w	$CO_3^=$
Pure Limestone	1420 b,m	1420 w	1420 v.w.	1420 v.w.	$CO_3^=$
	1150 b,m	1150 w	1155 w	1150 v.w.	SiO
	1130 s,w	1120 w	1120 w		SiO
	1000 m,b	1000 m	1000 m	1050 v.w.	SiO
	920 m,b	920 m	920 m	930 mb	SiO
	880 sh, w	890 w, sh	890 m	890 m,b	SiO
	840 s,w	845 m	850 m	850 m	SiO
Iron Cont. Dolomite	1430 w	1430 w	1430 v.w.	--	$CO_3^=$
	1150 w,sh	1150 v.w.	1150 v.w.	--	SiO
	1100 w	1110 w	1110 w	1110 w	SiO
	995 s	1000 s	1005 m	1020 w	SiO
	920 v.s.	920 v.s.	920 s	920 w	SiO
	900 v.s.	900 v.s.	900 s	900 w	SiO
	845 s	845 s	845 s	845 v.s.	SiO
	800 w	800 w	800 v.w.	800 v.w.	SiO
Silica Cont. Dolomite	3650 w	3650 w	--	--	OH^-
	1420 w	1420 v.w.	1420 v.w.	1420 v.w.	$CO_3^=$
	1240 v.w.	1240 v.w.sh	1240 v.w.	--	?
	1090 v.w.	1110 v.w.	1110 v.w.	--	SiO
	1000 s	1000 s	995 s	1010 w	SiO
	--	950 v.w.sh	950 v.w.	--	SiO
	920 s	920 s	925 s	920 s,b	SiO
	890 s	890 s	890 s	880 s	SiO
	845 w	850 w	845 w	--	SiO
	740 w	730 w	730 w	740 w	SiO

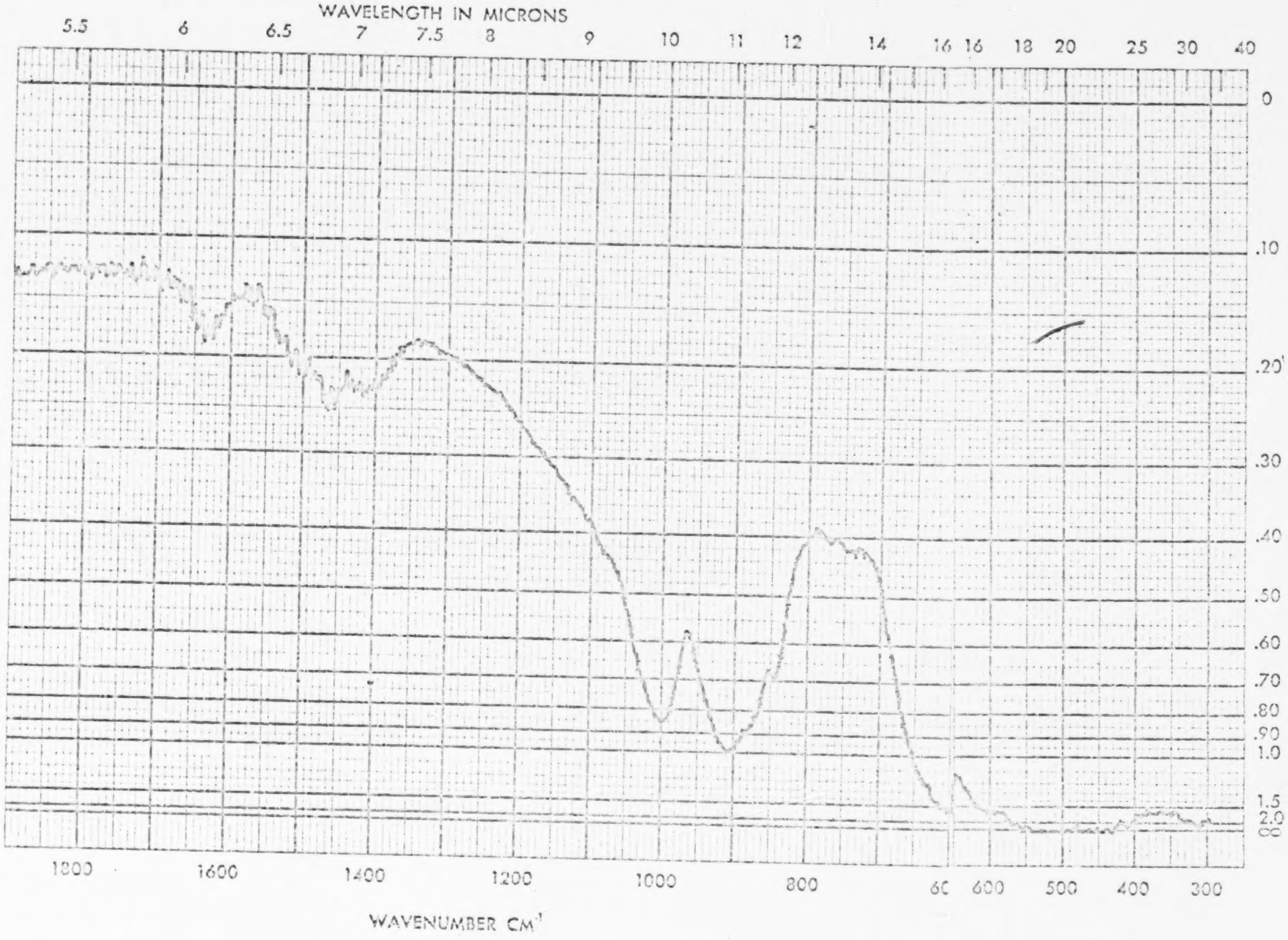

Figure 31A. Dolomite High in Silica at 1700°F

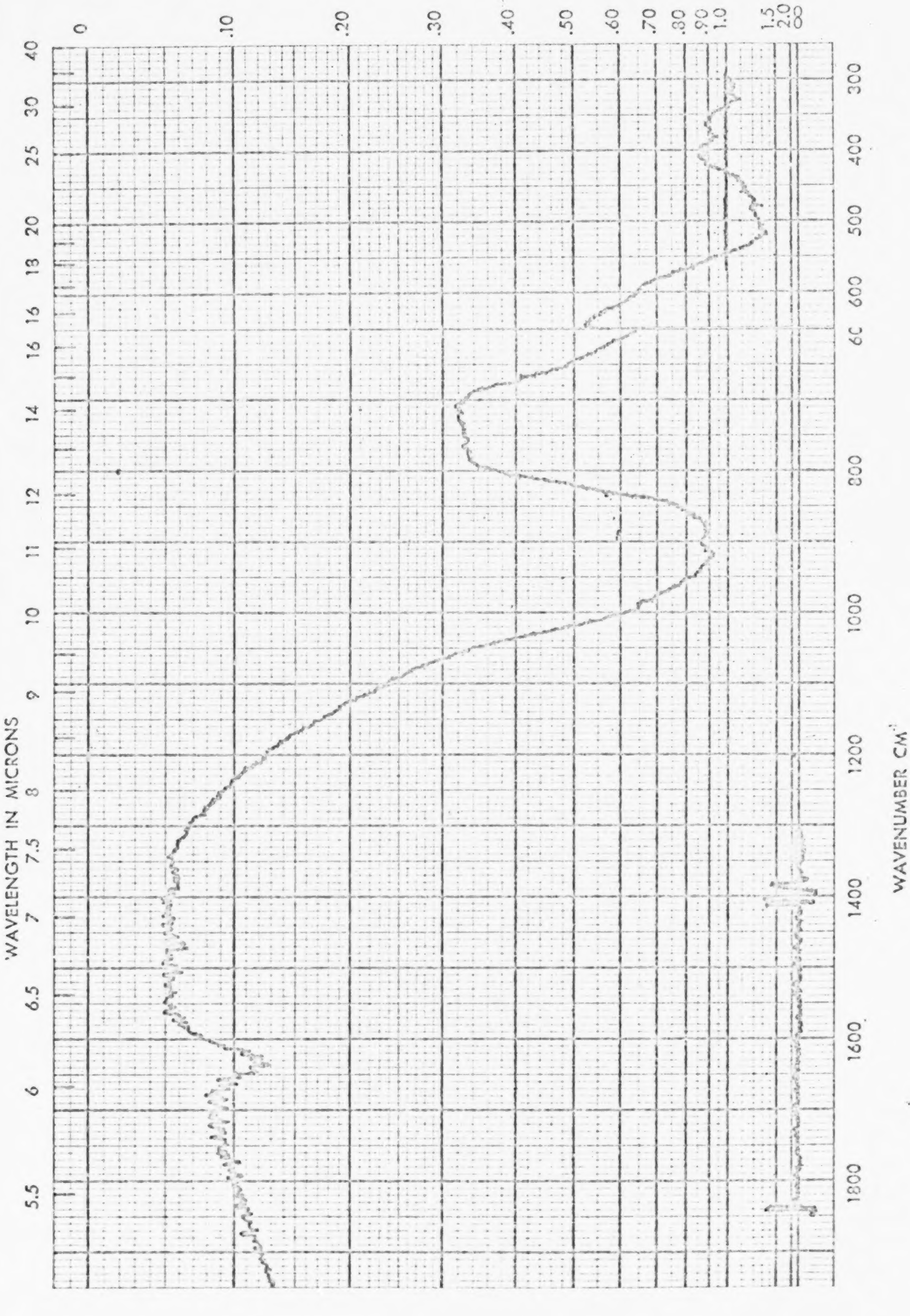

Figure 31B. Dolomite High in Silica at 2600°F

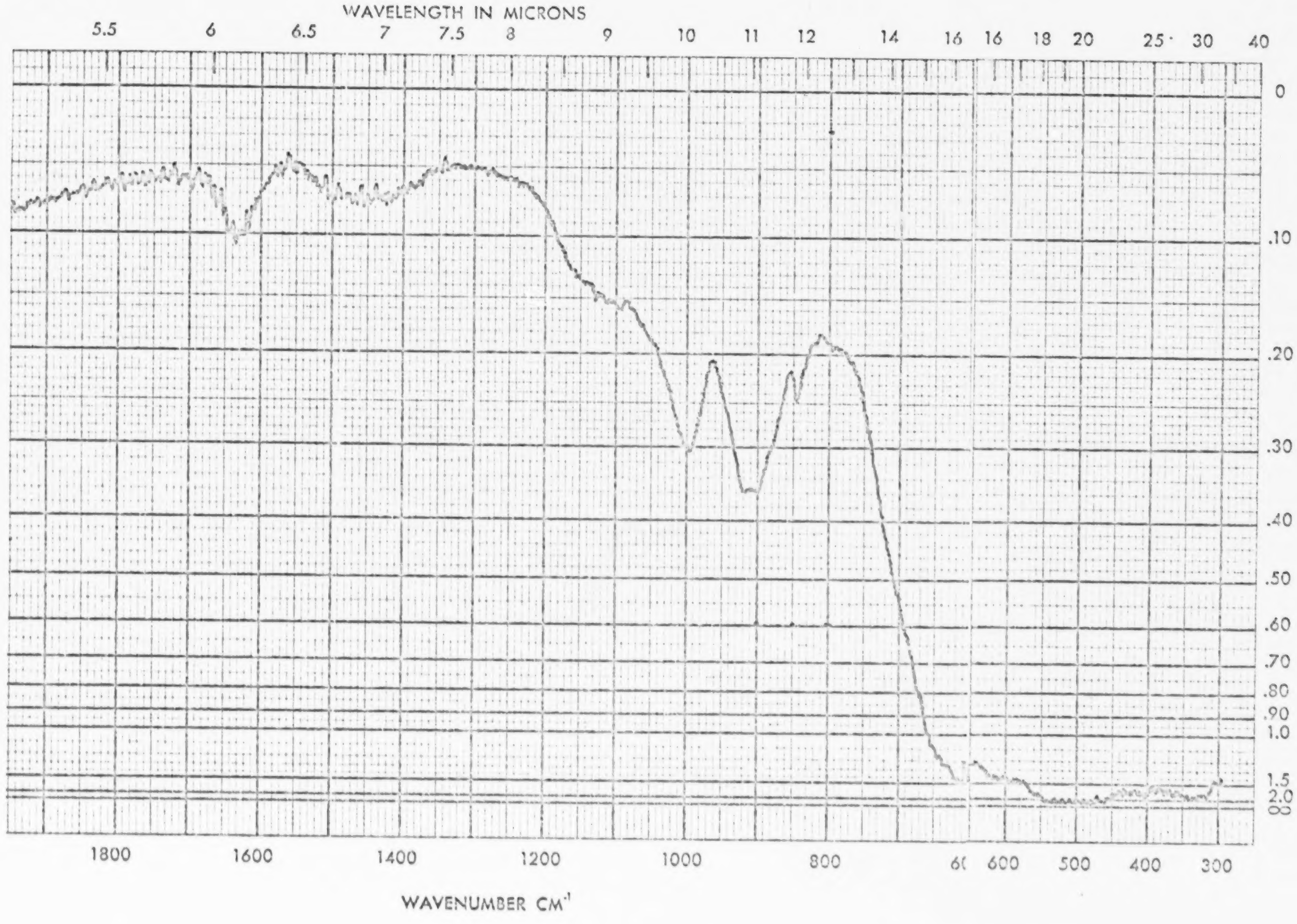

Figure 32A. Iron Containing Dolomite at 1700°F

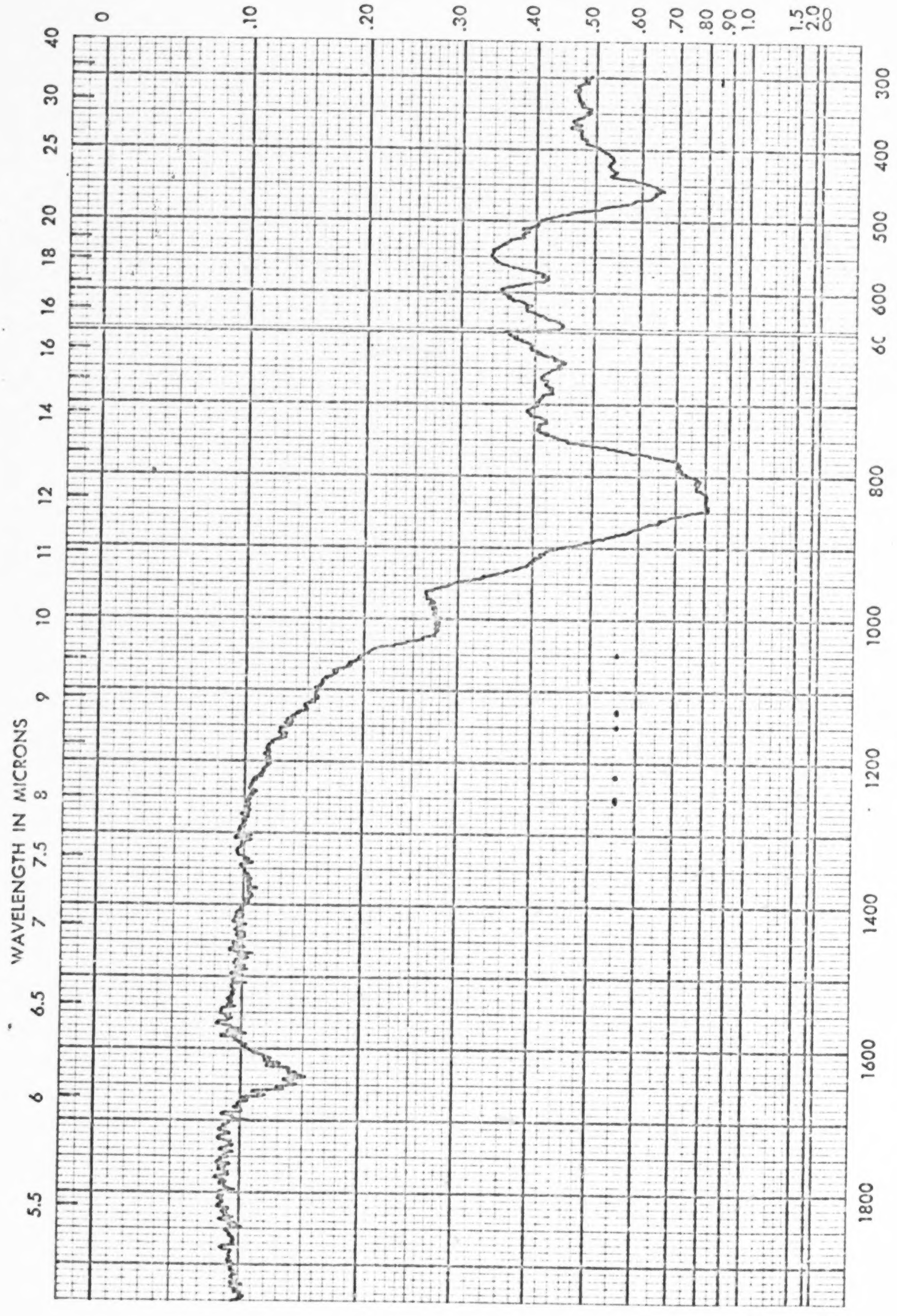

Figure 32B. Iron Containing Dolomite at 2600°F

Table VIII Band Positions Near 1000 cm^{-1} for Known Silicates

Material	Band Data				
α Quartz (SiO_2)	1160 s	1087 s	800 m	913 w	
Chert (SiO_2)	1160 s	1087 s	800 m		
Opal (SiO_2 in H_2O)	1160 s	1087 s	952 m	790 m	
Olivine $(Mg, Fe)_2SiO_4$	1000 s	952 s	893 s	840 m	
Garney ($Fe_3Al_2Si_3O_{12}$)	1020 m	966 s	900 s	870 s	
Augite ($CaMg(SiO_3)_2$)	1067 s	1020 s	963 s	918 m	874 s
Tremolite - $(OH)_2Ca_2Mg_5(Si_4O_{11})_2$	1110 s	1010 s	950 s	921 m	
Actinolite - $(OH)_2Ca_2(Mg, Fe)_5(Si_4O_{11})_2$	1110 s	990 s	955 s	921 s	
Hornblende	1020 s	784 w			
Wallastonite ($CaSiO_3$)	1090 s	1025 s	970 s	933 s	905 s
Hematite (Fe_2O_3)	980 s	820 w			

Table IX Spectra of HCl Insoluble Residues from Limestone Calcines

	Bands		
Material	1700°F	2600°F	Assignment
Iceland Spar	1420 v.w.	1420 v.w.	$CO_3^=$
	1100 v.w.	--	SiO
	1020 w	1020 v.w.	SiO
	805 w	--	SiO
Aragonite	1170 w sh	1170 w sh	SiO
	1085 v.s.	1095 s	SiO
	950 m	950 m	SiO
	780 s	790 s	SiO
	690 s	700 s	SiO
	460 s	465 s	SiO
Pure Dolomite	1160 m sh	1160 m sh	SiO
	1080 s	1080 s	SiO
	935 m	940 m	SiO
	795 s	800 s	SiO
	775 w	--	SiO
	690 w	--	SiO
	455 s	460 s	SiO
Pure Limestone	1155 w sh	1155 w sh	SiO
	1085 s	1090 s	SiO
	1050 v.w. sh	--	SiO
	920 m	940 m, sh	SiO
	780 s	790 m	SiO
	460 s	470 s	SiO
Dolomite Containing Silica	1170 m sh	1179 m sh	SiO
	1090 v.s.	1090 v.s.	SiO
	920 m sh	950 m	SiO
	870 v.w. sh	865 v.w. sh	SiO
	780 w	800 m	SiO
	450 s	460 s	SiO
Iron Containing Dolomite	1160 w, sh	1160 w, sh	SiO
	1100 s, b	1100 s, b	SiO
	940 m	945 m	SiO
	795 s	800 s	SiO
	775 s	775 s	SiO
	690 s	690 m	SiO
	455 s	460 s	SiO

considerable importance and any future studies of this type should be aimed at finding which silicates are present.

For the silica containing dolomitic material, efforts were also made to obtain spectra of the HCl soluble materials. Specifically, the HCl solutions of the 2000 and 2300°F calcines were first filtered to remove particulate matter and then evaporated to dryness and spectra obtained by the KBr pellet technique. The results are given in Table X. Weak bands were obtained in the silicate region indicating the presence of some soluble silicates. As metasilicates are the only silica containing material present known to be soluble in HCl, it can be concluded that some metasilicates may be present in the samples. Unfortunately, as these materials are decomposed by HCl dissolution, it is impossible at present to state which metasilicate materials are present.

Table X Spectra of HCl Soluble Residues from Limestone Calcines

Material	Bands	Assignment
Silica Containing Dolomite-2000°F	1020 vw, b	SiO
Silica Containing Dolomite-2300°F	1160 w	SiO
	1105 s, b	SiO
	1020 w, sh	SiO
	950 w	SiO

To gain further information on types of silicates present, spectra were also run of the EDTA insoluble residues of the 1700°F and 2600°F calcines of the iron and silica containing dolomites and of the pure limestone. The procedure used was to dissolve the limestone in tetrasodium EDTA saturated water, and collect the insolubles by filtration. The insolubles were then washed several times with distilled water to free them from EDTA. The residues were then dried and examined. For all of the low temperature calcines, visual examination revealed the presence of white and darker individual particles. These were separated for recording of spectra and KBr pellets of each type were prepared. The white materials yielded spectra identical to those seen for the HCl insoluble species (i.e. with the strongest band at ~1080-1100 cm^{-1} and additional bands at ca. 950 and 800 cm^{-1}). This separate phase, present in the low temperature calcines is undoubtedly some form of SiO_2. Spectra of the darker phase materials were somewhat more complex and are listed in Table XI. These spectra are difficult to interpret in terms of single sample silicates and are probably due to mixtures of silicates present.

From the results presented above, certain conclusions concerning the role of impurities in deadburning can be drawn:

Table XI Spectra of EDTA Insoluble Residues

Material	Bands 1700°F	 2600°F
Dolomite Containing Silica	1050 w, sh 1010 vs 980 w, sh 940 w, sh 780 w 560 m 460 s	1100 vw 1020 vs, b 950 w, sh 870 m 515 s 430 w
Pure Limestone	1160 w 1090 s 1040 w, sh 940 w, sh 795 s 775 s 690 s 460 s	1160 w, sh 1100 s, b 1020 w 985 w 940 w 790 m 705 m 430 m
Dolomite Containing Iron	1050 w, sh 990 s, b 900 w, sh 780 w 460 s	1020 s, b 940 w, sh 880 b, w 500 m

(1) The limestone materials, at low calcination temperatures contain some free SiO_2. At higher temperatures, apparently, some or all of this impurity undergoes reaction with CaO and other impurities to yield complex silicates.

(2) There is a definite change in the types of silicates present with an increase in calcination temperature, as is evidenced by spectral changes. Evidence accumulated to date suggests formation of comlex silicates.

(3) Differences between the EDTA residue and untreated material spectra can be explained in terms of reactions of EDTA with complex silicates which remove some of the metal ions (such as Fe^{+3}) from these solid materials and convert them into other insoluble silicates.

(4) For the relatively pure materials (Iceland Spar, aragonite and the pure dolomite) no major spectral changes, aside from small band shifts could be seen with increasing calcination temperature. For these materials, apparently, insufficient impurities are present to cause formation of significant amounts of complex silicates.

(5) For the iron and silica containing specimens and the "pure" limestone, pronounced changes in spectra were seen in increasing calcination temperature. Most of the major changes occurred between 2300 and 2600°F indicating that at or below ca. 2300°F little reaction has occurred. Above this temperature, apparently, chemical reaction of the SiO_2 or silicate present with lime or impurities occurs readily.

(6) From the infrared work alone, no conclusions can be drawn as to the locations of the SiO_2 or silicates with respect to the surface as a function of calcination temperature.

b. Microprobe Studies

(1) General Statement

In order to gain some insight into the location of silicate and other impurities with respect to both pores and surfaces, electron microprobe studies were undertaken. This work consisted of three phases of study: (1) An initial brief study of all six materials, (2) A detailed study of effect of calcination temperature for the silica and iron-rich samples and (3) An investigation of the effects of calcination times for these same two materials.

(2) Initial Studies

From the initial studies, results for the pure limestone, aragonite and pure dolomite were of little interest except for the presence of a few regions of high impurity content. Throughout the rest of the samples, impurity contents were uniform and very low. For example, the pure limestone particles showed a few regions in which there were high iron, aluminum and silica concentrations (all in some regions) and a few in which only silica was high. This result was expected for, as was stated earlier, both silica and silicates apparently exist in these samples. In general, regions of high iron content also yielded high aluminum indicating some pairing of these elements. From these runs, no clearcut evidence for diffusion to the surface of impurities with increasing calcination temperature could be obtained. Figures 33 and 34 show typical probe traces for Si, Al and iron on some particles of pure dolomite.

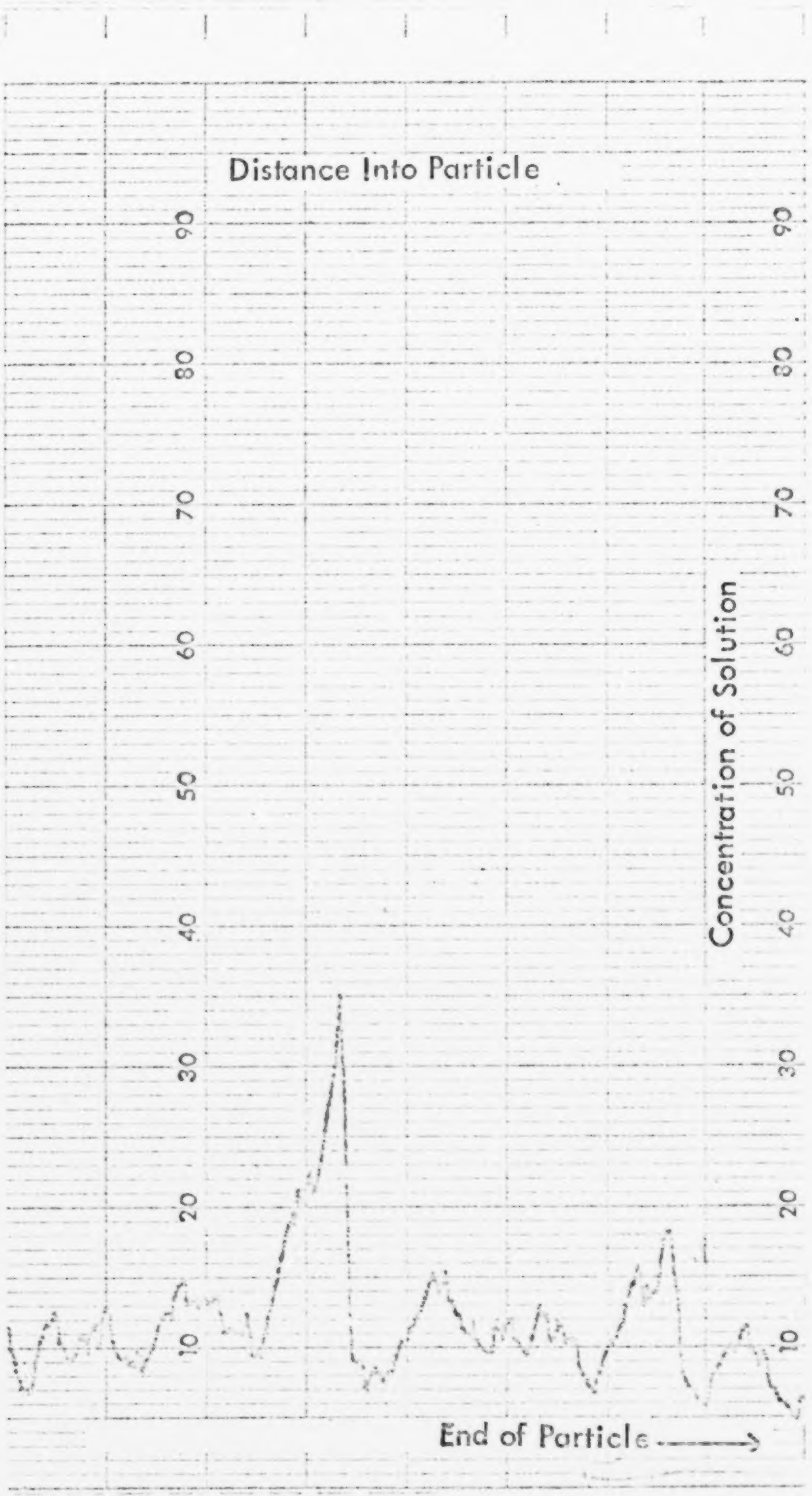

Figure 33. Microprobe Trace for Silicon on 1700°F Calcined Limestone

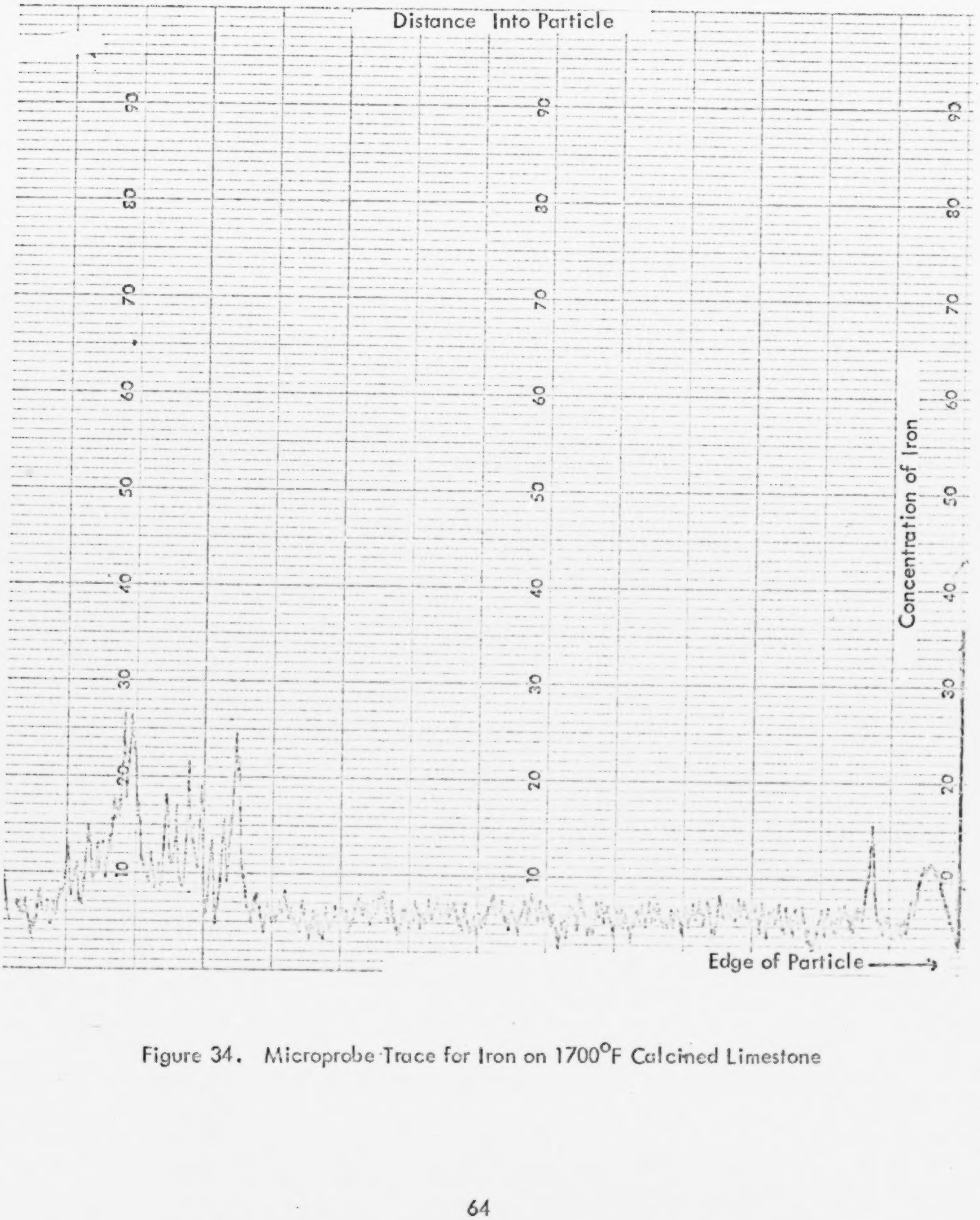

Figure 34. Microprobe Trace for Iron on 1700°F Calcined Limestone

Detailed studies at scan speeds of 12 μ/min were conducted on the 1700 and 2600°F calcines of these materials. For the 1700°F calcines the following were initially found:

(a) At surfaces impurity contents were about the same as those for the bulk for silicon, aluminum and iron.

(b) Most of the regions of high aluminum content also had high iron content although the aluminum/iron ratio did not remain constant from impurity region to impurity region. This coincidence of concentration maxima occurred in most of the high impurity regions traversed.

(c) The regions of high silicon content in some cases coincided with the above mentioned regions. Others, of quite high Si content did not correspond to either high Al or Fe concentrations giving further evidence for the presence of some free SiO_2.

(d) Examination under the microscope of trace paths for the high silica 1700°F sample showed that several of the Al maxima corresponded closely with the positions of sample pores. This indicates, in line with the above findings, the presence of Al and Fe at pore surfaces.

For the 2600°F calcines, the following initial results were obtained:

(a) The Fe and Al maxima again corresponded closely in position. However, about 80 percent of these maxima positions now correspond to pore positions.

(b) Again the Fe/Al ratio for impurity regions varied considerably.

(c) There was now a higher aluminum content at the particle surfaces than in the average bulk.

(d) The silicon maxima only in some cases corresponded to Al maxima. Those which did were almost always located in positions identical with those of pores.

(e) In some cases, the concentration of iron also appeared higher at the surface than in the bulk. No similar evidence was obtained for silica.

The above findings can be taken as evidence for:

1. Diffusion of aluminum (possibly as oxide) to the surface at higher calcination temperatures.

2. Aggregation of impurity phases in pores.

Figure 35 shows both effects for one particle. At the particle edge, as noted on the microprobe trace, there is a high concentration of aluminum on the aluminum concentration then declines as one moves toward the particle interior until a number of regions of high Al content are traversed. These appear as peaks on the microprobe trace and were found on examination to correspond to regions in which pores were present.

(3) Detailed Calcination Temperature Studies

Further microprobe studies were then conducted on the high silica and high iron content samples. In these investigations, the 1700, 2000, 2300 and 2600°F calcines of the two series were examined in detail with multiple line scans being run across several particles, for each sample, for iron, silicon and aluminum.

Table XII gives the ratios of surface to bulk (i.e. average bulk excluding the high impurity content discrete regions to be described later in this report) concentrations of the three impurities as a function of calcination temperatures. Each of the values reported in this table is the average of at least 3 particle scans for each material. The results, as can be seen, clearly show the following conclusions:

(a) At 2600°F there is definitely some diffusion of aluminum to the particle surfaces during calcination. This effect was more pronounced for the high iron content samples and may have something to do with the stabilities of the impurity phases present toward reaction with CaO. At 2300°F and below, no appreciable surface buildup occurs within a two hour interval of calcination.

(b) At all the calcination temperatures examined (1700-2600°F) there is no surface buildup of silica or iron as a result of calcination for 2 hours. It may be noted that here we are discussing only the main exposed surface and not the pores within the sample.

Scanning electron microscope photos, of the regions traversed by the microprobe on the series 6 and series 9 samples studied were taken and, from measurements of positions on the photographs, correlations were then attempted between the positions of pores and separate phases, seen in the photographs and those of maximum concentrations for silicon, iron and aluminum. Table XIII shows one such correlation in which all pores and separate phases along the trace are compared in position with observed

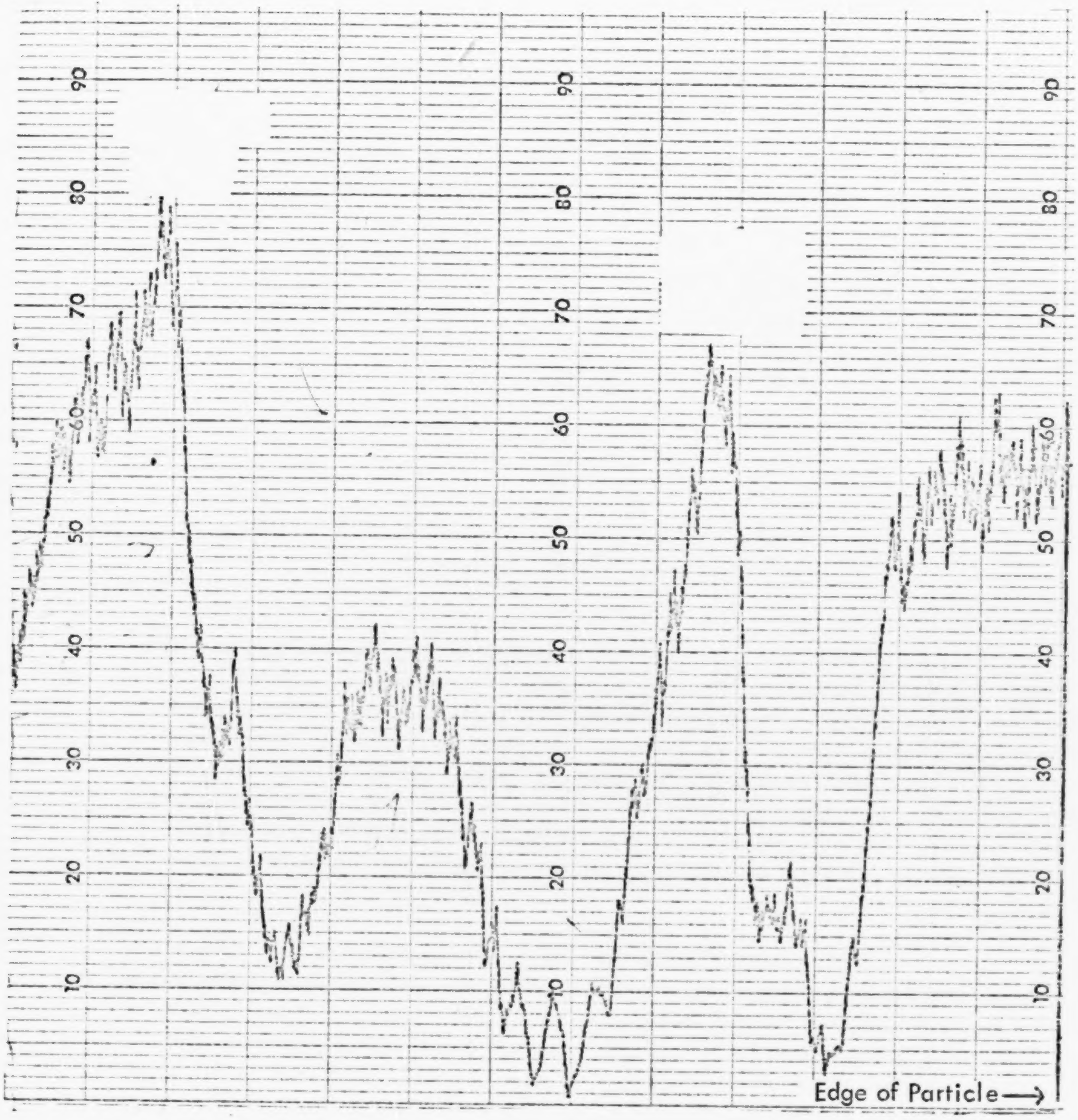

Figure 35. Microprobe Trace for Aluminum on 2600°F Limestone

impurity maxima positions. As can be seen from the table, excellent agreement exists. Furthermore, for all such tables prepared, for each of the particles traced, very few impurity peaks did not correlate with either phase boundaries, pores or separate phases in position.

Table XII Surface to Bulk Concentration Ratios for Impurities as a Function of Calcination Temperature

Material	Calcination Temperature	Surface/Bulk Ratio Al	Fe	Si
Series 6 (High Silica)	1700	1.30	1.05	1.20
	2000	0.90	0.80	1.25
	2300	1.20	0.85	0.90
	2600	2.05	1.15	1.15
Series 9 (High Iron)	1700	1.00	0.95	1.00
	2000	1.00	1.12	0.95
	2300	1.05	0.85	1.00
	2600	5.60	0.85	1.15

Table XIV shows the percentage of pores traversed by the microprobe for each specimen possessing more than ten times the average bulk concentration of the three impurities studied. For each calcination temperature, the sample studied was scanned a sufficient number of times to traverse at least 20 pores. As can be seen from the data, the fraction of pores with high alumina content increases with rising calcination temperature. The data for silicon and iron are less clearcut. For the discrete phases traversed, attempts were made to correlate impurity content with calcination temperature. However, no clear picture, such as that emerging for the pores in Table XIV, was seen to develop.

It may be mentioned that there was considerable variation in the number of pores and discrete phases from particle to particle. Thus, some of the particles studied were essentially pure limestone containing only a few regions of high impurity content, while others appeared to be filled with impurity phases, pores and other high impurity regions. For all of the above studies, a number of particles of each of the eight calcines were examined. Hopefully, this led to some type of average situation for which the results are reported above.

(4) Calcination Time Studies

Studies were also then conducted on the effects of calcination time on impurity contents at surfaces and in pores for the 2600°F calcines of the high iron

Table XIII Correlation Between Scanning Electron Microscope Positions of Pores and Phases and Microprobe Concentration Maxima-High Silica 2000°F Calcine Particles

Position* on S.E.M. Photo (in inches from start)	Phenomenon	Si$^+$	Fe$^+$	Al$^+$
0.5	pore	no effect	no effect	no effect
1.5	pore	maximum	maximum	large maximum
3.25	pore	maximum	maximum	large maximum
3.45-4.0	discrete phase	maximum	maximum	large maximum
5.4	discrete phase	no effect	maximum	no effect
6.0	pore	maximum	no effect	no effect
6.5	discrete phase	maximum	maximum	maximum
8.0	discrete phase	no effect	maximum	no effect
8.4	pore	no effect	no effect	maximum
9.0	pore	no effect	maximum	no effect
10.5-11	discrete phase	maximum	no effect	no effect
11.5	pore	no effect	maximum	maximum
13.0	phase boundary	minimum	maximum	strong maximum
13.7	pore	maximum	maximum	maximum
16.1	pore	maximum	no effect	no effect
17-17.5	discrete phase	no effect	maximum	maximum
19.1-20	discrete phase	no effect	maximum	minimum
20.6	pore	maximum	no effect	maximum

---

* Total trace region length on S.E.M. Photograph was 21.1 inches.
+ No effect means concentration remained at background level.

Table XIV Effect of Calcination Temperature on Concentrations of Impurities in Pores

Material	Calcination Temperature (°F)	% Total Pore Containing in Excess of 10 Times Bulk Impurity Concentration		
		Fe	Al	Si
High Silica (series 6)	1700	0	23	23
	2000	22	33	22
	2600	25	55	25
High Iron (series 9)	1700	40	25	18
	2000	55	36	16
	2600	94	50	20

and high silica limestones. In the preparation of these samples, as in all of the above and previous work, the stones were encapsulated in degassed epoxy disks and the epoxy and lime polished away with diamond to expose particle cross sections. All polishing was done with diamond only and care was taken to avoid contamination by iron, silica or alumina. The oil used in the diamond polishing was removed by washing with methanol. No water was used to avoid dissolution problems. The microprobe traces were run on several particles of each calcine under the same conditions (12 μ/min. scan rate) as before.

Table XV shows the effect of calcination time on impurity concentrations at the bulk surfaces. The surface to bulk ratios are seen to vary little with calcination time over the 20-120 minute interval studied. Similar analyses were also carried out for the pores. These results are given in Table XVI. Again, it can be seen that little variation can be observed with time, showing that the diffusion and agglomeration of these materials in pores is apparently fairly rapid at 2600°F and may play a considerable role in the deadburning process. For these samples, as for all earlier cases, the Si, Fe and Al were seen to exist mostly in high local concentrations in discrete phases, at phase boundaries and in pores.

Infrared spectra of KBr pellets of the 20 and 60 minute calcines of these 2600°F materials were also run. These spectra, on examination, proved to be identical to those reported earlier for the two hour calcines of the same materials. All of the same bands, in about the same intensity ratios appeared for the 20 and 60 minute calcines as for the 2 hour heated materials for each of the limestones studied. Thus, from the infrared evidence, no differences appear to exist between these materials. This would seem to indicate that the chemical reactions responsible for the marked differences between the 2600 the 2600°F and lower temperature calcines reported in an earlier letter are quite rapid. As the microprobe results indicate diffusion is also quite fast, it is possible that these diffusion processes govern both the rates of reaction and of diffusion of impurities into the pores. If this is true, then measurement of the infrared spectra may prove to be a valuable tool in determining the degree of deadburning of impure limestones, as the same diffusion processes control both the reactions and accumulation of impurities. With present arrangements, it was not possible to verify such conjecture directly. The samples used were calcined in crucibles at NAPCA for the desired fixed intervals. As the heatup time for the crucibles was a few minutes, it was not possible to investigate short calcination times using the microprobe technique. Possibly the alternative approach, such as using Auger spectroscopy and in situ heating may prove to be a means of verifying the above proposed mechanisms.

In these studies, we may note, some of the calcinations were conducted in pure Al_2O_3 crucibles and others in nickel crucibles. No major differences could be seen between the two preparation techniques. For the alumina boat calcines, some bits of Al_2O_3 could be seen by the microprobe to be present, but these were readily discernible from the remainder of the samples. The alumina boat calcined limestones themselves exhibited the same patterns of concentrations and diffusion behaviour as the nickel boat calcines.

Table XV Effect of Calcination Time on Surface/Bulk Impurity Ratios

Material	Calcination Time at 2600°F (mins.)	Surface/Bulk Ratio Al	Si	Fe	Mg
High Iron (series 9)	20	3.35	1.0	1.40	2.5
	60	3.00	1.30	1.40	3.0
	120	5.60	1.15	0.85	---
High Silica (series 6)	20	2.0	1.05	1.0	---
	60	2.5	1.00	1.0	2.0
	120	2.1	~1.15	~1.15	---

Table XVI Fraction of Pores Possessing Specific High Concentrations of Impurities (More than 10 Times Bulk Impurity Level)

Material	Calcination Time at 2600°F (mins.)	Si	Fe	Al
High Iron (series 9)	20	20	90	45
	60	20	90	55
	120	20	94	50
High Silica (series 6)		30	20	45
		30	25	50
		25	25	55

In these studies of shorter calcination times, the distribution of magnesium in some of the particles was also examined. As can be seen from the incomplete set of data in Table XV, some diffusion of magnesium to the surface may occur during calcination. The bulk of the magnesium, however, was seen to occur in discrete phases and at pores. Many of the Mg maxima observed also corresponded closely to those for at least one other impurity; however, there were a few maxima for MgO in positions where similar local high concentrations of the other impurities did not occur. This may be taken as evidence for the existence of discrete phases of both complex magnesium compounds and MgO itself within the calcines.

c. Auger Spectroscopy

To verify the diffusion of aluminum found by the microprobe studies, a single auger experiment was performed. Specifically, auger spectra were obtained for the surfaces at 3 discrete points each for the 1700°F and 2600°F iron-rich samples. The auger method has a dual advantage in that it can confirm the electron microprobe results and also show concentrations only with the first 50 Å of the surface, whereas the microprobe averages concentrations at depths up to 1 micron. The averaged results for the 1700 and 2600°F iron-rich calcines are given below:

1700°F -	Magnesium	11.0 at %
	Aluminum	1.0 at %
	Silicon	2.5 at %
	Iron	1.2 at %
2600°F -	Magnesium	11.0 at %
	Aluminum	2.5 at %
	Silicon	2.5 at %

As can be seen, the aluminum content has increased and is clearly above the 0.7 weight percent (Al_2O_3) bulk value found by APCO for this material. It may be noted that bulk values found by Harvey(16) (15.33% MgO; 0.7% Al_2O_3; 5.9% SiO_2 and 1.8% Fe) by chemical means are in only fair agreement with the Auger surface values reported above. This may be due to either differences in concentrations between surface and bulk or to difficulties with the Auger method of analysis. Nevertheless, the findings quoted above do support the conclusion drawn from the microprobe studies of diffusion of aluminum to the surfaces with increased calcination temperatures.

It should be noted that the above surface concentrations are for the surfaces and not for pores. Personnel conducting the above experiment measured only a few randomly chosen surface positions for each of the materials. The Auger spectrum of the 2600°F material is displayed in Figure 36.

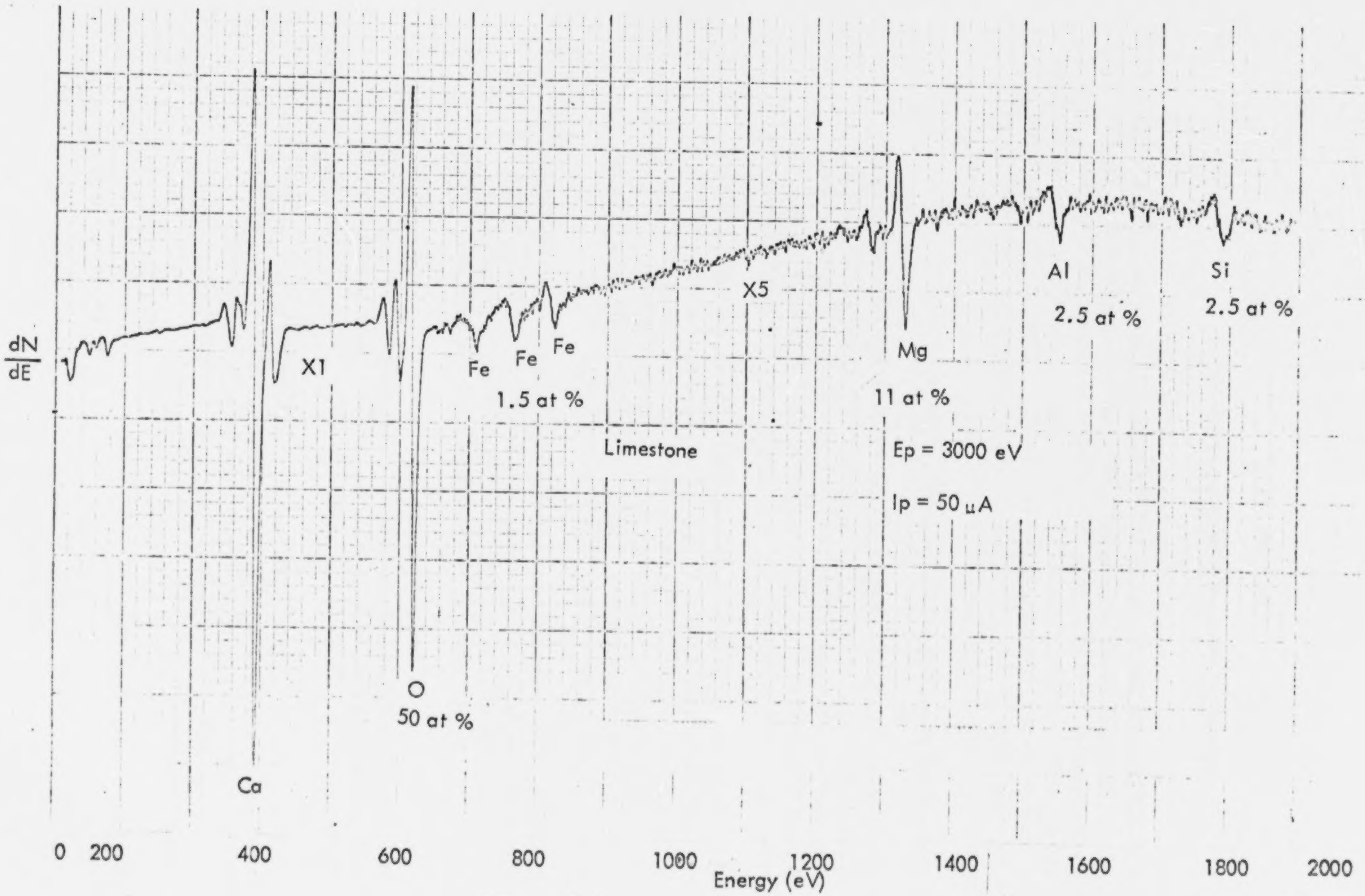

Figure 36. Auger Spectrum of 2600°F Limestone Calcine

SECTION III

CONCLUSIONS AND RECOMMENDATIONS

This study has illustrated the applicability of infrared methods to the study of problems involved in various limestone scrubbing processes. Using infrared spectroscopy in combination with electron microprobe studies, it has been possible to demonstrate reactions of impurities at high calcination temperatures with limestone and to show diffusion of some of these impurities or reaction products into pores and to bulk surfaces. Using the infrared method alone, new thin film cells have been developed and the groundwork has been laid for extending the analysis techniques developed to slurries.

The results of this program may be summarized as follows:

1. Two varieties of thin film infrared cells have been developed, using Irtran 2 as the window material, which possess better wear resistance than the AgCl cells used in earlier work. The sealed evacuable variety of cells has about as many filling and cleaning problems as the old AgCl cells. The new demountable cells developed, however, appear to be free of such difficulties.

2. Using the demountable cells, calibration curves for nitrate, nitrite, sulfate and sulfite have been developed for three solvent systems and lower limits on the general usefulness of the method have been established for all cases. For the case of water as the solvent, lower limitations are $1\text{-}5 \times 10^{-2}$ g/100 cc for all of the species of interest. Similar values were found using saturated aqueous KF and saturated aqueous tetrasodium EDTA.

3. Evaluation of the results obtained with the three solvent systems has shown that water is by far the easiest one to use. For the case of EDTA, interference from the solvents presents high accuracy analyses for carbonate and nitrate. For KF solutions, problems have been encountered for $CaSO_4$ analysis.

4. The analyses developed were checked, for a few cases against results obtained with ultraviolet spectroscopy for the same samples. Good agreement was obtained.

5. Infrared studies of deadburning have shown that reactions of silica and other impurities with lime and limestone do occur readily above 2300°F. The products of these reactions appear to be complex silicates with spectra very different from those of the impurities present before high temperature calcination.

6. Electron microprobe studies have shown that:

a. Impurities present in the limestones studied tend to be congregated in discrete phases, a larger number of which tend to congregate at pores as the calcination temperature is increased.

b. There is a diffusion of aluminum (probably as oxide or aluminate) to the surface of the limestone during high temperature calcination. No similar evidence was obtained for either the silica or iron impurities. These results were verified with auger spectroscopy.

To further utilize the techniques developed in this study and to gain further needed information by infrared methods on some of the problems involved in limestone scrubbing processes, the following set of recommendations are made:

1. The methods developed for sulfate, sulfite, nitrate and nitrite should be checked in detail against classical methods of analysis and their precision and accuracy assessed for the concentration ranges (0.05-3 g/100 cc) to which they are applicable. After this, the methods may be directly used to supplement wet limestone scrubbing studies. Here, the buildup of and reactions between reaction products could be studied directly by these methods and the infrared techniques could also aid in assessing the effects of product buildup in scrubber waters on reaction efficiencies and rates.

2. The methods developed for solids analyses should be assessed for accuracy by comparison of results obtained with those given by classical methods. These new techniques then could be put to use in several ways in conjunction with studies of dry scrubbing processes.

3. The methods developed, once fully assessed, may be useful for rapid analytical work required in conjunction with pilot plant studies.

4. The investigation of deadburning has shown the existence of solid state reactions during high temperature calcination and has also demonstrated buildups of inert materials in pores and at surfaces at higher calcination temperatures. However, the degree to which these phenomena influence overall process efficiencies has not been assessed. Specifically, both the above noted and sintering processes are expected to occur during calcination and efforts should be made to assess the amounts of reactivity losses due to each of these processes for limestones of interest. Also, determination should be made of maximum tolerable levels of specific impurities for limestones to be used for the wet and dry scrubbing processes. For this to be done, perhaps a study of the effects of impurities and calcination conditions on hydration rates may have to be undertaken.

SECTION IV

REFERENCES

1. Jones, R. N. and Sandorfy, C., "Infrared and Raman Spectra--Applications in Chemical Applications of Spectroscopy", W. West Ed., Interscience, New York, N. Y., 1959, p. 246.

2. Nachod, F. C. and Martin, C. N., Applied Spectroscopy, 13, p. 45, 1959.

3. Steinglanz, H., Applied Spectroscopy, 10, p. 77, 1956.

4. Kulbom, S. D., and Smith, H. F., Analytical Chemistry, 35, p. 912, 1963.

5. Thompson, W. K., Trans Faraday Science, 61, p. 2635, 1965.

6. Senior, W. A. and Vernall, R. E., J. Phys. Chem. 73, p. 4242, 1969.

7. Rissmann, E. F. and Larkin, R. L., Analytical Chemistry, 42, p. 1628, 1970.

8. Rissmann, E. F., Final Report, Contract CPA 22-69-59, National Air Pollution Control Administration, April, 1970.

9. Rissmann, E. F., Manual for Uses of Thin Film Infrared Cells, Interim Report, This Program, March, 1971.

10. Sulfur Oxide Removal from Power Plant Stack Gas--Tennessee Valley Authority, 1968.

11. Hatfield, J. D., Report for 3rd Limestone Symposium, Clearwater, Florida, Dec., 1967.

12. Potter, A. E., Report for 3rd Limestone Symposium, Clearwater, Florida, Dec., 1967.

13. Boynton, R. S., Chemistry and Technology of Lime and Limestone, New York, 1965, p. 17-20.

14. Ibid, p. 17-21.

15. Lee, H.,"Refractives from Ohio Dolomite", Ohio State Union Eng. Ext. Str. News, XIX, April, 1947, p. 2.

16. Harvey, Richard D., Interim Report, Contract CPA 22-69-65, June 22, 1970.

SECTION V

ACKNOWLEDGMENTS

The author wishes to thank Mr. Robert Larkin, Dr. Robert Statnick, and Dr. Dennis Drehmel of the Office of Air Programs, Fairfax Facility, Cincinnati, Ohio for helpful discussions and for providing some of the samples used in this study.

The author also wishes to thank Dr. Robert G. Shaver of General Technologies Corporation for helpful discussions and Mr. Frank Lysy, also of GTC for excellent experimental assistance on parts of this program.